

Electronic Thesis and Dissertation Repository

12-11-2013

Reaching for the light: The prioritization of conspicuous visual stimuli for reflexive target-directed reaching

Daniel K. Wood, *The University of Western Ontario*

Supervisor: Dr. Melvyn A. Goodale, *The University of Western Ontario*

A thesis submitted in partial fulfillment of the requirements for the Doctor of Philosophy degree in Neuroscience

© Daniel K. Wood 2013

Follow this and additional works at: <https://ir.lib.uwo.ca/etd>



Part of the [Behavioral Neurobiology Commons](#), [Cognitive Neuroscience Commons](#), and the [Systems Neuroscience Commons](#)

Recommended Citation

Wood, Daniel K., "Reaching for the light: The prioritization of conspicuous visual stimuli for reflexive target-directed reaching" (2013). *Electronic Thesis and Dissertation Repository*. 1759.
<https://ir.lib.uwo.ca/etd/1759>

This Dissertation/Thesis is brought to you for free and open access by Scholarship@Western. It has been accepted for inclusion in Electronic Thesis and Dissertation Repository by an authorized administrator of Scholarship@Western. For more information, please contact wlsadmin@uwo.ca.

REACHING FOR THE LIGHT: THE PRIORITIZATION OF CONSPICUOUS VISUAL
STIMULI FOR REFLEXIVE TARGET-DIRECTED REACHING

(Thesis format: Integrated Article)

by

Daniel Kent Wood

Graduate Program in Neuroscience

A thesis submitted in partial fulfillment
of the requirements for the degree of
Doctor of Philosophy

The School of Graduate and Postdoctoral Studies
Western University
London, Ontario, Canada

© Daniel Kent Wood, 2013

Abstract

The degree to which something stands out against the background of its environment communicates important information. The phenomenon of camouflage is a testament of the degree to which visual salience and probability of survival tend to overlap. Salient stimuli often elicit fast, reflexive movements in order to catch prey or avoid a predator. The overarching goal of the work presented in this thesis is to investigate how the physical salience of visual stimuli influence the programming and execution of reaching movements. I approached this question by recording kinematics and muscle responses during reaching movements. Broadly, this thesis investigates the effect of the physical salience of targets on the magnitude and latency of involuntary, spatially tuned muscle responses toward those targets.

In Chapters 2 and 3, subjects reached toward an array of potential targets on a touchscreen. The final target was cued only after the reaching movement was initiated. From trial to trial, targets differed in their numerosity (i.e., how many on the left versus the right) and in their salience (i.e., their relative contrast with the background). Different amounts of delay were introduced between the appearance of the targets and the cue to move. The results from these two studies demonstrate that the physical salience of (i.e., the luminance contrast differences between) targets influences the timing and the magnitude of involuntary deviations toward the most salient target(s) during reaching movements. At the level of individual subjects, the degree to which someone involuntarily reached toward the salient stimulus was predicted by the relationship between processing speeds for the different target contrasts.

In Chapter 4, subjects reached toward individual targets that varied in luminance contrast. Muscle activity in the right pectoralis major was recorded with intramuscular electrodes. Consistent with past studies, there was a consistent muscle response that was time-locked to the appearance of the target, regardless of the reaction time for the ensuing reaching movement. The same processing speed differences and magnitude modulations observed in Chapters 2 and 3 (due to different luminance contrast values of the targets) were observed in these stimulus-

locked muscle responses. Further testing revealed that stimulus-locked responses were elicited by a delayed, spatially uninformative go-cue.

Keywords

Saliency, uncertainty, affordances, reaching, global effect, EMG, superior colliculus, vision, motor control, individual differences

Co-Authorship Statement

All of the studies contained in this dissertation were carried out in collaboration with my supervisor, Dr. Melvyn A. Goodale. For Chapters 2 and 3, Dr. Craig Chapman, Dr. Jason Gallivan, and Jennifer Milne (and Dr. Jody C. Culham for Chapter 2) also assisted with the experimental design and data collection. While not listed as official authors, Alex Major and Alvi Islam also assisted with data collection for Chapter 3. For Chapter 4, Dr. Brian Corneil and Dr. Paul Gribble assisted with experimental design, data collection, and data analysis. Chao Gu assisted with data collection and data analysis. While not an official author, Dr. Jeremy Wong assisted with initial programming of the task. My supervisor, Dr. Goodale, assisted in all aspects of the writing process. However, the material in this thesis is my own work, and I take full responsibility for any mistakes.

As of the publication of this dissertation, only Chapter 2 is currently published in a peer-reviewed journal:

Wood, D.K., Gallivan, J.P., Chapman, C.S., Milne, J.L., Culham, J.C., & Goodale, M.A. (2011). Visual salience dominates early visuomotor competition in reaching behaviour. *Journal of Vision*, 11(10):16, pp. 1-11.

Acknowledgments

I spent six years of my life at what is now known as the Brain and Mind Institute at Western University. I was there during the formation of the institute, and so I was able to observe the coalescence of several fantastic research groups into one space. The atmosphere of collaboration and cooperation there is unlike anything I've seen at other institutions. The number of friends and collaborators I've had over the years, therefore, is probably too great for me to list all of them here. But I am grateful for each and every one of those collaborations.

All of the members of my advisory committee ended up being co-authors and collaborators. I'm grateful for their excellent mentorship. Specifically, Dr. Brian Corneil, Dr. Paul Gribble, and Dr. Jody Culham. Each of them has helped refine me as a thinker and as an experimentalist.

The staff members at the BMI are world class. Two of them need to be mentioned by name. Paula Perdue is the metaphorical thalamus of the BMI. All information passes through, and is filtered by her. And she handles it with humor and skill. If I have forgotten how many times her ability to organize has saved me, I could probably just go and ask her and she would have a record of it. Dr. Haitao Yang is a legend at the BMI. His ability to fix virtually every mechanical or technological bug with speed and precision is an incredible asset to the Institute. I have learned a great deal during my conversations with him. I'll never get tired of seeing how excited he gets whenever someone brings a baby to the lab.

The most successful collaboration during my time at Western was with Dr. Craig Chapman, Dr. Jason Gallivan, and Jen Milne. Our work on trajectory averaging has captured my fascination and, clearly, has heavily influenced the trajectory of my future research. Not only are these people fantastic scientists; they are also good friends, and I thank them for including me in that (ongoing) collaboration.

A special thanks to Dr. Brian Corneil who provided important mentorship in electromyography during the last year of my PhD. Our conversations have further

ignited my interest in the oculomotor system and provided a springboard into my postdoctoral work with nonhuman primates.

I thank Dr. Mark SeGRAves and Dr. Konrad Koerding, my current postdoctoral supervisors. They have supported and encouraged me during the last stages of my dissertation writing. I am thrilled to work with such talented scientists for the next few years.

Dr. Melvyn Goodale is nearing retirement. I will be one of the last of his graduate trainees. It has been a pleasure and an honor to work with Mel. Not simply because he is a giant in the field of visual neuroscience. Not simply because he is a brilliant writer and thinker. But mostly because he is a generous, kind person, and certainly among the few people who contribute to my image of an ideal scientist.

I want to thank my parents, Kent and Kathy Wood, for everything. For believing, sometimes irrationally, that I could do anything I wanted to do, and supporting me in it, whether it was being a professional musician, an academic philosopher, or a neuroscientist. I thank my mother for her impeccable balance of tenacity and flexibility, both in her approach to goals and in her moral navigations of social situations. She left a legacy of tireless charity and service that has changed me forever. I thank my father for his unquenchable curiosity (a trait he inherited from his own parents), his devotion to family and God, and his friendship. He really is one of my best friends.

Thank you to Rhonda, my step-mother, and to my parents-in-law, John and Janell Pallin, for their support and encouragement. I feel like I won the cosmic lottery when it comes to parental figures in my life.

Finally, there is Kristen, my wife. And Evelyn, my daughter. These two people mean everything to me. Kristen is my best friend and my best-kept secret; she kept me on track and motivated me during the frequent lulls in my own motivation during my graduate studies. Evelyn kept me sane with her ability to take my mind off of everything in the world other than how beautiful and hilarious and perfect she is. Thank you for joining me on this adventure, my girls.

Table of Contents

Abstract	ii
Co-Authorship Statement	iv
Acknowledgments	v
List of Abbreviations	x
List of Figures	xi
List of Appendices	xviii
Chapter 1 : General Introduction	1
1.1 An evolutionary perspective on reaching	1
1.1.1 The value of an ethological approach	3
1.1.2 Numerosity and salience	5
1.2 Affordance competition	6
1.2.1 Curved and averaged trajectories	10
1.2.2 Compelled response paradigms	18
1.3 Salience	23
1.3.1 Bottom-up salience in the oculomotor network	23
1.3.2 Bottom-up salience in the skeletomotor network	27
1.4 Thesis Objectives and General Overview	28
Chapter 2 : Visual salience dominates early visuomotor competition in reaching behaviour	31
2.1 Abstract	32
2.2 Introduction	33
2.3 Experiment 1	36
2.3.1 Methods.....	36
2.3.2 Results	39
2.4 Experiment 2	41
2.4.1 Method	43
2.4.2 Results	43
2.5 General Discussion	46
2.5.1 Salient targets dominate early visuomotor competition.....	46
2.5.2 Visual salience is a factor only during early visuomotor competition	49

2.5.3 Conclusion.....	51
Chapter 3 : Individual differences in the speed of visual processing predict capture by target salience	52
3.1 Abstract.....	53
3.2 Introduction	54
3.3 Methods	56
3.3.1 Data Processing and Analysis	60
3.4 Results	64
3.4.1 Characterization of bias over time.....	65
3.4.2 Target salience affects the timing and magnitude of trajectory biases	71
3.4.3 Individual differences in maximum salience bias are predicted by target enumeration speed	74
3.5 Discussion	77
3.5.1 Target salience persistently influences reach directions over a broad temporal range	78
3.5.2 Range of visual processing speed predicts susceptibility to capture by target salience	79
3.5.3 Conclusions.....	81
Chapter 4 : Target luminance contrast modulates stimulus-locked responses on human pectoralis major.....	83
4.1 Abstract.....	84
4.2 Introduction	85
4.3 Materials and Methods	86
4.3.1 Experimental tasks	89
4.3.2 Data Analysis	90
4.4 Results	93
4.4.1 Luminance contrast task	93
4.4.2 Delay task.....	99
4.5 Discussion	106
4.5.1 Conclusions.....	112
Chapter 5 : General Discussion.....	113
5.1 Summary of objectives and findings	114
5.2 Future directions.....	117
5.3 Conclusions.....	119

Appendix A: Supplemental Information for Chapter 2.....	134
Appendix B: Copyright Permissions	147
Appendix C: Ethical Approval	150
Curriculum Vitae	153

List of Abbreviations

PMd: dorsal premotor cortex
MT: middle temporal area
LIP: lateral intraparietal area
V4: visual area 4 in extrastriate visual cortex
SC: superior colliculus
SNr: subthalamic nucleus pars reticulata
PPRF: paramedian pontine reticular formation
PPC: posterior parietal cortex
PFC: prefrontal cortex
M1: primary motor cortex
RT: reaction time
fMRI: functional magnetic resonance imaging
OTid: optic tectum, intermediate and deep layers
Imc: nucleus isthmi pars magnocellularis
Ipc: nucleus isthmi pars parvocellularis
EMG: electromyography
MTR: multiple target reaching
E1: experiment 1 (experiment 2, etc.)
ANOVA: analysis of variance
FANOVA: functional analysis of variance
cd/m²: candela per square meter
SAL: salience differences in a target display
NUM: numerosity differences in a target display
AUC: area under the curve
MAD: median absolute deviation
SEM: standard error of the mean
SSE: sum squared error
SLR: stimulus-locked response
cPM: pectoralis major clavicular head
TC1-4: target contrast conditions 1 through 4
ROC: receiver operating characteristic

List of Figures

Figure 1.1 Competition between potential actions. A, Population activity, over time, in dorsal premotor cortex during a delayed reach-selection task. Cells (on the ordinate axis) are sorted according to spatial tuning. B, A sketch of the affordance competition hypothesis. Blue arrows represent action specification processes. Red arrows represent selection processes in the form of biasing signals from basal ganglia and prefrontal cortical regions. Taken from Cisek and Kalaska (2010). 8

Figure 1.2 Comparison of initial trajectory distributions from reaching and saccade performance for two target separation magnitudes. Modified from Ghez, et al., 1997 and Van der Stigchel & Nijboer, 2013. 20

Figure 2.1 Illustration of the experimental setup and typical arm trajectories (A), the tasks (B), and the experimental stimuli (C). The three-dimensional view of the experimental setup (A) depicts reach trajectories for example target displays, averaged across 27 participants. The colour of the trajectory corresponds to the initial target displays (inset right) and, in the case where potential targets appeared on both sides of space (i.e., blue and red targets), the final target location. The shaded bands surrounding the trajectories represent average standard error. The size of the three darkened ovals is proportional to velocity in the x and y dimensions at 25%, 50%, and 75% of movement distance. Colours are for purposes of illustration only. (B) Following the presentation of a fixation cross for a random interval, potential targets were displayed on the left and/or right sides of a touch screen. In E1 and the E2 no-delay group, the appearance of the potential targets was accompanied by an auditory cue for the participants to release a start button and initiate reach with the index finger toward the target display within 325 ms. In the E2 delay group, the auditory cue to move came 500 ms after the initial target display had appeared. In every case, the appearance of the final target (indicated by one of the potential targets filling in black) was triggered by the release of the start button as participants initiated their reaches. Participants had to touch the final target within 425 ms after button release. As displayed in (C), targets in experiment 1 (E1:

top row) consisted of black circles with contours of either 100% (high salience) or 50% (low salience) pixel concentration. In experiment 2 (E2), the high-salience target consisted of a black circle overlaid with a black cross, while the low-salience target consisted of a black circle with pixels removed where a cross would have intersected with the circle. 38

Figure 2.2 Results from experiment 1: an overhead plot of average reach trajectories (A) toward the target displays indicated above the plot. Only trials in which the left target was cued are shown. Shaded areas in the trajectory plot represent average standard error. The dark lines in (B) indicate the lateral deviation difference between trajectories in the H:L (i.e., *high* salience target left versus *low* salience target right) and L:L conditions (magenta) and between trajectories in the L:H and L:L conditions (cyan). Shaded areas in the difference plot represent 95% confidence intervals.... 40

Figure 2.3 Results from Experiment 2. The two plots on the left show an overhead view of average trajectories for the no-delay (top plot) and delay (bottom plot) groups in response to a target display with two low salience and two high salience targets. The colour of the trajectories correspond to the colour-coded target displays depicted between the two plots. In these plots, and in all other plots in the figure, only trials where the final target appeared on the left are shown. The two plots on the far right show average trajectories of the no-delay (top plot) and delay (bottom plot) groups in response to four low salience and two high salience targets. Shaded areas in the trajectory plots (i.e., blue and red) represent average standard error. Colours are for purposes of illustration only. The two plots in the center of the figure show the difference in lateral deviation (between the red and blue trajectories; i.e., the difference between responses to the two spatial arrangements of a given target display) as a function of the distance between the hand and the touchscreen. Shaded areas in the difference plots represent 95% confidence intervals. 44

Figure 3.1 Task and stimuli. A, Temporal sequence of a single trial in the reaching task. After a variable fixation period, the array of potential targets appeared. An auditory go-cue was presented either simultaneously with or up to 450 ms (50 ms increments) after the target array onset. After the go-cue, participants had 325 ms to

begin reaching. Only after reach onset was the final target cued by filling in one of the potential targets. Participants had 425 ms from reach onset to touch the final target. *B*, A single trial in the enumeration task. After a variable fixation period, a cluster of targets appeared on the screen for 16.7ms, along with an auditory go-cue. Participants had 1500ms to report (with a numeric keypad) the number of targets detected. *C*, The eight possible target displays, grouped into four basic patterns. Note that the uniform clustering of targets depicted here is only for illustrative purposes. See *Methods* for a description of the actual target locations in a display. *D*, Luminance and Weber contrast values for the potential targets. *E*, All three experimental groups had the same high contrast target, but differed with respect to the low contrast target that they encountered. 57

Figure 3.2 Analysis of reaching performance for a single participant in the MID salience group. *A*, During trials with the SAL-NUM target display, this participant was strongly biased toward salience at the minimum delay (0 ms) and strongly biased toward numerosity at the maximum delay (450 ms). We show only the first 10 cm (out of 40 cm) of the reach. Colored patches between the trajectories indicate the area under the curve (AUC). *B*, By taking the AUC (up to 20% or 8 cm of the reach) between the average trajectories toward the two mirror-image displays for each of the four target display conditions, we calculated the overall reach bias (on a continuum of salience to numerosity bias) at each of the parametric delays. The result is a bias function (shown in green bordering). *C*, To describe the shape of each participant's bias transition function (i.e., the bias function for the SAL-NUM target display), we fitted linear (not shown), cubic, and logistic functions. *D*, Finally, we characterized reach bias as a function of a continuous temporal metric (Delay + RT). We used this continuous bias transition function to define the max salience bias for each participant. 62

Figure 3.3 The interaction of salience and numerosity over time. These plots show average bias functions for the four target conditions of interest. Red traces show the bias transition function, which is the response to displays where luminance contrast and numerosity bias the reach in different directions (i.e., SAL-NUM). Green traces show the response to displays that differed only in luminance contrast (i.e.,SAL).

Magenta traces show the response to displays that differed only in numerosity (i.e., NUM). Blue traces show the response to displays where luminance contrast and numerosity bias the reach in the same direction (i.e., SAL+NUM). *A*, Bias functions averaged over all salience groups. *B*, Bias functions averaged within salience groups. Shaded regions indicate bootstrapped 95% confidence intervals. 66

Figure 3.4 Pure salience (SAL) and pure numerosity (NUM) bias functions over time. *A*, Salience and numerosity bias strength averaged over all salience groups. *B*, Salience and numerosity bias functions averaged within salience groups. Note that the trace for the SAL condition is inverted for display purposes. Shaded regions indicate bootstrapped 95% confidence intervals. 68

Figure 3.5 Between-group differences in salience-based bias function overlap. *A*, The degree of spread between the three salience-based bias functions (i.e., SAL- NUM, SAL, and SAL+NUM), compared across salience groups. The magnitude of salience bias spread is inversely proportional to the influence of numerosity within a given target salience group. Error bars indicate SEM. * $p < 0.05$. *B*, Target contrast values of the three salience groups, mapped onto the logarithmic contrast response function. This figure illustrates the proposed mechanism underlying the results depicted in *A*. 69

Figure 3.6 Maximum salience bias and bias transition latency. *A*, Measures of bias transition latency extracted from cubic and logistic fits to individual performance in the SAL-NUM display condition (see Figure 3.2D). In spite of the resemblance of the two fits, there were no significant latency differences between salience groups for the logistic fits, due to significantly higher variability. *B*, Average latency of the maximum salience bias for the respective salience groups. *C*, Average maximum salience bias for the respective salience groups. *D*, The magnitude of the maximum salience bias predicts the latency of the point where the maximum is reached. Participants with a stronger maximum salience bias tended to reach that maximum earlier than others. Histograms depict, on their respective axes, the distribution of data points for the three different salience groups. All error bars indicate SEM. 72

Figure 3.7 Target enumeration accuracy and RT are correlated with max salience bias. The RT difference between low- and high-contrast conditions is correlated with max salience bias in the reaching task. The black regression line represents the regression over all three salience groups, and corresponds to the Pearson's r value in black text. ** $p < 0.01$, *** $p < 0.001$ 75

Figure 3.8 Numerosity-tuning in a subset of participants. We regressed max salience bias (taken from SAL+NUM performance) against the mean of the entire bias function for the SAL-NUM display trials. We then divided participants according to negative or positive max salience bias scores (blue and red dots, respectively). The resulting groups showed a striking reversal in the relationship between the two variables, revealing a subset of participants who were tuned to the numerosity of the target display, regardless of which targets were salient. * $p < 0.05$, *** $p < 10^{-7}$ 76

Figure 4.1 Experimental paradigm. *A*, Subjects held the handle of a robotic arm, with their arm supported by an air sled. They viewed both the reach targets and a cursor representing real-time position of their hand on a mirror surface that reflected the output of a downward-facing LCD screen. *B*, The arrow indicates the approximate placement of electrodes in the clavicular head of pectoralis major (cPM). *C*, Trials in the luminance contrast task started with subjects holding the cursor in the central fixation circle (CF). The CF disappeared 200 ms prior to target (T) onset, after which subjects immediately reached toward the target. *D*, Trials in the delay task also started with the cursor in the CF. The target then briefly flashed for 150 ms. The CF disappeared either at target onset, or after a 1 sec delay. CF disappearance was the cue to reach toward the remembered location of the target. 88

Figure 4.2 Exemplar EMG recordings from pectoralis major (clavicular head; cPM) of a single subject in the luminance contrast experiment. The top row of panels depicts activity for movements toward the upper-left target, where cPM acts as an agonist. The middle row depicts cPM activity for movements toward the lower-right target. Data are aligned to visual target presentation (black vertical line at 0 ms) and are sorted according to RT in descending order. Manual RT for each trial is marked with red (agonist) or green (antagonist) circles. Bottom row depicts mean EMG traces.

The width of the trace subtends SEM. Columns are grouped by target contrast (TC) condition, with TC4 being the highest contrast. 94

Figure 4.3 Detection of stimulus-locked activity. *A*, Exemplary EMG data, sorted by RT and locked to stimulus onset (black vertical line at time 0). Red circles indicate RT for a given trial. Trials were either discarded (due to temporal overlap between robust voluntary movement-related activity and the stimulus-locked band of activity) or separated into early (red) or late (blue) RT groups. *B*, Area under the ROC curve was calculated for each EMG sample (here, from Figure 4.3A) between 100 ms before and 300 ms after stimulus presentation (only a constrained time window is displayed here), for both RT groups (i.e., early and late). ROC discrimination time (RDT) was defined as the time at which the ROC area first surpassed a value of .675. Red (early RT) and blue (late RT) transparent bands indicate samples at which the corresponding ROC area is over threshold. *C*, The slope of the relationship between RDT and average RT for early and late RT groups was calculated. Shown here is the slope for the data depicted in *A* and *B*. *D*, The slope threshold for detecting a SLR was set at 67.5 degrees (horizontal dotted line). Performance of all subjects in the luminance contrast task is shown. Individual dots represent the slope of the relationship between RDT and RT for the fast and slow RT trials, and the intensity of the dot corresponds to different target contrast conditions (see legend). The subjects are grouped into those who show the presence of stimulus-locked activity in at least one target contrast condition (SLR+) and those who do not (SLR-). 96

Figure 4.4 Contrast-modulated latency and magnitude of stimulus-locked activity. *A*, Average SLR magnitude (squares in upper axis) and latency (circles in lower axis) for the four target contrast conditions. Error bars (within the circles for latency values) indicate SEM. With the exception of TC2 vs TC3 in the magnitude data, all comparisons between conditions were significant for both measures, $p < 0.05$. *B*, Exemplary data from a single subject (different from individual subjects in Figures 4.2 and 4.3), illustrating the identification of peaks and their latencies in the ROC time course (black trace plotted above) for the four target contrast conditions. Black dotted line is .5 (chance discrimination), and red dotted line is .675 (discrimination

threshold). Average EMG traces for agonist (red) and antagonist (green) movements are plotted below. Width of traces subtends SEM. Magenta vertical line indicates timing of SLR peak in the ROC time course. Black vertical line at time 0 indicates stimulus onset..... 98

Figure 4.5 Exemplar recordings from a single subject in the delay experiment. Both panels contain EMG activity for individual trials, sorted by RT. Darker colors represent greater EMG activity. Red (agonist movement) and green (antagonist movement) dots represent manual RT. Mean EMG traces are plotted above each pair of panels. *A*, Data from the no-delay condition, locked to stimulus onset. *B*, Data from the delay condition. The first 800 ms (i.e., -100 to 700) are locked to stimulus onset, while the last 800 ms (i.e., -300 to 500) are locked to disappearance of central fixation. Approximately 150 trials are depicted in each cluster (on the ordinate). .. 101

Figure 4.6 Stimulus-locked activity in the delay task. ROC discrimination slopes (67.5% RDT versus RT) for individual subjects in three different epochs: (1) locked to stimulus onset, no delay, (2) locked to stimulus onset, delay, (3) locked to fixation disappearance, delay. Slopes over the cutoff of 67.5° (SLR detected) are in pink solid lines, while slopes below the cutoff (no SLR detected) are in blue dotted lines. 103

Figure 4.7 Stimulus-locked oscillations in muscle activity. *A*, EMG activity for individual trials, sorted by RT and locked to stimulus presentation (red vertical line), for 5 of the subjects in the delay experiment. Red (agonist movement) and green (antagonist movement) dots represent manual RT. Darker colors represent greater EMG activity. Approximately 150-200 trials are depicted for each subject (on the ordinate). *B*, Single-sided frequency-amplitude spectra for the corresponding epochs (sampled between 50 and 250 ms) in *A*. The two vertical lines indicate the location of 10 and 20 Hz. Note that peak amplitude consistently occurs between 12 and 15 Hz. 105

List of Appendices

Appendix A: Supplemental Information for Chapter 2	134
Appendix B: Copyright Permissions	147
Appendix C: Ethical Approval	150

Chapter 1 : General Introduction

1.1 An evolutionary perspective on reaching

While it has become a well-worn trope in grant applications and introduction sections, it is still worth mentioning here that the imperative to study visually-guided movement of the limbs is partially driven by the practical medical outcomes of such research. For patients suffering from paralysis or amputation, neuroprosthetic limbs offer the hope of being able to manually interact with the world once again. For example, recent studies have reported successful neuroprosthetic control of an anthropomorphic robotic limb (for both reaching and grasping) by individuals with tetraplegia (Collinger et al., 2013; Hochberg et al., 2012). These exciting developments have been built upon the foundation of decades of basic research on the neural circuits that mediate skilled, visually guided reaching and grasping.

Basic research on visually guided movements has its own intrinsic sources of motivation. Beyond the genuine fascination and awe that most researchers experience as they confront the elegance of the sensorimotor system, it is also the case that this system (in particular, the oculomotor system) is an ideal model for understanding the rest of the brain. This is partly due to the fact that we know, relatively speaking, a great deal about the visual system (at least in comparison with other sensory modalities). Many of the computational algorithms that describe the behavior of cells in the visual system are also implemented in other systems. There is constant cross-pollination of ideas between and within the various levels of analysis in neuroscience, and the systems-level approach to visuomotor processing is one of the more productive pollinators.

A deeper philosophical point, however, provides a broad motivation for studying the motor system: our brains evolved to control movement. In order to eat, to escape threats from inanimate and animate sources, and to reproduce,

organisms need to move. The nervous system of any organism, vertebrate or invertebrate, is a solution to the problem of movement. This insight carves out a general approach to studying the brain, semi-seriously referred to as “motor chauvinism” by Daniel Wolpert (Wolpert, Ghahramani, & Flanagan, 2001), in which everything we learn about perception, language, emotion, and every other capacity of the nervous system, is filtered through and indexed back to movement.

If this seems to be too extreme a position, at least consider that this motor chauvinism is part of larger constellation of ethological approaches to the study of the brain. All of these emphasize a point that was aptly expressed by Cisek and Kalaska: “One of the most important facts we know about the brain is that it evolved” (Cisek & Kalaska, 2010 pg. 275). In a broader sense, ethological approaches attempt to maintain a focus upon the organism’s role as part of an ecosystem; the behavior and neurophysiology of the organism cannot be understood apart from its evolutionary past and its current interactions with its environment.

Given any consistent empirical observation about the nervous system, there are infinite ways of making sense of it. But the theoretical structures that end up making sense of our empirical observations have tangible, long-lasting consequences for our ability to make progress in science. This is primarily due to the fact that our theories not only make sense of existing empirical findings, but also shape our understanding of what constitutes a good empirical question. Considering the brain in light of (1) the selective pressures under which it evolved, and (2) the biological idiosyncrasies flowing from those pressures as they play out in the interactions between the animal and its environment, has proved to be a fruitful approach.

Of course, the theory of natural selection is so pervasive in every branch of the biological sciences that one would be hard-pressed to find a scientist that is not explicitly or implicitly operating under the assumption that it is true. And yet, the

life sciences are littered with examples of frameworks that explain phenomena in ways that are (at the worst) at odds with or (at the best) redundant with respect to the more established and far more coherent framework of natural selection. In systems and cognitive neuroscience, the most frequent examples of this occur when principles from other fields make a helpful contribution, but then decide to move in and take over the whole operation. Perhaps two of the more frequent offenders in this regard are philosophy and engineering. Both (obviously) vitally important fields in their own right, they have also bled into neuroscience in immeasurably productive ways. But when, for example, a particularly useful engineering principle is able to reproduce certain biological phenomena, it will often bring with it some unhelpful conceptual baggage that may ultimately eclipse, as Cisek and Kalaska put it, one of the most important facts about the brain: that it evolved.

1.1.1 The value of an ethological approach

A good example of how an ethological approach clarifies empirical findings can be found in the development of the dual streams hypothesis of the primate visual system. Ungerleider and Mishkin (Ungerleider & Mishkin, 1982) famously outlined a theory of two basic visual processing streams that branch off from primary visual cortex. The dorsal stream (the “where” stream), which extends from occipital cortex to parietal cortex, was described as being responsible for processing the spatial location of objects. The ventral stream (the “what” stream), which moves from occipital cortex to inferior temporal cortex, was allegedly responsible for processing the identity of objects. Note that this distinction is consistent with the view that vision (at least in humans) is primarily for building a central, knowledge-based representation of the external world. This view of the senses has dominated throughout the history of philosophy, in various forms, until perhaps the last two centuries, and even now it still reverberates through the impact that it has had on virtually every field that studies humans.

Goodale and Milner (Goodale & Milner, 1992), while retaining in their model roughly the same anatomical features of the two streams, approached the data from an ethological perspective. For example, they proposed that the primary role of the dorsal stream is to control visually-guided behavior. In other words, visuomotor processing in the dorsal stream extracts the spatial features of objects from the incoming visual signal not so that it can populate a centralized representation of space (presumably to be used by both perception and action) or to generate beliefs about the world, but rather to specify potential actions and control ongoing actions. And while Goodale and Milner, for reasons of simplicity, characterize ventral stream processing as “vision for perception”, a close reading of their view makes it clear that the ventral stream is, ultimately, also vision for action. In other words, while our rich, detailed visual experience of the world relies upon ventral stream processing, the biological purpose served by that visual experience is not to provide humans with something to contemplate and enjoy, but rather to make movement more flexible and adaptive. Ventral stream processing essentially unyokes our movements from the immediate incoming visual information and provides the possibility of top-down, selective modification of the locally competitive processes governing the dorsal stream processing of visual information. It just so happens that an eventual byproduct of that evolutionary innovation is the ability to experience the visual signal as a unified scene, rich with meaningful categories.

Since the time that this ethologically inspired view of the dual visual processing streams was first published, it has become clear that the primate dorsal visual processing stream consists of a stunning mosaic of reference-frame- and effector-specific sub-streams that allow for an unparalleled degree of precision and flexibility in the visually guided control of eye and limb movements (Goodale & Milner, 2013). Indeed, the fecundity of the dual streams framework has been demonstrated over the past 20 years, as it has spawned countless studies and profoundly influenced the way we think about the cortical processing of sensory signals. It is an instructive example of the importance of the ethological approach.

1.1.2 Numerosity and salience

It is perhaps no coincidence that the only exclusively carnivorous primate, the tarsier (family *Tarsiidae*), has remarkably large eyes that are as big as its entire brain. The tarsier hunts at night, and it uses its acute vision to locate, leap toward, and grasp its prey (e.g., insects, small birds, bats), often in mid-air. The speed and accuracy necessary to accomplish this feat are mediated by a visuomotor system that is finely tuned for guidance through fast visual feedback (Wong, Collins, & Kaas, 2010). Across the entire animal kingdom, there are many species that, like the tarsier, rely upon fast, visually guided limb movements for their survival. In spite of this, relatively little is known about this behavior as distinguished from slower, less urgent limb movements that, while more frequent, play a different role in the survival of the animal.

Tarsiers and other predators are notable because of the speed and precision of their movements, but even more impressive is the fact that they often perform these movements in conditions of high uncertainty and urgency. For example, a cheetah pursuing a herd of gazelle must track multiple targets simultaneously until one is within reach or the cost of not committing becomes too high, all while reacting to obstacles in the terrain. Of course, many of the same things can be said of the prey that must rely upon the same behaviours to escape from predators. In the case of humans, flexible intelligence has considerably reduced our dependence upon fast, precise movements toward multiple targets. And yet this behavior, a gift from our evolutionary ancestors, persists in activities like hand-to-hand combat, sports, and even something as modern as the avoidance of high-speed traffic collisions. Again, this highlights an important and yet relatively ignored class of limb movements: those that are fast, urgent, and directed toward multiple potential targets.

The primate visual system evolved to give considerable priority to stimuli with features that differ from their background or context. As will be demonstrated throughout the course of this thesis, this conspicuity affects movements most

profoundly during a short period immediately after we first see them. Indeed, it is often the case that involuntary, coordinated muscle responses are elicited by sufficiently salient stimuli. Such a feature makes sense: the ubiquitous evolutionary phenomenon of camouflage is testament to the frequency with which visual salience and relevance for survival tend to overlap. For an animal constantly on the lookout for predators, the small cost of many false positives is greatly outweighed by the ultimate cost of a single false negative (i.e., becoming something else's lunch).

This overlap between bottom-up salience (i.e., conspicuous visual event) and top-down relevance (i.e., whether the visual event is something dangerous) is a key feature of salience map models, which assume a final, central topographical map that combines salience information from many feature-specific maps (Bisley & Goldberg, 2010; Fecteau & Munoz, 2006; C. Koch & Ullman, 1985). The computational strategy of combining top-down and bottom-up priority information into one common neural currency necessarily leads to states of the priority map where it is impossible to distinguish between something shiny and something that has life or death consequences.

The research presented in this thesis is focused upon this unique subset of reaching movements: those that involve fast, often involuntary deviations toward salient stimuli, primarily in situations with many simultaneous stimuli that are potential targets. Hopefully, approaching this behavior from an ethological perspective helps make it clear that this phenomenon (i.e., the fact that salient stimuli exert such a strong influence over our behavior) is something more than just a bug in the system. It is a fundamental behavior that was selected by evolutionary pressures because it increased (or did not decrease) the survival rates of those organisms in which the mutation first appeared.

1.2 Affordance competition

The visual system is arguably one of the most-studied and best understood topics in behavioral and systems neuroscience. The fact that there is still so

much that we do not understand about it (especially in primates) is a testament to the rich complexity of this system. There are still some basic questions that have not been answered. For example, what is the mechanism by which the individual objects in our visual surroundings are parsed and categorized in terms of priority for action? Currently, the most successful hypothesis is that a topographic map incorporates many features of a visual stimulus, from bottom-up feature contrast to top-down feature search relevance, into a common (although perhaps distributed) map, often called a salience map (Itti, Koch, & Niebur, 1998) or a priority map (Bisley & Goldberg, 2010; Fecteau & Munoz, 2006). This unified representation of the processing priority of the objects in visual space determines the probability that the next movement will be directed to the corresponding location.

An ethological extension of this hypothesis comes from Cisek and Kalaska, who emphasize the fact that the majority of our interactions with the world involve a multiplicity of possibilities for action, at any given moment (see Figure 1.1). The classic evidence for this view comes from a study in which monkeys were briefly presented with two differently colored spatial cues (Cisek & Kalaska, 2005). The monkeys then waited for a few seconds until the fixation spot changed into one of the target colors, signaling to the monkey which of the initial stimuli was the final target. They recorded from cells in dorsal premotor cortex (PMd). The population response is depicted in Figure 1.1 A. Upon presentation of the initial stimuli, two distinct populations (each with a roughly Gaussian distribution of tuning to the respective stimuli) of cells became active and persisted simultaneously until the presentation of the color cue. Following this, cells preferring the cued location showed a sharp and persistent rise in activity, while cells preferring the non-cued location were suppressed.

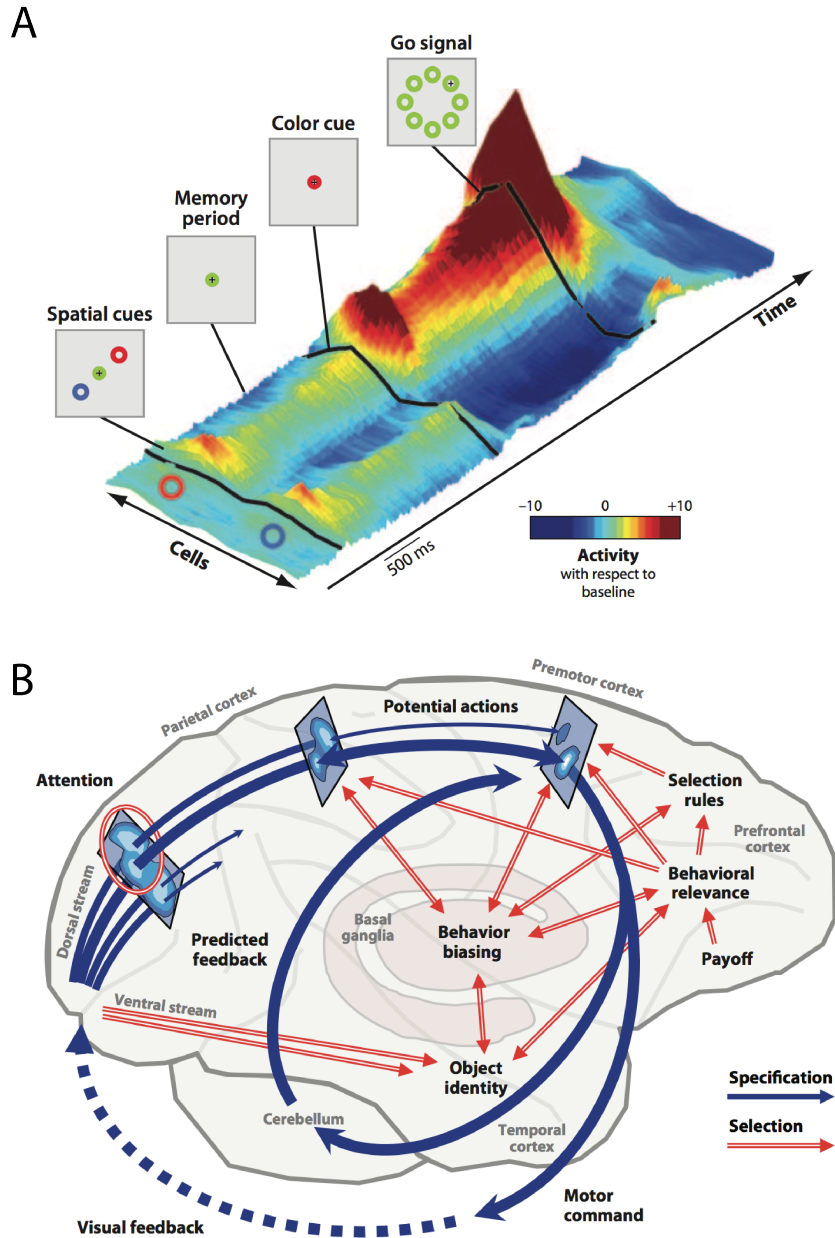


Figure 1.1 Competition between potential actions. A, Population activity, over time, in dorsal premotor cortex during a delayed reach-selection task. Cells (on the ordinate axis) are sorted according to spatial tuning. B, A sketch of the affordance competition hypothesis. Blue arrows represent action specification processes. Red arrows represent selection processes in the form of biasing signals from basal ganglia and prefrontal cortical regions. Taken from Cisek and Kalaska (2010).

Similar dynamics had already been observed in the ventral stream (Desimone, 1998) and have since been replicated in the dorsal stream (Baldauf, Cui, & Andersen, 2008; Pastor-Bernier & Cisek, 2011). Essentially, these studies imply that the specification of potential actions occurs in parallel throughout the sensorimotor continuum. The operations of the dorsal stream upon the incoming visual signal are best characterized as extracting the possibilities for action available within the signal (Tipper, Howard, & Houghton, 1998; 2000). These possibilities for action, sometimes referred to as affordances (Cisek, 2007; Cisek & Kalaska, 2010), compete with each other for further processing until bottom-up or top-down mechanisms bias the competition enough that one of the potential actions wins out. This is a high-level description of what the brain is doing, and is in no way meant to replace the lower-level descriptions of the sensorimotor transformation. For example, when monkeys try to discriminate the dominant direction of a field of moving dots and report their decision with a saccade to the appropriate target, neurons in middle temporal cortex (MT) represent the constant quality of information for the various alternatives (i.e., the conspicuity of the motion in a given direction) and neurons in lateral intraparietal cortex (LIP) integrate the signal from MT over time until enough evidence has been collected and the cells preferring one of the alternatives have reached a firing threshold, at which point the saccade is executed (Churchland, Kiani, & Shadlen, 2008; Gold & Shadlen, 2007). These sensorimotor decision-making mechanisms have been described in great detail, and it does not diminish the descriptions at this lower level to also assert that these mechanisms are engaged in the process of extracting possible actions from the visual signal (Furman & Wang, 2008).

For reasons of simplicity (and conformity), from this point forward I will refer to this map of potential actions as the salience map or priority map. One fascinating question about the functioning of these maps concerns how they are finally transformed into a final movement vector. This “readout stage” is poorly understood in the eye movement literature, and has hardly been touched in the reaching literature. In the next section, I will spend some time discussing the literature on curved and averaged trajectories. The motivation for this should be

immediately apparent: averaged trajectories occur because the readout mechanism was applied prior to the competition between actions being resolved in the priority map. As such, they provide a unique opportunity to dissect the computations involved in the final stages of sensorimotor processing.

1.2.1 Curved and averaged trajectories

The study of involuntary deviations of goal-directed movements in the presence of distractors and/or multiple targets, despite being around for some time now (Yarbus, 1967), is still a vibrant and growing field. The ongoing fascination with these behavioral phenomena derives from the assumption that they tell us something important about the underlying neural processes; that they provide a readout, of sorts, of the sensorimotor system in an instructive boundary condition.

Trajectory curvature typically occurs during short-latency responses (Van der Stigchel, Meeter, & Theeuwes, 2006). In fact, there is a limited time (~200 ms) following stimulus presentation during which the trajectory will deviate toward a distractor (Welsh & Elliot, 2004; Welsh, Neyedli, & Tremblay, 2013). After this period, there is often a deviation away from the distractor, in both arm and eye movements (C. S. Chapman & Goodale, 2008). In keeping with the overarching goals of this thesis, I will focus my remarks on the early stages of that continuum, where low-latency responses are drawn toward the distractor or competing target.

1.2.1.1 Eye movements

When saccades are performed to targets in the presence of nearby distractors, in the context of a visual search, or in a double-step task, the result is often an averaged trajectory (i.e., the endpoint lands between two stimuli). This phenomenon, often referred to as the “global effect”, is related to the more common but less dramatic phenomenon of saccade curvature, where the

endpoint of the saccade lands on an actual stimulus, but not before curving toward another stimulus.

Before quickly moving on to mechanisms, I will briefly touch upon a highly relevant behavioral study. In an effort to quantify just how global the global effect actually is, Van der Stigchel and Nijboer (2013) parametrically manipulated the angular distance between a target and a distractor. They found that angular distances below 35 to 40° elicited a unimodal distribution of saccade endpoints, with the peak of the distribution directly between the two distinct locations of target and distractor. For 45° separations and greater, the resulting distributions were increasingly bimodal. The boundary between unimodality and bimodality, however, was fuzzy; as angular distance increased, there was a linear decrease in the number of saccade endpoints that ended up between the two stimuli. This linear decrease in the probability of the global effect is consistent with classic surround mechanisms that increasingly inhibit cells with increasingly distant spatial preferences—a hallmark of lateral inhibition.

The purely behavioral literature on saccadic averaging is vast and daunting, with applications spanning across multiple disciplines. Since this thesis is primarily concerned with reaching movements, the primary reason for discussing eye movements here is that the neural mechanisms governing saccadic averaging are far better understood than those governing reaching trajectory averaging. Accordingly, I will focus upon the latest developments in the search for those mechanisms in the oculomotor literature.

Trajectory averaging and curvature are thought to reflect the state of a population code found in a priority map at the time of the readout stage (Tipper et al., 2000). While the vast majority of mathematically elaborated priority map models remain agnostic as to where such a map might be found, there have nonetheless been many proposals. For example, the priority map has been attributed to lateral intraparietal area, the frontal eye fields, area V4, and primary visual cortex (Kusunoki, Gottlieb, & Goldberg, 2000; Z. Li, 2002; Mazer & Gallant, 2003;

Thompson & Bichot, 2005), just to name a few. One possibility is that the priority map is distributed over many areas, with no single map performing a final integration of all other feature maps. At this point, it is not important to take a position on where the priority map might be. However, even if the priority map is distributed, it is still the case that the sensorimotor circuits have a beginning and an end. One of the areas closest to the end of the oculomotor pathway, and which also shows properties of a priority map, is the intermediate and deep layers of the superior colliculus (SC).

With regard to the role of SC in the programming of curved and averaged saccades, there are two main questions to ask:

1. Is SC the site at which separate spatial representations for the two targets (or target and distractor) are combined into a final movement vector?
2. Regardless of whether the final vector is coded in SC or somewhere downstream, what is the computation that transforms two separate vectors into one final vector?

The answer to the first question has been, for the most part, settled. Studies have consistently found that, even by the time the curved saccade has been initiated, there are still two discrete populations of activity. In one study, monkeys made saccades to one or two targets. On two-target trials where the saccade was averaged or curved, the spatial pattern of discharge was consistent with two separate visually indexed responses rather than one single perimotor response at an intermediate location (Edelman & Keller, 1998). In line with this, Port and Wurtz (Port & Wurtz, 2003) showed that it is the relative timing of the distinct activity peaks for different targets that determines the spatial and temporal profile of saccade curvature. Monkeys reached toward the first of two targets presented in rapid succession. In cases where the saccade trajectory deviated toward the first target but ultimately landed at the second target, the activity profile for cells that preferred the first target's location peaked earlier than the profile for cells preferring the second target. In cases where the trajectory landed at an averaged

position, the peaks for the two profiles overlapped temporally. A similar effect was reported by McPeck et al. (McPeck, Han, & Keller, 2003).

Another indirect demonstration that the final movement vector is encoded downstream of the SC comes from a study in which the order of operations for the decoding of SC activity was investigated. Two basic steps are necessary to transform SC activity into a saccade. First, the activity must be read out through vector averaging or summation. Second, there must be an exponential transformation from SC coordinates to visual coordinates (to reverse the logarithmic transformation inherent in the spatial organization of the map in SC). If the exponential transformation occurs prior to the vector summation, then the vector summation cannot be occurring within SC. By simultaneous microstimulation of two SC sites, Katnani and Gandhi (Katnani & Gandhi, 2011) found that the pattern of saccade endpoints was consistent with the model in which the exponential transformation occurred prior to vector summation. Thus, the balance of the empirical evidence is consistent with the “downstream hypothesis”; i.e., the encoding of final saccade vector direction occurs downstream of the SC.

The one exception to this, it seems, is a study by Glimcher and Sparks (Glimcher & Sparks, 1993) in which they observed increased activity at an intermediate location between two distinct locations of activity during averaged saccades. Edelman and Keller (1998) pointed out that Glimcher and Sparks found no significant statistical difference between spatial profiles of one and two-target saccade movement fields, and further suggested that any legitimate intermediate activity may have been a function of the task. The task involved making saccades to a target that was defined by color, which required the monkey to select one of the two targets. The activity at the intermediate location may have been the result of an upstream (e.g., frontal eye fields) error in target selection, and would thus be reflected in SC as a single movement vector to an erroneous location. This explanation has some interesting implications. If an upstream area is consistently making selection errors to a location in between two legitimate

locations, it suggests that vector averaging is taking place upstream. Given that competition exists at multiple levels of the visuomotor processing pathway, it is not out of the question that this could be the case. Indeed, it is consistent with recent suggestions that sensorimotor decisions are ultimately the product of a distributed consensus of competitive processes operating at multiple scales, from low-level feature contrast to relative reward valuations of the targets (Cisek, 2012).

Given the strong evidence for the downstream hypothesis, what is the computation that ultimately transforms two separate vectors into one final vector during curved saccades? A model of SC processing that accounts for saccade curvature was developed by Arai et al. (Arai & Keller, 2005). Based on the work of Hikosaka and Wurtz (Hikosaka & Wurtz, 1983a; 1983b; 1983c; 1983d), they show that broadly distributed inhibitory inputs to SC from the subthalamic nucleus pars reticulata (SNr) were able to produce physiologically realistic variability in saccade trajectories, including the type of modest curvature commonly observed in visual search tasks. However, in order to produce the strongly curved saccades that are occasionally observed, the model had to assume a separate, parallel input to the saccadic burst generators in the brainstem. Arai et al. propose that this parallel input could come from the caudal fastigial nucleus of the cerebellum.

A more recent (and more parsimonious) model comes from a series of studies, in which Goossens and van Opstal (Goossens & Van Opstal, 2006; 2012; Van Opstal & Goossens, 2008) have reported strong evidence for the dynamic ensemble coding hypothesis. This hypothesis essentially holds that saccadic burst generator cells in the paramedian pontine reticular formation (PPRF) receive and sum the vector contributions of descending SC projections, weighted by the spike rate at the synapse. Thus, the motor command that is ultimately sent to the eye is a dynamic population signal consisting of a weighted sum of all SC site-specific movement vector contributions. Two simultaneous peaks of activity in the SC would be summed by the burst generator cells and emerge as an

intermediate vector. This model is currently the most robust downstream model with respect to predicting the various behavioral features of saccades, including saccadic averaging and curvature.

At least one significant weakness of the dynamic ensemble coding hypothesis has been identified in the literature. Katnani et al. (Katnani, Van Opstal, & Gandhi, 2012) point out that, according to this hypothesis, the contributions of the individual SC cells should only be taken into account after a threshold is reached. This predicts that when low signal intensity of simultaneous stimuli results in low, sub-threshold activity in SC, the final saccade vector should resemble a linear addition of the two single-site vectors, in contrast to the weighted vector average that would be expected when SC activity is over threshold. Interestingly, Katnani et al. found that at both high and low stimulation intensities, the resulting saccade more closely resembled a weighted vector average. They conclude that the dynamic ensemble coding hypothesis requires an extra computational step that would enable the model to generate flexible categorization and competition processes that can scale their dynamics to the overall intensity of the incoming stimuli. They offer no strong hypotheses regarding what this mechanism might be. This will be addressed later, when we come to the discussion on the encoding of salience in the SC.

As I see it, another possible weakness of the dynamic ensemble coding hypothesis is that it has no straightforward way of accounting for the well-defined range of angular separation (between targets) within which saccadic averaging occurs (Van der Stigchel & Nijboer, 2013). Unless there is evidence of strong lateral interactions between cells in the PPRF (and I was unable to find any such evidence), there is no a priori or empirical reason why the burst generators would be unable to sum vectors from targets separated by, say, 70 degrees (i.e., well out of “global effect” range), and generate a saccade toward the midpoint of those two targets.

This turns out to be an interesting test of the dynamic ensemble coding hypothesis. By performing microstimulation within the pontine reticular formation (Cohen & Komatsuzaki, 1972; Keller, 1974; Sparks, 2002), one could first identify sites that result in eye movements separated by a given angular magnitude. Then, using dual-site stimulation, both sites could be stimulated simultaneously. By co-stimulating while parametrically varying the distance between landing locations for individual stimulation sites, it should be possible to identify the range of angular target separation within which saccadic averaging does or does not occur as a direct function of PPRF dynamics.

My prediction would be that such an experiment would yield averaged saccades across a much wider range than what is observed through natural sensory stimulation. This prediction is largely based upon the fact that the PPRF performs a constant linear integration of its inputs (Cohen & Komatsuzaki, 1972). If it is receiving signals from SC that are based upon widely separated activation peaks, it may be the case that, as far as the PPRF is concerned, the upper limits of target separation for averaged saccades are determined by the range of downstream ocular musculature that can generate forward movement during co-recruitment of agonist/antagonist pairs.

We are still faced with the fact that there are only two plausible explanations for the results of Van der Stigchel et al. (2013). Either the modulation occurs at the level of the SC or it occurs at the level of the PPRF. The former seems unlikely. Whether such modulation would be occurring through intrinsic, long-range inhibitory interconnections in SC (which likely do not exist, see Ozen, Helms, & Hall, 2004), or from inhibitory inputs from a possible third node in the critical circuit (which would have to possess the strong winner-take-all competitive dynamics that are not prevalent in SC), one would still expect to see stronger competitive dynamics in the SC than are typically observed. Specifically, one would not expect the frequent observation of discrete activation peaks separated by 40° or more (Edelman & Keller, 1998; McPeck et al., 2003; Port & Wurtz, 2003).

Thus, it may be the case that extra-collicular inputs into the PPRF gate and/or filter the incoming SC inputs if the angular separation between targets is too large. Candidates for this might include omnipause neurons (gating) or, as suggested by Arai et al. (2005), the caudal fastigial nucleus of the cerebellum (filtering).

1.2.1.2 Reaching

In terms of suggesting actual mechanisms for the phenomenon of trajectory curvature, the reaching literature is sparse. A general mechanism is described by Tipper et al. (2000). An on-center, off-surround organization among topographically organized and directionally selective cells creates the dynamics necessary to account for deviations toward distractors. This is the same lateral inhibition mechanism that is assumed to play a role in many of the more competitive nodes within the oculomotor path. What we get from Tipper et al., however, is not much more than a descriptive model.

At least one computational model directly addresses the question of how (and possibly where) multiple potential reach targets are encoded. Cisek (Cisek, 2006) developed a model of the parieto-frontal circuit that mediates the planning and control of goal-directed reaching. The model consisted of 7 layers of leaky-integrator neurons, with the 7 layers corresponding to the following areas: posterior parietal cortex (PPC), 2 layers of prefrontal cortex (PFC) corresponding to two color cues given in the task, 3 layers of dorsal premotor cortex (PMd) to simulate a rostro-caudal gradient of activity, and primary motor cortex (M1). The PPC, PMd, and M1 layers all contain lateral inhibition to varying degrees, and thus they possess many of the properties described by Tipper et al. (2000). Cisek used this model to simulate the task from his 2004 study with John Kalaska, described above.

One of the key features of the model is that PMd is the last area in the processing chain to show distinct, simultaneous peaks of activation. Area PMd feeds directly into M1, where intensely competitive lateral interactions rule out the

possibility of multiple peaks. In essence, the dynamics of M1 force the system to make a selection. Moreover, reciprocal connections with PMd can apply those same dynamics to force PMd to make a selection if things are taking too long (i.e., if the go cue has been given and a decision has still not been made).

In one of the simulations of Cisek's model, the go cue is presented just 20 ms after the color cue (which identifies one of the two previously presented targets as the final target), with targets either near or far from each other. When the targets are far from each other in this urgent condition, the winner-take-all dynamic introduced by feedback from M1 causes the peak with the highest activity to be selected. Since the 20 ms of processing time is insufficient to overcome the influence of random noise in the system, the wrong target is selected nearly half the time. When the targets are near each other, however, the outer tails of the two distributions in PMd get suppressed, while the overlapping portions of the two populations mutually facilitate each other, resulting in an intermediate peak in PMd. Thus, in response to the question of whether or not the final movement vector is actually encoded in a map somewhere, Cisek answers in the affirmative. There has been no electrophysiological confirmation of this hypothesis, as of yet.

1.2.2 Compelled response paradigms

It is a familiar trope in old Western movies. A cowboy walks into a saloon, struts over to a poker table, and accuses a shady character of cheating his tragically impulsive, but ultimately well-meaning younger brother out of his inheritance. Insults are exchanged. The cowboy kicks over the poker table, draws his pistol, and utters the dreaded words: "Dance, varmint." At this point, the poker cheat is faced with an embarrassing and slightly dangerous problem—a problem that, in various forms, has fascinated neuroscientists for years. He must execute a movement before he has all the information about what the right movement is. Given the speed with which the cowboy can modify the direction of the bullet, and given the speed of the actual bullet, the cheat has no way of knowing what

the final location of each bullet will be. At the same time, he cannot afford to stand still, or he risks being hit by one of the bullets. Socially, the resulting behavior is a humiliating display of hopping around while the cowboy hoots and hollers. Scientifically, the resulting behavior tells us something important about how the brain transforms visual information into action.

The “dance, varmint” scenario is an example of a compelled response paradigm. This, in essence, was the paradigm emulated by Cisek’s model when the go-cue was placed just 20 ms after the informative color cue. The system lacked the processing time necessary for a smooth relaxation into one or the other response, so it was forced to either select one of the targets at random (if the targets were far apart) or create an intermediate vector between them (if the targets were close together). This pattern of results closely resembles the results found in (at least) two studies. The first, from the saccade literature, we already encountered. Van der Stigchel and Nijboer (2013) showed that saccade endpoints formed a unimodal distribution between the two target locations when they were close together. As the targets grew further apart, the distribution become increasingly bimodal.

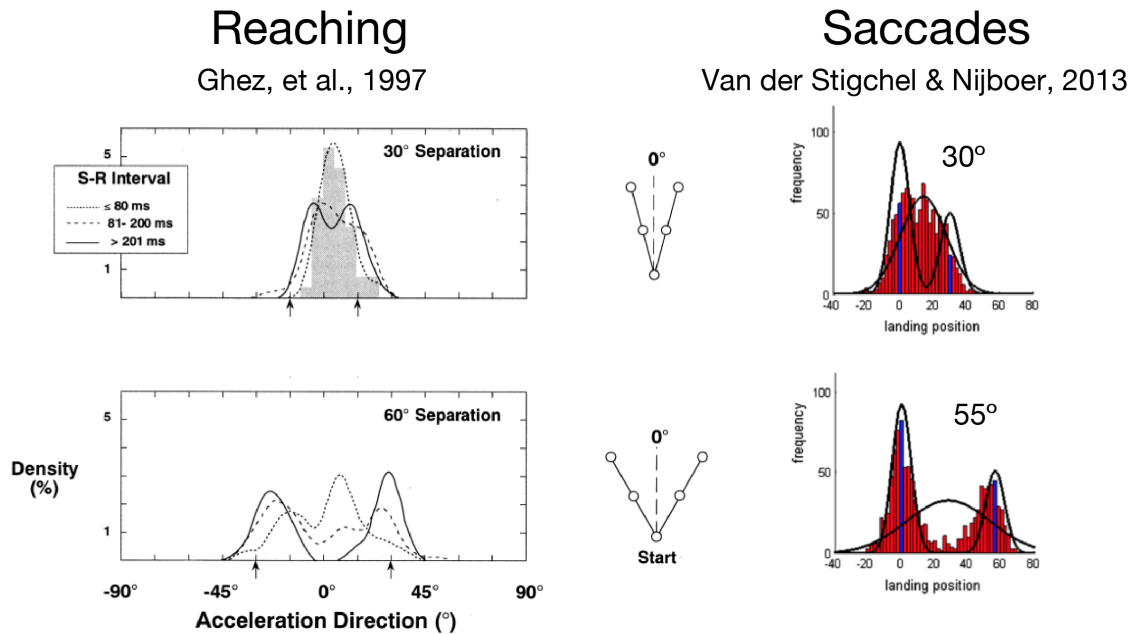


Figure 1.2 Comparison of initial trajectory distributions from reaching and saccade performance for two target separation magnitudes. Modified from Ghez, et al., 1997 and Van der Stigchel & Nijboer, 2013.

The second study that reported this same pattern of results was a reaching study that employed the compelled response paradigm. Ghez et al. (1997) presented single reach targets selected from a pair of targets divided by varying degrees of angular separation. Critically, the target only appeared between 400 and 0 ms before the last of four rhythmically spaced beeps. The last beep served as the cue to initiate the reach (i.e., reaches were to start at the same time as the cue). Thus, there were some trials where there was plenty of time to see the target and plan an appropriate reach vector. However, as the interval between target onset and the fourth tone grew shorter, there was an increase in the probability that the reach would have to be initiated with insufficient information. Indeed, on many trials, the reach was merely a guess, given that no target had yet appeared.

Interestingly, the pattern of results was highly similar to that of Van der Stigchel and Nijboer (Figure 1.2). Ghez et al. measured the lateral position of the hand at

the time of peak acceleration. The distribution of lateral positions was unimodal for target separations under ~45 degrees. For larger target separations, distributions were bimodal.

In light of the differences between the proposed mechanisms for mediating averaged trajectories in arm and eye movements, the similarities between the empirical findings of Van der Stigchel et al. and Ghez et al., along with the implications of Cisek's model, are striking. Such similarities speak to the possibility of shared mechanisms, if not shared pathways, in the reading out of population codes during reflexive movements toward multiple stimuli. Given the fairly robust performance of oculomotor models that are far more committed to specific biological implementations in mapped out circuits, any hope of specifying points of convergence between the oculomotor and skeletomotor the burden of proof is on the side of skeletomotor models when it comes to resolving discrepancy.

1.2.2.1 Reaching to multiple targets

We have argued that one way of behaviorally sampling the state of the priority map (or, more broadly, the parallel representation of targets in the visuomotor system) during a state of unresolved competition is by way of a compelled response paradigm involving reaches to multiple potential targets, all of which have an equal probability of becoming the final target (C. S. Chapman, Gallivan, Wood, Milne, Culham, & Goodale, 2010a; 2010b; Gallivan et al., 2011; Milne et al., 2013). In this paradigm, the final target is selected from the array of potential targets, but this final target appears only after a reach has been initiated. By imposing strict RT and movement time constraints upon the movements, we create a situation where the participants must plan and initiate a reach vector based upon the only information available at the time: the numerosity and spatial distribution of the targets. Consistently, initial trajectories in this paradigm are directed toward the centre of gravity of the potential target display. If, for example, there are two targets on the left and two targets on the right,

trajectories will go directly up the middle, between the two targets, correcting to the final target at about 60% of the spatial extent of the reach. If there are 30% more targets on the left, the initial reach vector will be proportionally biased toward the left.

This paradigm is unique in the sense that, while most tasks involve a distractor (or multiple distractors) that must be inhibited in order to successfully perform the task, the multiple target pointing task requires that all stimuli on the screen be treated as targets. It is a task that is designed to provide a glimpse into the unresolved competition between multiple targets for action within the priority map.

The studies presented in chapters 2 and 3 of the present thesis make use of this paradigm. Specifically, they explore a set of predictions that flow from one important theoretical nuance in the priority map account: at any given time, the firing rate of a given cell in the priority map is a dynamically weighted function of the bottom-up and top-down features of the stimulus within its receptive field. For example, if a stimulus is a potentially rewarding target, that top-down feature will result in stronger activity. If a stimulus has a high luminance contrast ratio, that bottom-up feature will also result in stronger activity. And while bottom-up and top-down facilitation follow different temporal profiles (Schütz, Trommershäuser, & Gegenfurtner, 2012), there will be times when the respective contributions of the two will be impossible to pin down. The result of this is that the encoding of stimulus conspicuity is indistinguishable, at times, from the encoding of reward likelihood associated with the stimulus. The clear prediction that follows from this is that, all other things being equal, potential targets with high luminance contrast should be given more weight in the priority map than targets with low luminance contrast, despite their equal value. In the multiple target pointing task, this should result in trajectories being heavily biased toward high-contrast stimuli, even when there is a greater number of low-contrast stimuli on the other side of the display.

1.3 Saliency

Computational models of natural scene processing can predict, with a relatively high degree of success, which parts of the scene are most likely to elicit ocular fixations (Itti & Koch, 2001; Torralba, 2003). Among the most successful of these models are those that assume a unified topographical map that describes the saliency landscape of a visual scene by combining saliency information from multiple feature-specific maps (Itti et al., 1998). The most active location on this saliency map denotes the location of the most salient object and, consequently, the location toward which attention and eye movements should be directed. In order to emphasize that such a map would also incorporate top-down inputs carrying information about goals and stimulus value, some have suggested that priority, rather than saliency, is the more accurate description of what the map encodes (Bisley & Goldberg, 2010; Fecteau & Munoz, 2006). For the purposes of this thesis, however, I will be limiting myself to a discussion of the manipulation that was used in the original research that I will present: differences in bottom-up saliency.

1.3.1 Bottom-up saliency in the oculomotor network

1.3.1.1 In humans

A good portion of the studies that have investigated bottom-up saliency in the human brain have been behavioral. Trajectory averaging in response to salient stimuli has been demonstrated before (Bonin, Mante, & Carandini, 2005; Deubel, Wolf, & Hauske, 1984), typically in response to distractors (Busse, Wade, & Carandini, 2009; Dombrowe, Olivers, & Donk, 2010; Donk & Soesman, 2010; Donk & van Zoest, 2008; van Zoest, Donk, & Van der Stigchel, 2012). These latter studies all share a common empirical result: that saliency typically exerts a capturing influence on movements until ~250 ms after stimulus presentation.

In terms of mechanisms, we know that there is a logarithmic response function for visual contrast (Bell, Meredith, Van Opstal, & Munoz, 2006; Heeger, Huk,

Geisler, & Albrecht, 2000; X. Li & Basso, 2008; Marino et al., 2012) in various circuits throughout the brain. This response function is the result of divisive normalization (Carandini & Heeger, 2012; Heeger, 1992; White & Munoz, 2011), a fundamental neural operation that has been observed at nearly every major way station of the visual pathway, including the retina (Demb, 2002), lateral geniculate nucleus (Bonin et al., 2005; Port & Wurtz, 2003), primary visual cortex (Busse et al., 2009; Martin, 1982), and parietal cortex (Knudsen, 2011; Louie, Grattan, & Glimcher, 2011). Schneider and Kastner (Schneider & Kastner, 2005) attempted to characterize the contrast response function in human SC using fMRI. What they saw was broadly consistent with a logarithmic contrast function. Interestingly, they interpreted the small change in signal intensity in response to the shift from 25% to 100% contrast (which would be expected if the rate of rise in intensity is logarithmic) as evidence that the SC was indifferent to luminance contrast.

1.3.1.2 In non-human primates

In line with the emphasis placed upon the SC during my discussion of saccadic averaging in monkeys, I will also focus my remarks here on the role of the SC in the encoding of salience. Electrophysiological studies on the salience response in SC have primarily focused on the mechanisms responsible for the hastening of saccadic reaction times in the presence of high contrast stimuli. For example, SC visual responses increase in magnitude and decrease in latency as the luminance contrast of a visual stimulus increases (Bell et al., 2006; X. Li & Basso, 2008; Marino et al., 2012). These modulations of the timing and intensity of SC visual responses, in turn, predict the timing and metrics of saccades. The faster and more intense the visual response, the faster the initiation of the saccade. There is evidence that the mechanism responsible for triggering a saccade in response to incoming luminance contrast information is distinct from the mechanism that triggers saccades after a discrimination (e.g., between two different colors) has been made (White & Munoz, 2011).

To my knowledge, there have been no studies that have examined SC activity when a saccade trajectory is averaged or deviated precisely because of a luminance contrast difference. However, given that luminance contrast differences lead to latency differences between visual responses (Bell et al., 2006; X. Li & Basso, 2008; Marino et al., 2012), and given that timing differences between firing profiles for simultaneous stimuli result in curved saccades (Port & Wurtz, 2003), it is not difficult to predict what the outcome of such a study would be.

1.3.1.3 In barn owls

At first glance, the barn owl seems an odd choice to study the encoding of salience in the oculomotor system; barn owls, to put it plainly, cannot move their eyes. Rather, their uniquely flexible neck can rotate the head nearly 270 degrees. In general, owls have abnormally large retinal surfaces that increase the amount of information available. The downstream integration of retinal signals is specially tuned to extract spatial information from the nocturnal luminance range (Martin, 1982). The high spatial resolution and sensitivity to luminance differences across a wide range make the visual system of the barn owl an ideal preparation to investigate how incoming visual stimuli are categorized in terms of their bottom-up salience. This is especially true given that the superior colliculus (i.e., the optic tectum in non-mammals) and other nearby midbrain structures have been preserved across vertebrate evolution (Knudsen, 2011).

In response to a single stimulus, cells in the barn owl optic tectum (OTid: intermediate and deep layers) display a very weak version of the typical properties of a classical centre surround inhibition, with inhibition profiles that gradually roll off in strength with increasing distance from the site of activity. However, when multiple stimuli are presented simultaneously, there is a global inhibition of all sites other than the most active location on the map (Mysore, Asadollahi, & Knudsen, 2010). This has the effect of quickly and flexibly selecting the most salient stimulus for further processing. These dynamics within the OTid

can be explained by the concerted effects of two nearby structures: the nucleus isthmi pars magnocellularis (Imc) and pars parvocellularis (Ipc).

The Ipc and Imc are reciprocally connected with the OTid. The Ipc sends back cholinergic, excitatory projections. The Imc, in contrast, sends back GABAergic, inhibitory projections. In Ipc, when multiple stimuli of varying salience (e.g., looming discs expanding at different speeds) were presented, the cells displayed a switch-like property. There was an abrupt drop in signal strength as soon as the disc in the receptive field ceased to be the most conspicuous stimulus in the display (Asadollahi, Mysore, & Knudsen, 2010). These switch-like properties suggest that Ipc coded relative stimulus strength and facilitated processing of salient stimuli with its selective excitatory feedback to OTid.

Mysore et al. (2012) suggest that lateral inhibitory connections aren't sufficient to mediate flexible categorization of salience among stimuli in a salience map, contra Lee et al. (1999) and Cisek (2006). They point out that if the overall magnitude of competing stimuli changes, lateral inhibition (including feedforward lateral inhibition) is unable to accommodate the requisite shift in the boundary for categorization of stimulus strengths. Interestingly, variable overall magnitude of the competing stimuli is the condition that the dynamic ensemble coding hypothesis couldn't account for, adding to the evidence that the SC and burst generators are insufficient to carry out this operation on their own.

In support of this assertion, Mysore et al. (2013) showed that focal, reversible inactivation of Imc results in the abolishment of competitive interactions within the intermediate and deep layers of the optic tectum. This is consistent with the idea that, without the reciprocal inhibition supplied by the Imc, the innate, local selection mechanisms of the OT are not sufficient to mediate competitive dynamics between multiple sites of activation.

This series of elegant studies from Knudsen and colleagues clearly identifies mechanisms in the avian midbrain that are able to flexibly and effectively mediate the competition between visual stimuli on the basis of their physical features. To

my knowledge, this is the only example of a salience or priority map that has actually been pinned down to the level of a circuit mechanism in a specific biological implementation. As such, and in spite of the fact that it was discovered in barn owls, it is a provocative finding in the context of the primate oculomotor system. While primate homologues for the itesm complex have been proposed (e.g., *Imc::periparabigeminal lateral tegmental nucleus*, *lpc::parabigeminal nucleus*; see Knudsen, 2011), there is little evidence, as of yet, that these areas play a similar role in the selection and categorization of salient stimuli in the primate SC. For the purposes of this thesis, one interesting and glaring gap between the owl and the primate tectal circuits is that the owl OT seems to have stronger winner-take-all dynamics than the primate SC. There have been no reports of “averaging” (in this case, of the head trajectory) with correlated persistent peaks of activity in the OT. It seems likely that this discrepancy is due to the global, rather than classical inhibition of the OT map outside of the location of the most salient stimulus. This dynamic is not observed in the primate SC in response to natural stimuli. On the other hand, the lack of such data may simply be due to fact that nobody has asked the right question, but it is nonetheless a curious missing link in the homological chain between these two structures.

1.3.2 Bottom-up salience in the skeletomotor network

To my knowledge, there have been no electrophysiological investigations into the role of bottom-up salience in the programming of reaches. In terms of behavioral approaches, it is a relatively common finding that trajectories toward oddball targets in search tasks consistently show deviations toward other targets in the array (Song & Nakayama, 2007; 2008). Similarly, trajectories will deviate toward a single, salient distractor (Kerzel & Schönhammer, 2013), but participants can learn to suppress such deviations if the target and distractor are sufficiently dissimilar and are presented in blocked sequences (Welsh, 2011). One unique study showed that reaches in a modified Simon task consistently deviated toward the stimulus onset, even if the color of that stimulus instructed the reach to go to the other side of the display (Buetti & Kerzel, 2009).

In all of the studies cited so far, however, it is important to note that the effect of the salience of a distractor on reach trajectories is impossible to disentangle from the effect of the mere presence of a distractor. This is especially troublesome in light of recent evidence that attentional capture occurs even in situations where the distractor is less salient than the target (Zehetleitner, Koch, Goschy, & Müller, 2013).

One important contribution comes from Zehetleitner et al. (2011), who showed that reaching and search tasks were similarly influenced by various manipulations of salience, including luminance contrast. From the similarity of the effects on the reaching and visual search performance, they argued that the priority map is shared between the oculomotor and skeletomotor systems. This is indirect, but provocative evidence that agrees with some of the findings already discussed above, including the striking similarity between target separation ranges within which averaged trajectories (for both reaches and saccades) tend to occur most frequently.

1.4 Thesis Objectives and General Overview

The overarching goal of the work presented in this thesis was to investigate how low-level visual differences between competing or singleton visual stimuli influence the programming and execution of reaching movements. I approached this question primarily through behavioural approaches. In each of the studies reported here, the kinematics of the reaching movements were recorded and analyzed. In Chapter 4, I also recorded chest muscle activity with intramuscular electromyography (EMG) while participants performed a reaching task. In each of the studies presented here, salience was operationally defined as the luminance contrast of targets with their background. In Chapters 2 and 3, where there were multiple targets with different contrast values, salience specifically refers to the relative contrast value of the highest contrast target (e.g., when the low-contrast target has a particularly low contrast value, it makes the high contrast target even

more salient). In Chapter 4, since there was only ever one target on the screen, salience is co-extensive with luminance contrast.

The first objective was to test the hypothesis that salience differences between stimuli introduce temporary biases into the competition between multiple potential actions. One prediction generated by this hypothesis is that compelled reaches toward arrays of potential targets would deviate toward targets that were more visually salient, and that introducing a delay between stimulus onset and the go-cue would diminish or eradicate this bias. The results reported in Chapter 2 supported these predictions, revealing that spatially averaged trajectories (toward an array of potential targets) are biased toward salient stimuli, even when there are twice as many targets (and therefore twice the likelihood of the final target appearing) on the other side of the display. After a 500 ms delay, initial trajectories were once again tuned to a spatial average of potential target locations.

The second objective was to characterize, in fine temporal detail, the transition from a salience bias during immediate responses to a traditional spatially averaged response after a delay. By building off of the findings reported in Chapter 2, I hoped to quantify the interaction between target salience and target numerosity as these two variables were dynamically reweighted in the parameterization of reach trajectories over a wide range of response delays. In Chapter 3, it was demonstrated that salience exerts a strong bias that overpowers the bias of numerosity at early latencies, after which it logarithmically decays and settles into a small, but still significant bias after a 450 ms delay. Numerosity was slower to exert an influence on the reach, but that influence remained constant over the course of 450 ms. Another fascinating outcome of the research presented in Chapter 3 was that individual differences in visual processing speed (as measured by a speeded enumeration task) predicted the degree to which salience targets biased reach trajectories, suggesting that the speed and the gain of transient salience representations during visuomotor processing are likely redundant in terms of the information they transmit.

The third objective was to conduct a test of the hypothesis that stimulus-locked activity in upper limb muscles during reaching is sensitive to the low-level features (e.g., luminance contrast) of the reach target. The results presented in Chapter 4 provided strong support for this hypothesis. Stimulus-locked activity appeared sooner, and with a greater magnitude, when stimulus contrast was higher. Further testing revealed that stimulus-locked activity can be evoked by a delayed, spatially uninformative cue to move.

Chapter 2: Visual salience dominates early visuomotor competition in reaching behaviour

2.1 Abstract

In this study, we investigated whether visual salience influences the competition between potential targets during reach planning. Participants initiated rapid pointing movements toward multiple potential targets, with the final target being cued only after the reach was initiated. We manipulated visual salience by varying the luminance of potential targets. Across two separate experiments, we demonstrate that initial reach trajectories are directed toward more salient targets, even when there are twice as many targets (and therefore twice the likelihood of the final target appearing) on the opposite side of space. We also show that this salience bias is time-dependent, as evidenced by the return of spatially averaged reach trajectories when participants were given an additional 500 ms preview of the target display prior to the cue to move. This study shows both when and to what extent task-irrelevant luminance differences affect the planning of reaches to multiple potential targets.

2.2 Introduction

Goal-directed movements are typically performed within a complex, target-rich visual milieu. How does the human visuomotor system select from among so many competing targets and distractors? One possibility is that the visuomotor system constructs maps that encode the behavioural priority of the respective stimuli in the visual scene (Bisley & Goldberg, 2010; Fecteau & Munoz, 2006). In these priority maps, cells facilitate activity in other cells with similar processing preferences and inhibit activity in cells with different preferences. The net result is a landscape of competing neural populations, each representing a potential target for attention and/or action (Baldauf & Deubel, 2010; Cisek & Kalaska, 2005). Some have argued that the activity within priority maps not only represents the behavioural priority of stimuli, but also constitutes an ongoing elaboration of parallel motor plans for interacting with the respective stimuli (Cisek, 2007).

While the majority of evidence for the parallel encoding of multiple motor plans has come from monkey electrophysiology (Baldauf et al., 2008; Basso & Wurtz, 1997; Cisek & Kalaska, 2005; McPeck et al., 2003), support can also be found in a large body of behavioural work. For example, when a target and a distractor are positioned in close proximity, eye movements tend to initially deviate toward the distractor, resulting in a curved trajectory (Godijn & Theeuwes, 2002; Sailer, Eggert, Ditterich, Straube, & undefined author, 2002; Theeuwes, Kramer, & Hahn, 1998; Van der Stigchel et al., 2006). Similarly, in reaching behaviour, this 'spatial averaging' has been observed between target and distractor (Sailer et al., 2002; Song & Nakayama, 2008) and in response to probabilistic information about eventual target location (Hudson, Maloney, & Landy, 2007). Models of saccade generation explain this spatial averaging effect as the result of unresolved competition between possible targets in the priority map (McPeck et al., 2003; Port & Wurtz, 2003).

In a series of recent studies, we set out to test a specific behavioural prediction arising from competition-based models of the spatial averaging effect; we predicted that if participants were forced to reach toward multiple potential targets, the unresolved competition between the potential targets would result in a spatial averaging of reach trajectories. In these studies, participants initiated rapid reaches toward multiple potential targets, all of which had an equal likelihood of being cued as the final target upon movement initiation. At movement onset, the final target was cued and participants corrected their reach trajectory in-flight to the cued location. Initial trajectories resembled a spatial average of individual trajectories toward all potential targets, reflecting biases from both the spatial location and number of potential targets on each side of space (C. S. Chapman, Gallivan, Wood, Milne, Culham, & Goodale, 2010a; 2010b; Gallivan et al., 2011). If, as we will argue, this paradigm allows researchers to get a real-time glimpse of an unresolved competition between *individual targets* represented in the priority map, then it could prove to be a useful, non-invasive technique for investigating the mechanisms of visuomotor decision-making in humans.

Note that the pattern of results described in the multiple target reaching (MTR) paradigm described above is consistent with any explanation based on the simultaneous encoding of multiple targets (and/or movement plans) within visuomotor planning networks. In other words, it leaves untouched the question of whether or not this type of processing is occurring in something like a priority map. Given that priority maps incorporate both cognitive and stimulus-driven inputs (Trappenberg, Dorris, Munoz, & Klein, 2001), and are especially modulated by stimulus salience (Findlay & Walker, 1999; C. Koch & Ullman, 1985), one should predict that the introduction of task-irrelevant luminance differences into an array of potential targets would result in the spatial averaging of reach trajectories being modulated and biased toward the high luminance targets. Indeed, there is evidence that the spatial averaging of saccades can be influenced by luminance differences (Deubel et al., 1984), but, to our knowledge, no one has investigated how task-irrelevant luminance differences in multiple

potential targets affect the planning of a reach to those targets. Thus, the present study utilizes the MTR paradigm to investigate the question of how the representation of visual salience in the priority map influences the evolution of competition between multiple potential targets for action.

To fully address the question of how salience influences the unfolding of visuomotor competition, it was necessary to probe the state of that competition at more than one time-point. This temporal aspect of the experimental design was also motivated by the finding that salience seems to exert only a transient effect upon visual selection (Theeuwes, 2010). For example, when reporting the location of the most salient singleton in a display, participants were most accurate at short response latencies and short presentation durations (Donk & van Zoest, 2008). In another study, when participants were asked to indicate the location of a probe, reaction times (RTs) were significantly faster when that location was previously occupied by a salient singleton than when it was occupied by a background stimulus. Importantly, this effect was observed only when the singleton display was presented for relatively short durations (e.g., 30-240 ms); by 480 ms, there was no RT difference (Dombrowe et al., 2010). Together, these studies suggest that there is an early and brief temporal window within which visual salience biases the competition for selection.

For the present study, therefore, we predicted that salience would overpower the spatial averaging effect when presentation durations were short, but that there would be no effect of salience (as evidenced by the return of spatial averaging) when presentation durations were relatively long. To test this, we manipulated the timing of the task such that some participants were required to begin their reaches immediately upon presentation of the potential targets, while others were required to wait 500 ms before being cued to begin their reach. Our results suggest that visual salience exerts a time-dependent bias upon the competition between multiple potential movement plans.

2.3 Experiment 1

2.3.1 Methods

Using OPTOTRAK (NDI, Waterloo), we recorded rapid reach movements (sampling the position of the right index finger at 150 Hz) in 22 right-handed subjects as they reached from a start button to a touch screen located 40 cm away (Figure 2.1A). Trials began with participants holding down the start button while fixating a cross at the center of the screen (for 1000 – 2000 ms). A beep signalled that the fixation cross had been replaced by a target display that consisted of one or two potential targets (hollow circles [2 cm diameter] of black pixels on a white background). This beep also served as a cue for subjects to initiate a reach toward the display (within 325 ms). It is important to note that fixation was no longer required after the target display replaced the fixation cross. Upon button-release, one of the targets in the initial display was cued (by filling in black) and subjects had to modify their trajectory in flight to that target location within 425 ms (Figure 2.1B). All targets in the display had an equal probability of filling in and becoming the final target. To encourage accurate performance, participants received trial-by-trial feedback on their fulfillment of the task's temporal and spatial constraints. There were four possible types of errors that caused the following text to be displayed: *Too Early* (if the start button was released before 100 ms had elapsed after the beep; this aborted the trial), *Time Out* (if the start button was not released within 325 ms; this also aborted the trial), *Too Slow* (if the screen was not touched within 425 ms of button-release) or *Miss* (if subjects did not touch within a 6 cm x 6 cm box centered on the target). *Good* was displayed on trials without errors. The timing constraints used in the present study have been used in past studies that employed a version of this task (C. S. Chapman, Gallivan, Wood, Milne, Culham, & Goodale, 2010a; 2010b; Gallivan et al., 2011). Participants performed an initial training session of at least 32 trials, followed by 160 test trials (across 10 blocks).

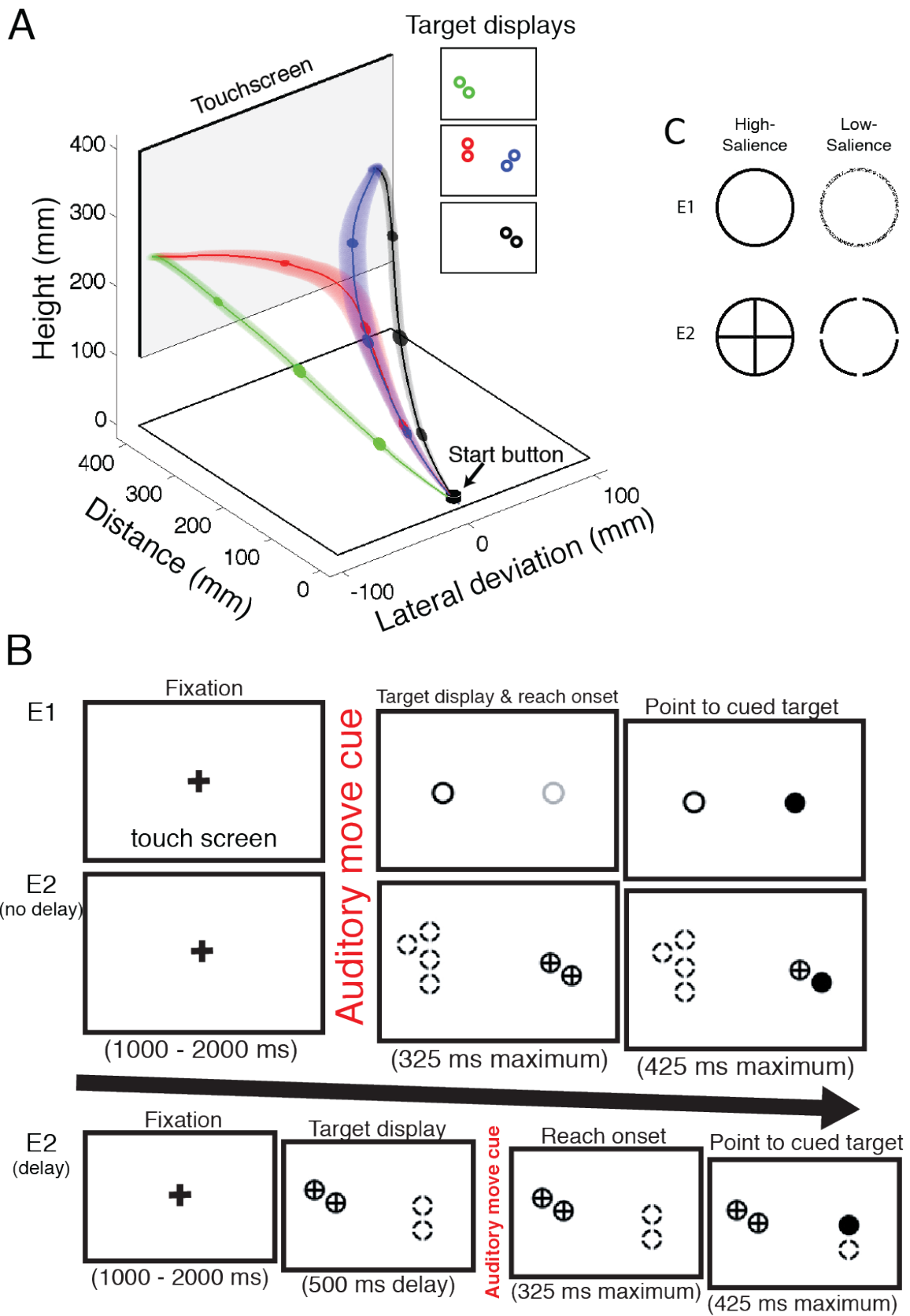


Figure 2.1 Illustration of the experimental setup and typical arm trajectories (A), the tasks (B), and the experimental stimuli (C). The three-dimensional view of the experimental setup (A) depicts reach trajectories for example target displays, averaged across 27 participants. The colour of the trajectory corresponds to the initial target displays (inset right) and, in the case where potential targets appeared on both sides of space (i.e., blue and red targets), the final target location. The shaded bands surrounding the trajectories represent average standard error. The size of the three darkened ovals is proportional to velocity in the x and y dimensions at 25%, 50%, and 75% of movement distance. Colours are for purposes of illustration only. (B) Following the presentation of a fixation cross for a random interval, potential targets were displayed on the left and/or right sides of a touch screen. In E1 and the E2 no-delay group, the appearance of the potential targets was accompanied by an auditory cue for the participants to release a start button and initiate reach with the index finger toward the target display within 325 ms. In the E2 delay group, the auditory cue to move came 500 ms after the initial target display had appeared. In every case, the appearance of the final target (indicated by one of the potential targets filling in black) was triggered by the release of the start button as participants initiated their reaches. Participants had to touch the final target within 425 ms after button release. As displayed in (C), targets in experiment 1 (E1: top row) consisted of black circles with contours of either 100% (high salience) or 50% (low salience) pixel concentration. In experiment 2 (E2), the high-salience target consisted of a black circle overlaid with a black cross, while the low-salience target consisted of a black circle with pixels removed where a cross would have intersected with the circle.

We manipulated the visual salience of the targets by varying the number of pixels contributing to the targets themselves (Figure 2.1C). High salience targets consisted of hollow, black circles (i.e., the line of the circle consisted of 100% black pixels). For the low salience targets (which were the same size as the high salience targets), we randomly replaced half of the black pixels of the circle with white pixels (the same colour as the background), thus yielding a stimulus with exactly half the contrast of the high salience target. The initial target display only ever consisted of one or two targets, with the two possible target locations being

in the same vertical plane and equidistant from the location of the central fixation cross, and separated by 18 cm.

Prior to statistical analysis, we removed trials with the slowest 5% of movement times (between subjects) as well as trials where participants missed the target. In order to be included in the final analysis, participants had to contribute at least four successful repetitions of each trial type across the experiment. After trial removal, 6 participants failed to meet this criterion and were excluded from analysis, leaving 16 of the original 22 participants for inclusion in the statistical analysis.

2.3.2 Results

We used repeated-measures functional ANOVAs (FANOVAs) to compare spatially normalized (in the Y dimension) trajectories across conditions of interest (Ramsay & Silverman, 2005). This technique allows one to examine both where and to what extent trajectories are statistically different within a given dimension (here we used deviation in the X dimension). Please see our previous work (C. S. Chapman, Gallivan, Wood, Milne, Culham, & Goodale, 2010a; 2010b; Gallivan et al., 2011) for a more detailed description of this analysis technique.

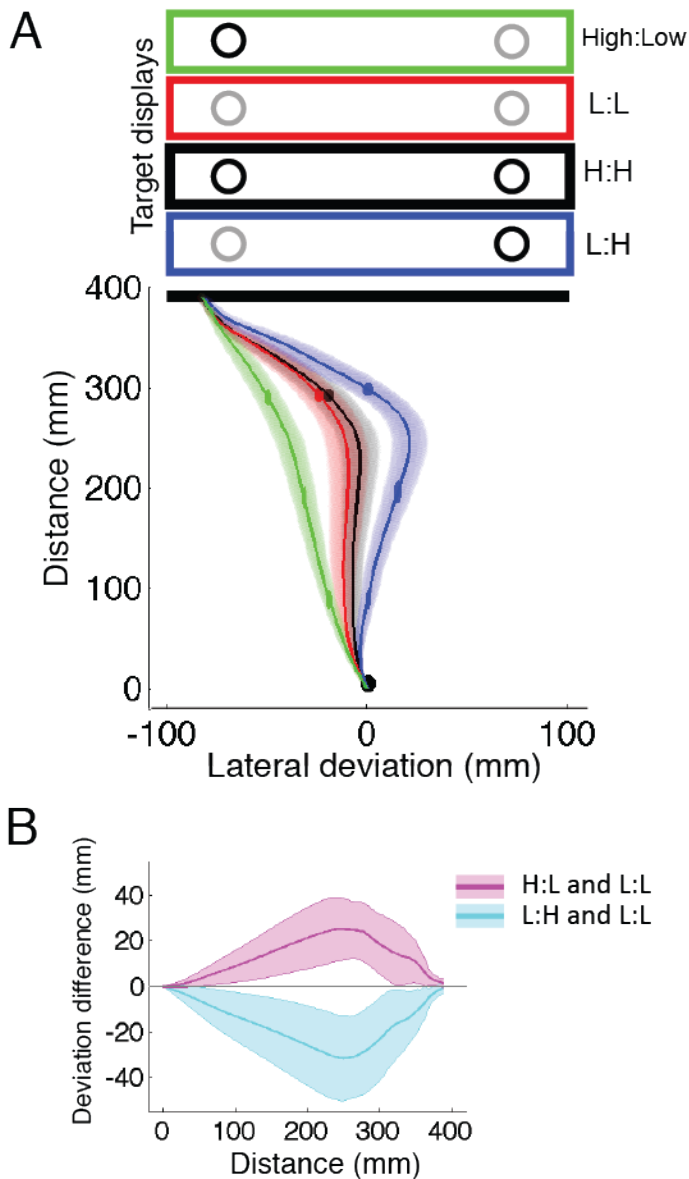


Figure 2.2 Results from experiment 1: an overhead plot of average reach trajectories (A) toward the target displays indicated above the plot. Only trials in which the left target was cued are shown. Shaded areas in the trajectory plot represent average standard error. The dark lines in (B) indicate the lateral deviation difference between trajectories in the H:L (i.e., *high* salience target left versus *low* salience target right) and L:L conditions (magenta) and between trajectories in the L:H and L:L conditions (cyan). Shaded areas in the difference plot represent 95% confidence intervals.

Initial trajectories showed a significant bias toward the higher salience target (Figure 2.2). When high salience targets were presented on the left, trajectories were biased toward the left side of space (green traces in Figure 2.2). Similarly, when high salience targets were presented on the right, trajectories were biased toward the right side of space (blue traces in Figure 2.2). Importantly, this was the case whether the final target was cued on the left or the right (Supplemental Figure 2.1). In contrast, when equally salient targets were presented on both the left and right sides of space (i.e., when both targets were either high or low salience), subjects showed no such biasing and initial trajectories aimed for a midpoint between the two targets (red and black traces in Figure 2.2). The FANOVA showed that trajectories toward targets of unequal salience (i.e., L:H and H:L) were significantly different from trajectories toward equally salient targets (i.e., L:L). These differences started early (2.5% of the reach) and continued until near the end of the reach (94% of the reach).

2.4 Experiment 2

There were at least three potentially relevant consequences of varying the concentration of pixels in the targets of experiment 1 (E1): first, the targets varied in number of pixels. Second, they varied in the luminance contrast of their contours (i.e., the luminance of the background vs. the luminance of the lines making up the target). Third, they varied in the overall luminance contrast of the target (i.e., the luminance of the background vs. luminance within the bounds of the target). Any of these factors could conceivably be responsible for the biasing of initial trajectories toward the high salience targets in E1.

The second experiment (E2) had three goals: first, to disentangle the influences of number of pixels and contour luminance contrast from that of target luminance contrast; second, to observe how salience interacts with the number of potential targets in the biasing of initial reach trajectories; third, to see whether the salience bias (if there is one) is constant within the timescale of a single trial, or whether it changes as a function of time.

To address the first goal of E2, we took a basic target (i.e., empty black circle) and either subtracted (low salience) or added (high salience) a cross at its center, with the arms of the cross spanning the diameter of the circle (see Figure 2.1C). The two resulting stimuli had equal contour luminance contrast, but they differed in target luminance contrast and the low salience stimulus still had half as many pixels as the high salience stimulus. Our interest in the question of pixel count was primarily motivated by a need to rule out the possibility that, in past versions of our task (C. S. Chapman, Gallivan, Wood, Milne, Culham, & Goodale, 2010a; 2010b; Gallivan et al., 2011), trajectory biases toward the side of space with more targets could be attributed to the fact that the side with more targets also always had more black pixels on a white background. In other words, rather than basing reach decisions on the probabilities inherent in the spatial distribution of targets, participants could have simply used differences in the amount of “stuff” on each side as a cue for initial trajectory formation. In theory, when presented with twice as many low salience targets on one side as there are high salience targets on the other side, participants could: 1) be pulled toward one side because of high salience targets, 2) be pulled toward the other side because of a greater number of targets (and thus a greater probability that the final target would appear on that side), or 3) not be pulled to either side and reach up the middle because there would be an equal number of pixels on each side of space.

Accordingly, we addressed the second goal of E2 by varying the number of potential targets that could appear on each side of the screen (Figure 2.1 B). Either 0, 2, or 4 targets could appear on each side of the screen (i.e., all permutations of 0:2, 0:4, 2:2, 2:4, and 4:4 across the two levels of the salience factor). Target locations were selected from a hexagonal cluster of possible locations (with one location at the center, resulting in 7 possible target locations) on each side of the screen, with the center target of the cluster being located 9 cm to the left or right of the central fixation cross (Supplemental Figure 2). The addition of more targets necessitated more trials to ensure a suitable number of trial-type repetitions. After an initial training session of at least 54 trials, an experimental session commenced, consisting of 540 trials (10 blocks of 54).

To address the third goal of E2, we tested two separate groups of participants. Participants in one group (no-delay group) were presented with the initial target display at the same time that they received an auditory cue to begin their reach. The other participants (delay group) received the auditory cue 500 ms after the presentation of the initial target display (Figure 2.1B). This time-dependent approach allowed us to investigate what effect, if any, target salience might have when subjects have been given more time to process the target display and plan their reaches.

We have emphasized that the targets employed in E2 differed in overall target luminance (i.e., luminance within the bounds of the target), but not in contour luminance (i.e., luminance of the lines that make up the target). We note here that another possible factor introduced by this salience manipulation is the relative closure of the target contours. The high-salience target had fully closed contours, while the low-salience target had open contours. In light of evidence that shape processing is fast for closed stimuli and slow for open stimuli (Elder & Zucker, 1993), we assumed that the degree of closure of the E2 targets also contributed to their overall salience.

2.4.1 Method

Aside from the differences mentioned above, the design and procedure of E2 were identical to those of E1. There were 31 participants in the no-delay group and 33 participants in the delay group. After trial removal and participant screening (using the same criteria that were used in E1), we were left with 27 participants in the no-delay group and 26 participants in the delay group.

2.4.2 Results

The primary finding of E2 was that salience differences (i.e., global luminance contrast) strongly biased the trajectories of participants in the no-delay group. This bias was strong enough to overpower the traditional spatial averaging (based on the distribution of targets) that we have observed in earlier studies (C.

S. Chapman, Gallivan, Wood, Milne, Culham, & Goodale, 2010a; 2010b; Gallivan et al., 2011). In contrast and rather importantly, we found no salience bias in the trajectories of participants in the delay group. Instead, their trajectories showed a return to spatial averaging behaviour (Figure 2.3).

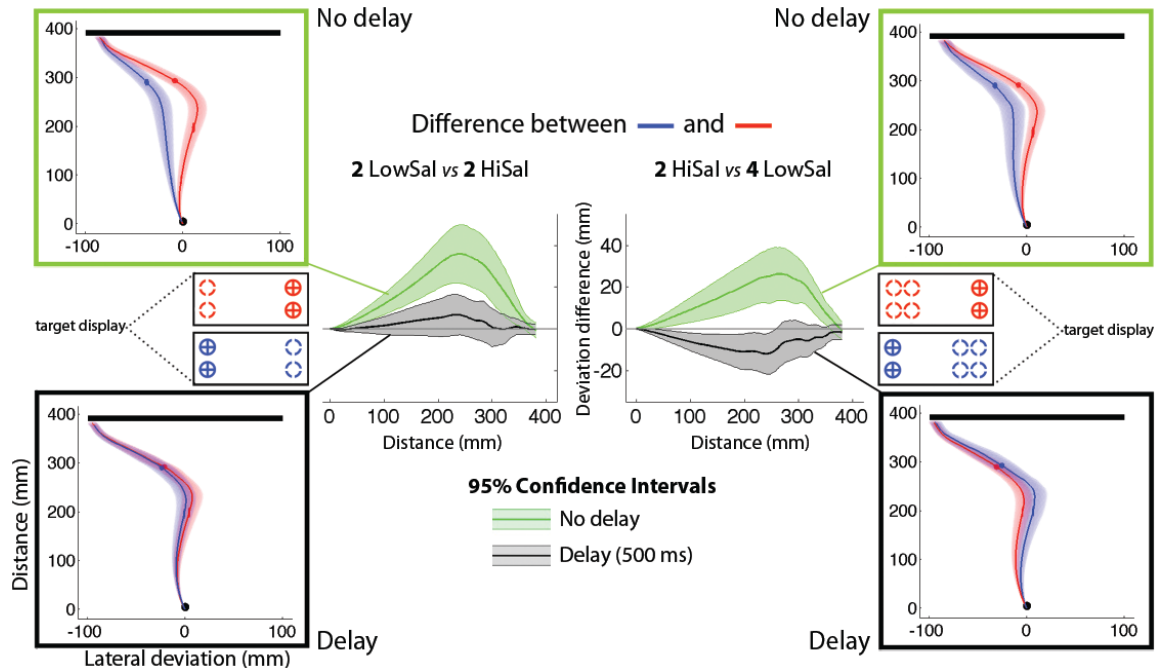


Figure 2.3 Results from Experiment 2. The two plots on the left show an overhead view of average trajectories for the no-delay (top plot) and delay (bottom plot) groups in response to a target display with two low salience and two high salience targets. The colour of the trajectories correspond to the colour-coded target displays depicted between the two plots. In these plots, and in all other plots in the figure, only trials where the final target appeared on the left are shown. The two plots on the far right show average trajectories of the no-delay (top plot) and delay (bottom plot) groups in response to four low salience and two high salience targets. Shaded areas in the trajectory plots (i.e., blue and red) represent average standard error. Colours are for purposes of illustration only. The two plots in the center of the figure show the difference in lateral deviation (between the red and blue trajectories; i.e., the difference between responses to the two spatial arrangements of a given target display) as a function of the distance between the hand and the touchscreen. Shaded areas in the difference plots represent 95% confidence intervals.

This time-dependent effect of salience can be observed in the comparison of 2H:2L (i.e., two *high*-salience targets on the left versus two *low*-salience targets on the right) and 2L:2H trials. Initial trajectories were biased toward the side with the high salience targets in the no-delay group. In the delay group, however, both of these trajectories ran up the middle, as would be predicted if participants in the delay group were simply averaging the spatial location of the potential targets.

A more striking illustration of this effect of salience came from the comparison of 4L:2H and 2H:4L trials. Even though the final target was twice as likely to appear on the side of space with the four low salience targets, initial trajectories of participants in the no-delay group were still strongly biased toward the two high salience targets. Critically, in the delay group, we observed a small but significant bias toward the side of space with more potential targets.

We observed an unexpected attenuation of spatial averaging sensitivity in the no-delay group, even in trials where all potential targets had equal salience. For example, when we compared 2H:4H and 4H:2H trials, the FANOVA showed that trajectories were only slightly biased to the left when there were four targets on the left, and only slightly biased to the right when there were four targets on the right (Supplemental Figure 3). Regardless of this attenuation, spatial probabilities still had a consistent effect on reaches such that trajectories were always biased toward the side of space with more targets.

As an alternative to the results of the functional data analysis presented here, we also performed a more traditional analysis of the same data, using a mixed-design ANOVA that compared averages of a selected data point (i.e., 30% of the reach trajectory) instead of the entire reach trajectory. This analysis was entirely consistent with the functional data analysis, and is included in the Supplemental Materials (see Supplemental Table 1). Also included in the Supplemental

Materials is an analysis of reaction time (Supplemental Table 2) and movement time (Supplemental Table 3) for E2.

2.5 General Discussion

We recorded trajectories while subjects performed reaches toward multiple potential targets of differing luminance. Two basic observations emerged: (1) when subjects were required to react immediately, trajectories were strongly biased toward the side of space containing targets of higher salience, even when a higher number of less-salient targets on the opposite side of space made this strategy sub-optimal, and (2) when subjects were given a 500 ms preview of the initial display of potential targets prior to being cued to move, the salience bias was profoundly diminished, as evidenced by the return of a spatial averaging trajectory bias that reflected the target probabilities inherent in the initial display. These results, to our knowledge, are the first to show that target salience exerts a time-dependent modulation of the spatial averaging of reach trajectories.

2.5.1 Salient targets dominate early visuomotor competition

The driving motivation behind the present study was to test the hypothesis that the neural mechanisms responsible for selecting a reach target would be influenced by luminance differences in the potential targets. More specifically, we hypothesized that the competition between representations of potential targets on a reach-specific priority map would be biased by salience differences such that the neural activity representing salient target(s) would be facilitated. In light of our claim that the spatial averaging effects observed in past iterations of the present task (C. S. Chapman, Gallivan, Wood, Milne, Culham, & Goodale, 2010a; 2010b; Gallivan et al., 2011) and other similar tasks (Hudson et al., 2007; Song & Nakayama, 2006; 2007; 2008) are a reflection of unresolved competition in the priority map at the time of reach initiation, one clear prediction from this hypothesis was that the unresolved competition would be biased in favor of the salient target(s), resulting in an initial trajectory bias toward the spatial location of the salient target(s). This prediction was also based upon an analogy with

models of saccade curvature (McPeck et al., 2003; Tipper et al., 2000; Van der Stigchel et al., 2006), in which saccade curvature during double-step (Van Gisbergen, Van Opstal, & Roebroek, 1987) or visual search (Godijn & Theeuwes, 2002; McPeck, Skavenski, & Nakayama, 2000; R. Walker, Mcorley, & Haggard, 2006) paradigms is a result of averaging disparate saccade vectors encoded simultaneously by competing clusters of activity within a priority map.

In the present study, when participants were required to initiate a reach as quickly as possible (E1 and no-delay group in E2), initial trajectories were strongly biased toward the high salience targets. This is in contrast to spatially averaged trajectories that aim for a midpoint location when the salience of the competing targets was equal. A more compelling demonstration of this salience bias (in E2) was found in the observation that when making rapidly initiated reaches, trajectories were biased toward high salience targets even when there were twice as many targets (and therefore twice the probability that the final target would appear) and an equal number of pixels on the other side of space. The fact that trajectories did not aim for a midpoint location in this condition (i.e., 2H:4L) suggests that the salience bias is driven not by the difference in salience between whole clusters of targets (i.e., the amount of pixels or “stuff” on a given side of space), but rather by the difference in salience between individual targets.

One surprising observation from E2 was that when salience was held constant (e.g., 2H:4H), initial trajectories were far less sensitive to spatial target probabilities than has been observed in past studies (C. S. Chapman, Gallivan, Wood, Milne, Culham, & Goodale, 2010a; 2010b; Gallivan et al., 2011). Perhaps the introduction of luminance differences, along with the overwhelming behavioural relevance of visual salience in most other contexts, cultivated a readiness for those differences even though they were task-irrelevant in this case. On a related note, the observed behaviour of participants in the no-delay group during the 2H:4L condition also shows that the salience bias exerts dominance not only in spite of the task-irrelevance of target luminance, but also in spite of a considerable decrease in movement efficiency. In other words,

reaching toward the 2H targets (as opposed to the 4L targets) in response to the 2H:4L display necessitated a greater frequency and magnitude of online corrections. This seemingly sub-optimal behaviour persisted throughout the entire session (i.e., there was no detectable difference between behaviour in the first three and last three blocks; see Supplemental Figure 4), suggesting that participants in the no-delay group never learned to ignore the salience of targets.

At least one study has previously examined the role of target salience in the selection of reaching movements. Zehetleitner, Hegenloh, and Müller (Zehetleitner et al., 2011) observed that when participants pointed to a target among a uniform field of distractors differing from the target in either orientation or luminance, reach durations and initiation latencies decreased as feature contrast increased. Since a similar effect has been consistently observed in saccades during visual search tasks (Wolfe & Horowitz, 2004), Zehetleitner et al. interpreted their results as evidence of a salience map. In the present study, we were unable to detect differences in initiation latencies between trials with and without luminance differences between targets. Indeed, we have never been able to detect reaction time differences in past implementations of the present paradigm--a fact that is likely a reflection of the stringent reaction time cutoff employed (i.e., 325 ms). Importantly, the failure to detect RT differences was not due to participants "timing out" more often on one type of trial than another, which would have led to a selective exclusion of the more difficult trials from analysis. Simply put, participants quickly learned to respond well ahead of the cutoff (the slowest average RT for any condition was 200 ms; see Supplementary Table 2), regardless of luminance conditions. Despite the lack of RT differences, the results of our trajectory analysis agree with the claim that reaching movements are selected on the basis of a motor map that incorporates visual salience into its computations.

Multiple studies indicate that there is typically a tight anchoring of ocular gaze to the target of ongoing pointing movements (Fisk & Goodale, 1985; Neggers & Bekkering, 2000). Indeed, it could be argued that eye movements are often an

integral component of visually guided reaching; we typically look at the target we are reaching towards. Given that eye movements were unconstrained in our study, one might argue that the observed effect of salience upon initial reach trajectories could be explained by salience-induced saccadic activity prior to the initiation of the reach. That is, salient targets could have captured attention and elicited a saccade, and pointing movements could have been drawn to where the participants were looking. We acknowledge this possibility and hope to pursue this interesting question in future studies.

2.5.2 Visual salience is a factor only during early visuomotor competition

One of the central goals of the present study was to test the prediction that, if salience did in fact bias initial reach trajectories, it would do so only within a short temporal window after the presentation of the potential targets. Positive support for this prediction was found in the striking reversal of trajectory biases as participants in the no-delay group were biased by target salience while, within the same condition, participants in the delay group were instead biased by the spatial distribution of potential targets (see Figure 2.3). These results agree with a number of studies showing that eye and arm movements following either a short SOA or a short response latency are more influenced by salience differences than are those that follow longer SOAs or response latencies (Dombrowe et al., 2010; Donk & Soesman, 2010; Donk & van Zoest, 2008; Stritzke, Trommershäuser, & Gegenfurtner, 2009). The results of the present study and these latter studies indicate that target salience biases selection only within a brief time span following stimulus onset.

Why does the salience bias seem to disappear after a few hundred milliseconds? One possible explanation is that stimulus salience results in an immediate and persistent boost in gain at the corresponding location on the priority map, and that the gain at this location can be suppressed by top-down inputs that take a few hundred milliseconds to appear. More specifically, some have proposed that

the initial sweep of activity during visual processing is entirely stimulus-driven, and that subsequent recurrent processing involves top-down regulation of early visual areas by way of long-range feedback connections (Lamme & Roelfsema, 2000; Theeuwes, 2010). This proposition finds some empirical support from a study in which Buschman and Miller (2007) recorded simultaneously from frontal (prefrontal cortex and frontal eye fields) and parietal (lateral intraparietal area, LIP) cortex while monkeys located a target in either a visual pop-out or a visual search task. These two tasks were meant to selectively elicit bottom-up or top-down attention, respectively. Interestingly, LIP cells represented the location of the target 150-200 ms earlier in the pop-out task than they did in the visual search task, suggesting that bottom-up attention has an influence upon the priority map in LIP significantly sooner than does top-down attention.

Of course, in everyday behaviour, visual information is not broken into the discrete, unpredictable bursts that characterize visual information within a laboratory setting. Rather, visual information tends to be continuous, contextualized, and statistically structured, which implies that anticipatory top-down modulation could occur in principle, allowing one to suppress task-irrelevant salience differences within a stimulus set. Indeed, Mazaheri et al. (2011) have demonstrated that pre-stimulus coupling between frontal and parietal areas predicted successful suppression of attentional capture by a salient distractor. Many other studies have demonstrated that it is possible to suppress attentional capture from the outset, specifically when sufficient practice or training has occurred (Ipata, Gee, Gottlieb, Bisley, & Goldberg, 2006; Kim & Cave, 1999), or when task-set (Yantis & Egeth, 1999) or distractor frequency (Geyer, Müller, & Krummenacher, 2008) increase the incentive to suppress salience differences (although the Yantis & Egeth results have been strongly contested; see Lamy & Zoaris, 2009) It is conceivable that, in our task, participants could have eventually developed the ability to suppress the salience bias had they been given more trials.

An alternative explanation of the eventual disappearance of salience biases is that salient stimuli are processed earlier than other competing stimuli, as indicated by electrophysiological studies (Hickey, McDonald, & Theeuwes, 2006; Töllner, Zehetleitner, Gramann, & Müller, 2011). In priority maps, where lateral inhibition results in winner-take-all dynamics (Bisley & Goldberg, 2010), a selective reduction in processing latency for salient stimuli would also result in the suppression of activity at other spatial locations prior to the appearance of activity representing less salient stimuli. After the appearance of the other stimuli, and in the absence of any continuous signal boost for salient stimuli, the competition would tend toward equalization until either endogenous or exogenous inputs identified and thus biased the competition for one of the targets. This “head start” is another possible mechanism that could explain the time-dependence of the salience bias in our data.

2.5.3 Conclusion

In conclusion, we show that salience exerts a time-dependent bias upon reach trajectories toward multiple potential targets, and that this salience bias overpowers the spatial averaging of initial trajectories toward those targets. Since this spatial averaging behaviour is widely thought to reflect unresolved competition in a priority map, we interpret our results as evidence that visual salience selectively increases the gain of target representations on the map, and that this early processing advantage for salient targets dwindles within 500 ms at most. It will be important for future studies to titrate the duration of the display presentation (prior to the movement cue) in order to better characterize the shape of the function describing the attenuation of the salience bias.

Chapter 3: Individual differences in the speed of visual processing predict capture by target salience

3.1 Abstract

Salient stimuli attract our movements, even when this is sub-optimal and contrary to our goals. Using a rapid reaching task, we show that the degree to which this happens in an individual depends on the range of their visual processing speeds. We also demonstrate that increasing the salience differences between stimuli makes the individual differences in processing speed matter less. This can be explained by response saturation due to normalization. Finally, we show that the biasing effect of visual salience upon behavior lasts much longer than the classical 200-250 ms (as reported by past studies) in conditions where all stimuli, both salient and inconspicuous, are task-relevant.

3.2 Introduction

When people reach toward multiple potential targets without knowing the final target location, initial reach vectors are sensitive to the numerosity of the target distribution, as evidenced by a trajectory bias toward the centre of gravity of the target array (C. S. Chapman, Gallivan, Wood, Milne, Culham, & Goodale, 2010a; 2010b; Gallivan et al., 2011; Milne et al., 2013). When there are salience differences between the potential targets, however, the initial trajectories are biased toward the high-salience targets, even in cases where there are twice as many low-salience targets on the other side of the display (Wood et al., 2011). Similarly, express saccades and fast, visually guided reaching movements will often deviate toward distractors (Song & Nakayama, 2007; Van der Stigchel, 2010). These examples illustrate the consistent finding that salient stimuli may elicit involuntary orienting responses and trajectory deviations, often in cases where such responses are explicitly contrary to overarching goals. Despite the considerable literature exploring these effects, we still understand very little about the mechanism(s) responsible. What is it about how salience is coded that causes trajectory deviations?

Visual stimuli with high luminance contrast are processed faster than low-contrast stimuli. This is a phenomenon that has long been known through classic behavioral studies (Cattell, 1886; Mansfield, 1973), but more recently demonstrated with electrophysiological techniques in occipital and parietal cortex (Gawne, Kjaer, & Richmond, 1996; Johannes, Münte, Heinze, & Mangun, 1995; Töllner et al., 2011). It is unclear, however, what this processing speed differential means for the encoding of salience in visuomotor circuits (e.g., in a salience map). Salience responses can be found in many areas involved in visuomotor processing, such as superior colliculus (Boehnke & Munoz, 2008), lateral intraparietal area (Gottlieb, Kusunoki, & Goldberg, 1998), primary visual cortex (Z. Li, 2002), area V4 (Mazer & Gallant, 2003), and frontal eye fields (Thompson & Bichot, 2005). The most influential computational models of visual salience simulate these salience responses through hierarchical centre-surround

mechanisms (Itti & Koch, 2001), but such approaches are, at best, indifferent to any possible role of differential processing speed in the computation of salience.

An alternative proposal suggests that salience could be computed by way of a temporal code that utilizes the relative timing of the arrival of the first spikes in response to a stimulus (Guyonneau, Vanrullen, & Thorpe, 2004; Vanrullen, 2003). While there is evidence that such a rank-order coding scheme is indeed used in sensory processing (e.g., Johansson & Birznieks, 2004), there is little empirical support for the provocative hypothesis that this mechanism is involved in the processing of salience.

If the encoding of visuomotor salience is influenced by the relative processing speeds for concurrent stimuli, then the degree of trajectory deviation toward a salient target in a reaching task should be directly related to the difference in processing speeds between the salient and less-conspicuous targets of the target display. In the present study, we tested this prediction by using (1) a speeded enumeration task with stimuli of varying contrast, and (2) a compelled reaching task with multiple potential targets that varied in contrast, sampled at ten different delay conditions. The latter task allowed us to characterize, over a broad temporal range, the respective biases of salience and numerosity.

We demonstrate that the degree to which behaviour is automatically influenced by salience differences in the visual scene is predicted by an individual's unique range of processing speeds for visual information. We also demonstrate that the biggest differences between individuals occur in the lower ranges of salience. In other words, as you increase the salience differences between stimuli (and, presumably, the spike arrival latencies between them), the individual differences in processing speed matter less. Finally, we show that, when both salient and inconspicuous stimuli are task-relevant, the biasing effect of visual salience upon behavior lasts much longer than the 250 ms reported by many past studies (Dombrowe et al., 2010; Donk & Soesman, 2010; Donk & van Zoest, 2008; van Zoest et al., 2012).

3.3 Methods

Using optoelectronic markers (Optotrak: NDI, Waterloo, ON), we recorded reaching movements (sampling the position of the right index finger at 150 Hz) in 79 right-handed participants (mean age 22; 48 females), distributed across three experimental groups (E1: 26, E2: 28, E3: 25), as they reached from a start button to a touchscreen (1024x768, 60 Hz refresh rate) located 40 cm away. Trials began with participants holding down the start button while fixating (for a variable delay of 1000–2000 ms) a point at the center of the touchscreen. The fixation point was then replaced by a target display that consisted of four to eight potential targets (i.e., clusters of two or four targets on each side of space) of varying luminance contrast. The ‘Go’ cue was an auditory ‘beep’ that occurred anywhere from 0 to 450 ms (in 50 ms increments) following the appearance of the target display, resulting in 10 parametric delay conditions. Following the Go cue, participants had 325 ms to initiate a reach toward the display. Once the reach began and the start button was released, one of the targets in the initial display was cued (by filling in black) and participants had to correct their trajectory in flight to that target location within 425 ms (Figure 3.1A). We emphasize here that the 425 ms movement time constraint precluded any strategies that involved a double-step movement, e.g., lifting the finger off the start button and waiting for the final target to appear, and then initiating a reach toward the final target. In other words, participants needed to commit to a reach vector and move forward, relying upon online correction later in the reach in order to hit the target within the allotted time.

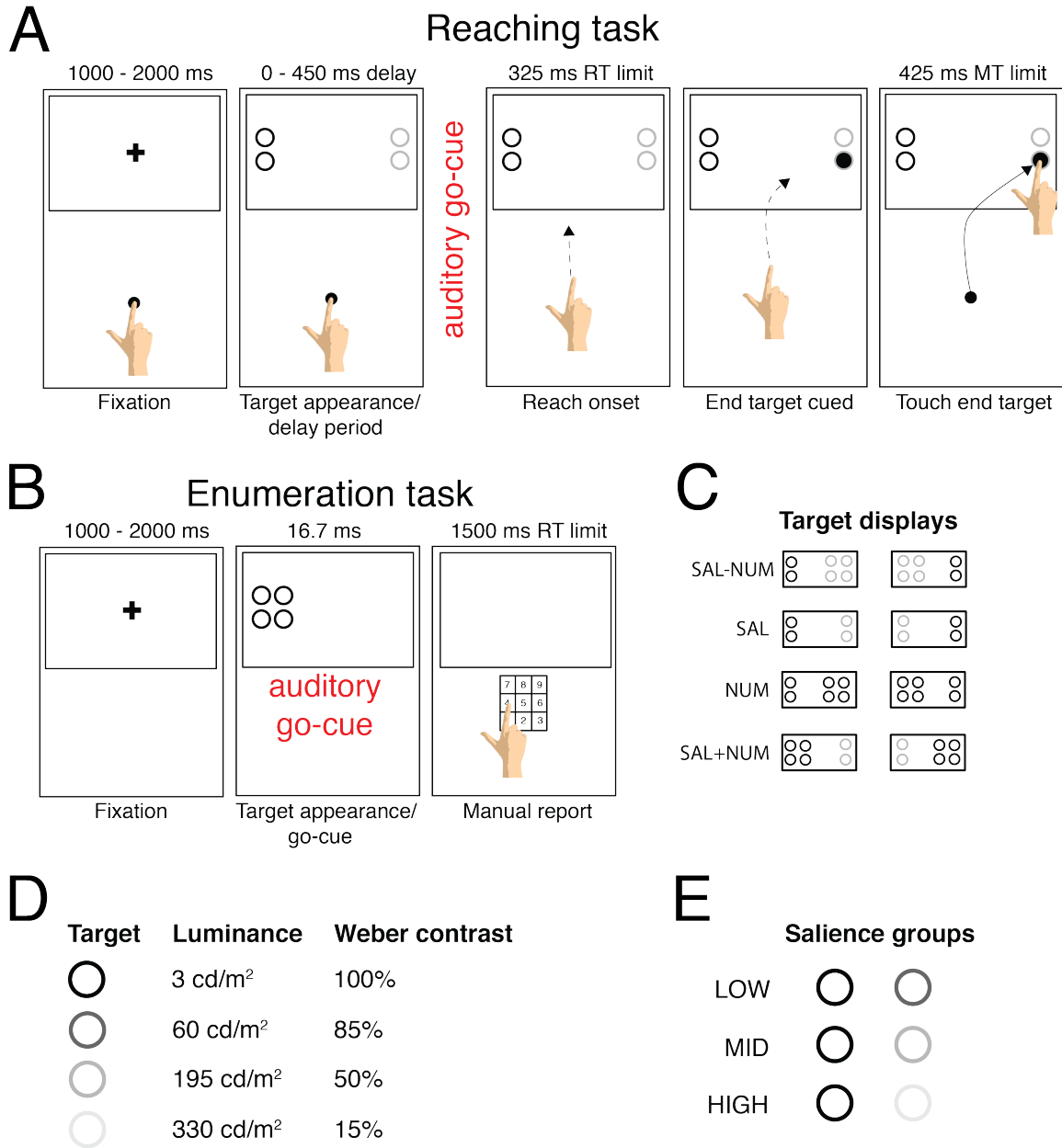


Figure 3.1 Task and stimuli. *A*, Temporal sequence of a single trial in the reaching task. After a variable fixation period, the array of potential targets appeared. An auditory go-cue was presented either simultaneously with or up to 450 ms (50 ms increments) after the target array onset. After the go-cue, participants had 325 ms to begin reaching. Only after reach onset was the final target cued by filling in one of the potential targets. Participants had 425 ms from reach onset to touch the final target. *B*, A single trial in the enumeration task. After a variable fixation period, a cluster of targets appeared on the screen for 16.7ms, along with an auditory go-cue. Participants had 1500ms to report

(with a numeric keypad) the number of targets detected. *C*, The eight possible target displays, grouped into four basic patterns. Note that the uniform clustering of targets depicted here is only for illustrative purposes. See *Methods* for a description of the actual target locations in a display. *D*, Luminance and Weber contrast values for the potential targets. *E*, All three experimental groups had the same high contrast target, but differed with respect to the low contrast target that they encountered.

All targets in the display had an equal probability of filling in and becoming the final target. To encourage accurate performance, participants received trial-by-trial feedback on their fulfillment of the task's temporal and spatial constraints. There were four possible types of errors that caused the following text to be displayed at the centre of the display screen: 'Too Early' (if the start button was released before 100 ms had elapsed after the beep cue; this aborted the trial), 'Time Out' (if the start button was not released within 325 ms; this also aborted the trial), 'Too Slow' (if the screen was not touched within 425 ms of button release), or 'Miss' (if participants did not touch the screen within a 6 cm x 6 cm box centered on the target). 'Good' was displayed on trials without errors. Participants performed an initial training session of at least 70 trials, followed by 1400 test trials (across 20 blocks).

Target stimuli were empty grey/black circles (presented against a white background) with a 2 cm diameter. They were pseudo-randomly selected from a possible target array of 14 targets (7 on each side of space). Each 7-target location array was essentially a hexagon with one target location in the center, with that center target located 10 cm to the left or right of the central fixation point. Each target in the array was 3 cm away from its nearest neighbors. In order to control for spatial biases due to differences in the visual eccentricity and spread of the potential targets, the central target position in the potential target array was always presented on each trial, with all other potential targets being randomly selected for presentation.

We manipulated the salience of individual targets by varying their luminance contrast ratio with the background (Figure 3.1 D and E). Luminance contrast was varied between, but not within, target clusters (i.e., between opposing sides of the target display and not within the same side of the target display). The background of the touch display was white (RGB: [255 255 255]) with a luminance value of 380 cd/m². For each of the three salience groups, high-salience targets were black (RGB: [0 0 0]) with a luminance value of 3 cd/m² (~0% of white luminance, ~100% Weber contrast ratio). The three salience groups differed only in the luminance value of the low-salience targets they viewed. In the LOW salience group, low contrast targets (RGB: [102 102 102]) had a luminance value of 60 cd/m² (~85% Weber contrast ratio). In the MID salience group, low contrast targets (RGB: [185 185 185]) had a luminance value of 195 cd/m² (~50% Weber contrast ratio). In the HIGH salience group, low contrast targets (RGB: [230 230 230]) had a luminance value of 330 cd/m² (~15% Weber contrast ratio). Luminance values were measured with a Minolta LS-110 photometer.

The target positions for a given trial in the reaching task consisted of a permutation of one of eight possible patterns: (1) The two opposite-bias target displays (i.e., SAL-NUM) consisted of two high contrast targets on one side and four low contrast targets on the other side. In this condition, the respective salience and numerosity biases pulled in opposite directions. (2) The two pure salience displays (i.e., SAL) pitted two high contrast targets against two low contrast targets, thus holding numerosity constant. (3) The two pure numerosity displays (i.e., NUM) pitted two high contrast targets against four high contrast targets, thus holding salience constant. (4) The two same-bias displays (i.e., SAL+NUM) consisted of two low contrast targets pitted against four high contrast targets. In this condition, the salience and numerosity biases pulled in the same direction.

Following the main reaching experiment, participants completed a short enumeration task (Figure 3.1B) in which they viewed anywhere from one to six

targets flash on the screen for one monitor refresh (i.e., 16.7 ms), and then reported with a number pad how many targets they detected. The stimuli were the same empty circles with the same two possible luminance values, randomly selected from the same 14 (i.e., 7 left and 7 right of fixation) possible locations that the participant experienced during the reaching task. The cluster of stimuli presented during a given trial, however, was always of a single salience value and only on one randomly selected side of the display. We collected RTs and instructed participants to respond as quickly and accurately as possible. If a participant failed to respond within 1500 ms, the trial aborted and the participant received a visual reminder to respond quickly.

3.3.1 Data Processing and Analysis

Other studies that have used a version of this task have shown that information about the final target (which is cued at movement onset) reliably begins to exert an influence on trajectories at about 60% of the spatial extent of the movement (C. S. Chapman, Gallivan, Wood, Milne, Culham, & Goodale, 2010a; 2010b; Gallivan et al., 2011). Since we were exclusively interested in the initial direction of reach trajectories, we focused the present analysis upon the first 20% of movement space. Sampling at this early stage isolated the initial reach plan and avoided contamination from visual processing of the final target location. Accordingly, we collapsed the final target cue variable for the purposes of analysis (since it should have no impact upon the reach trajectory until ~60% of the reach). To characterize the effects of target salience and numerosity over time, we averaged trajectories according to target display condition and delay condition.

Figure 3.2 A depicts, for two different delay conditions, the instantaneous spatial position of reach trajectories for a representative subject. Since we were interested in characterizing the entire first 20% of the movement trajectory (and not simply what is happening at a single point at 20% of reach distance), we took the area under the curve (AUC) for the first 20% of each trajectory. We found this

metric to be less noisy, and less susceptible to chance differences in instantaneous position at the point of sampling. To measure bias for each of the four target patterns (i.e., SAL-NUM, SAL, NUM, and SAL+NUM), we took the difference between the average AUC of the two opposing conditions within a display pattern (see Figure 3.1 C). Using this approach, a bias of zero would indicate that the average trajectories for the two opposite displays within a pattern are completely overlapping. Unless otherwise specified (for example, Figure 3.4), a negative bias value indicates a trajectory bias toward salience, and a positive trajectory bias value indicates a bias toward numerosity. Note that, in order to validate the choice of 20% of the reach as a sampling cut-off point for analysis, we also conducted the analysis with AUC at 50% of the reach. The differences were negligible and had no impact on the outcome of the analysis and its interpretation.

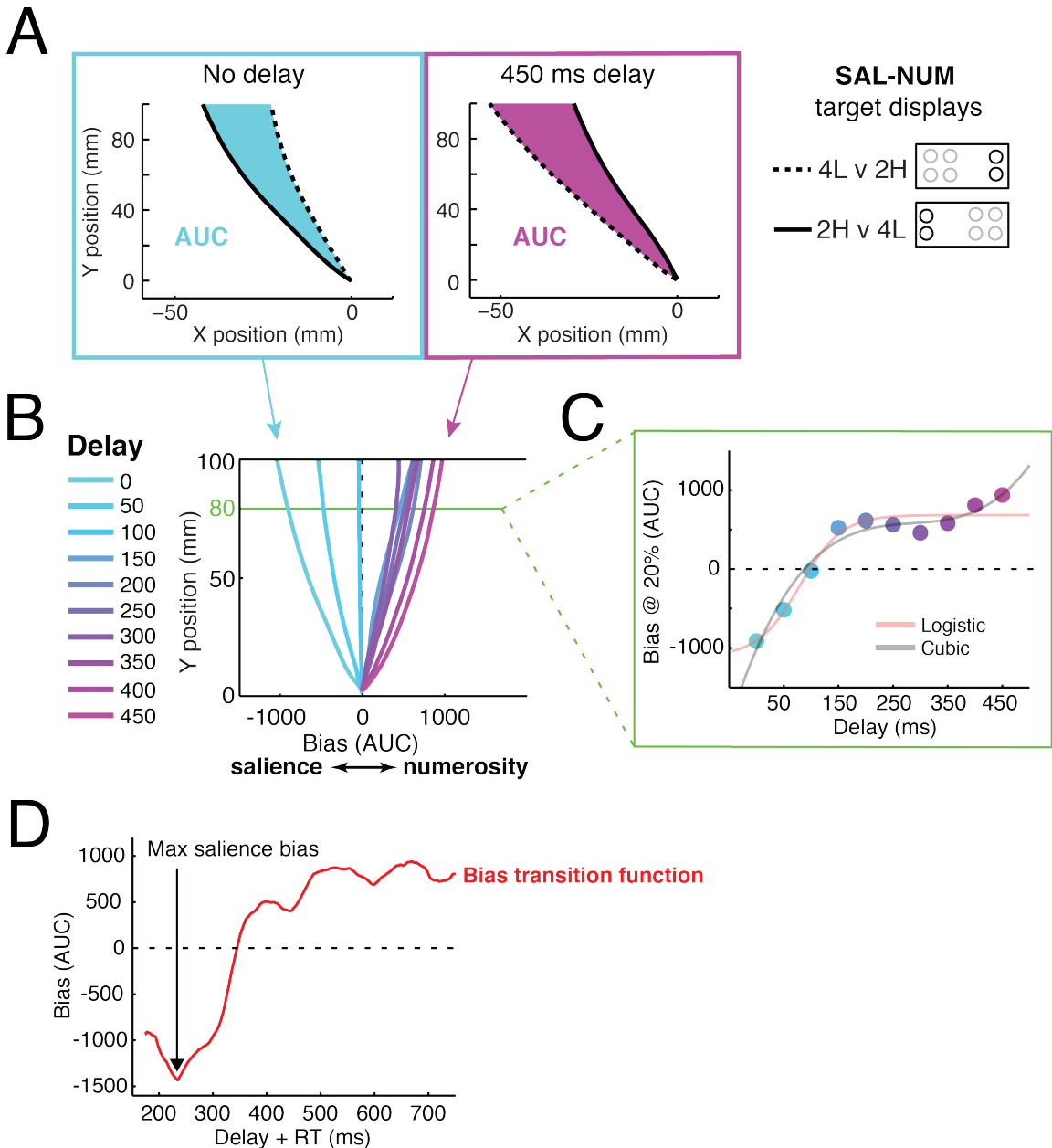


Figure 3.2 Analysis of reaching performance for a single participant in the MID salience group. **A**, During trials with the SAL-NUM target display, this participant was strongly biased toward salience at the minimum delay (0 ms) and strongly biased toward numerosity at the maximum delay (450 ms). We show only the first 10 cm (out of 40 cm) of the reach. Colored patches between the trajectories indicate the area under the curve (AUC). **B**, By taking the AUC (up to 20% or 8 cm of the reach) between the average trajectories toward the two mirror-image displays for each of the four target display conditions, we calculated the overall reach bias (on a continuum of salience to

numerosity bias) at each of the parametric delays. The result is a bias function (shown in green bordering). C, To describe the shape of each participant's bias transition function (i.e., the bias function for the SAL-NUM target display), we fitted linear (not shown), cubic, and logistic functions. D, Finally, we characterized reach bias as a function of a continuous temporal metric (Delay + RT). We used this continuous bias transition function to define the max salience bias for each participant.

Given the assumption of a non-uniform relationship between delay and RT (this was verified statistically, but not reported here) and given that our primary goal was to understand how different variables influence reaching vectors as a function of the time elapsed between visual presentation and movement onset, it was important to account for both delay duration and RT in our temporal measure. To do so we simply added RT to delay duration, resulting in a continuous (rather than a discrete) measure of stimulus visual feedback duration prior to movement onset. We then sorted the reach bias values by this continuous delay variable, and took the median bias value within a 70 ms sliding window (Figure 3.2 D). The resulting bias function was then smoothed with a 7-point (i.e., 7 ms) moving average filter. Many of the dependent measures used in the present study are derived from the bias function for the SAL-NUM display trials, which we call the *bias transition function*, since it theoretically involves the transition from a salience bias to a numerosity bias over time. For the remaining target displays, we refer to the change in bias over time as, simply, a bias function.

To verify that unnecessary distortions were not introduced into the bias functions by way of the 70 ms windowed median approach, we conducted the same analysis with various window sizes (50, 25, and 10 ms windows). In every case, the bias functions were nearly identical, with the only changes being (1) slightly higher frequency fluctuations and (2) the size of the confidence intervals, which naturally grew as the window was contracted. The conclusions of these analyses did not differ from those of the original analysis. For robustness, we also

performed the same analysis with a mean rather than a median of the data within the window. The only effect of this change was a negative translation of the bias function, demonstrating that the underlying distribution was skewed.

For the purposes of the kinematic analysis, we relaxed the movement time constraint to 500ms (instead of 425 ms) and we also included all trials where the final target was missed, so long as they touched the screen within the allotted time. This decision was based upon the assumption that an inaccurate (and perhaps slightly slower) reach is still highly informative, especially within the first 20% of the movement (when movement corrections have not yet taken place). These criteria resulted in a rejection of 14.5% of the trials for the kinematic analysis.

We removed outliers by calculating the median absolute deviation (MAD) and removing data points that were over 3 MADs from the median (Leys, Ley, Klein, Bernard, & Licata, 2013). Using this criterion, there was one outlier in max salience bias and four outliers in RT for the enumeration task. All reported ANOVAs were Greenhouse-Geisser corrected where violations of the sphericity assumption were observed. All reported t-tests were Bonferonni corrected to account for multiple comparisons.

3.4 Results

The primary goal of this study was to investigate the relationship between visual processing speed as measured in a target enumeration task and the degree of bias induced by target saliency in a rapid reaching task. To do this, we first characterized and quantified the interaction of target saliency and numerosity over time. Our main analytical approach to this problem was to construct continuous bias functions for the four target patterns (see Figure 3.1 *D*), and to compare them using confidence intervals. These four target display patterns captured four possible relationships between target saliency and numerosity: (1) subtractive, (2) saliency only, (3) numerosity only, and (4) additive.

3.4.1 Characterization of bias over time

We first report the results of our bias function analysis, which is depicted in Figures 3.3-5. The bias functions for each of the four target display patterns, averaged across all salience groups, are depicted in Figure 3.3 A. The three salience-based functions (i.e., SAL-NUM, SAL, and SAL+NUM) are almost indistinguishable up to 300-350 ms, at which point they begin to diverge from one another. This divergence is perhaps best conceived as a deviation from the SAL function in two different directions, due to either subtracting (i.e., SAL-NUM) or adding (i.e., SAL+NUM) the influence of numerosity.

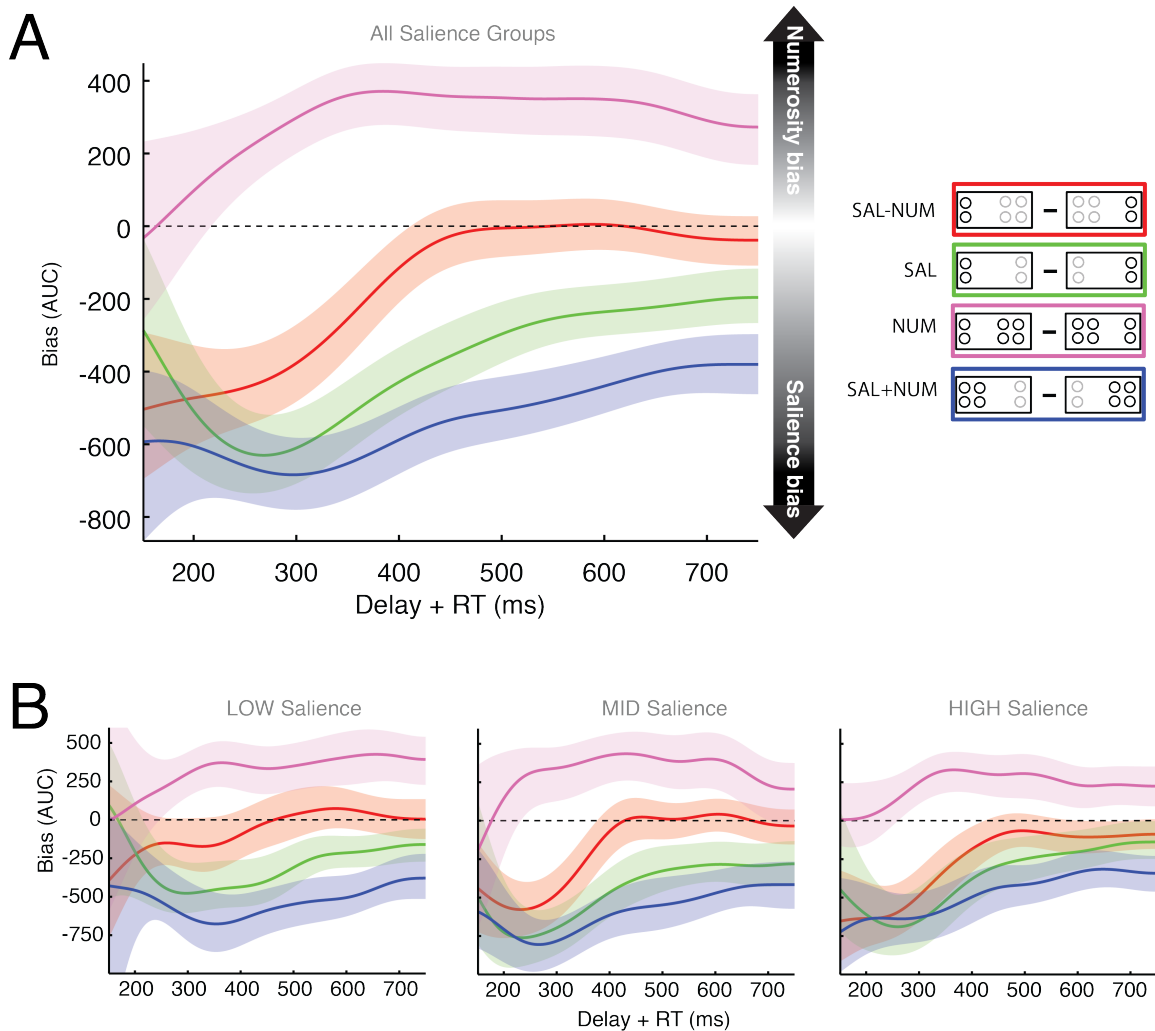


Figure 3.3 The interaction of salience and numerosity over time. These plots show average bias functions for the four target conditions of interest. Red traces show the bias transition function, which is the response to displays where luminance contrast and numerosity bias the reach in different directions (i.e., SAL-NUM). Green traces show the response to displays that differed only in luminance contrast (i.e., SAL). Magenta traces show the response to displays that differed only in numerosity (i.e., NUM). Blue traces show the response to displays where luminance contrast and numerosity bias the reach in the same direction (i.e., SAL+NUM). *A*, Bias functions averaged over all salience groups. *B*, Bias functions averaged within salience groups. Shaded regions indicate bootstrapped 95% confidence intervals.

One target pattern that was of special interest is the SAL-NUM pattern, in which there were two high-salience targets on one side of space and four low-salience

targets on the other side. This put the biases of target salience and numerosity into direct opposition, allowing us to observe their interaction over time. As expected, the influence of salience overpowered that of numerosity at the earliest time points (small Delay + RT). This was true even in the LOW salience group, in which the confidence interval briefly dipped below 0 at around 325 ms. Based on past work that showed a small but significant bias toward numerosity in response to a SAL-NUM display after a 500 ms delay (Wood et al., 2011), we had expected to see a transition to a numerosity bias by the end of the tested time range in the present study. Instead, we observed a stabilization of the bias transition function at equilibrium between salience and numerosity (Figure 3.3 *A* and *B*). This finding is even more striking when one considers the magnitude of the NUM bias function (plotted in magenta for Figures 3.3 and 3.4).

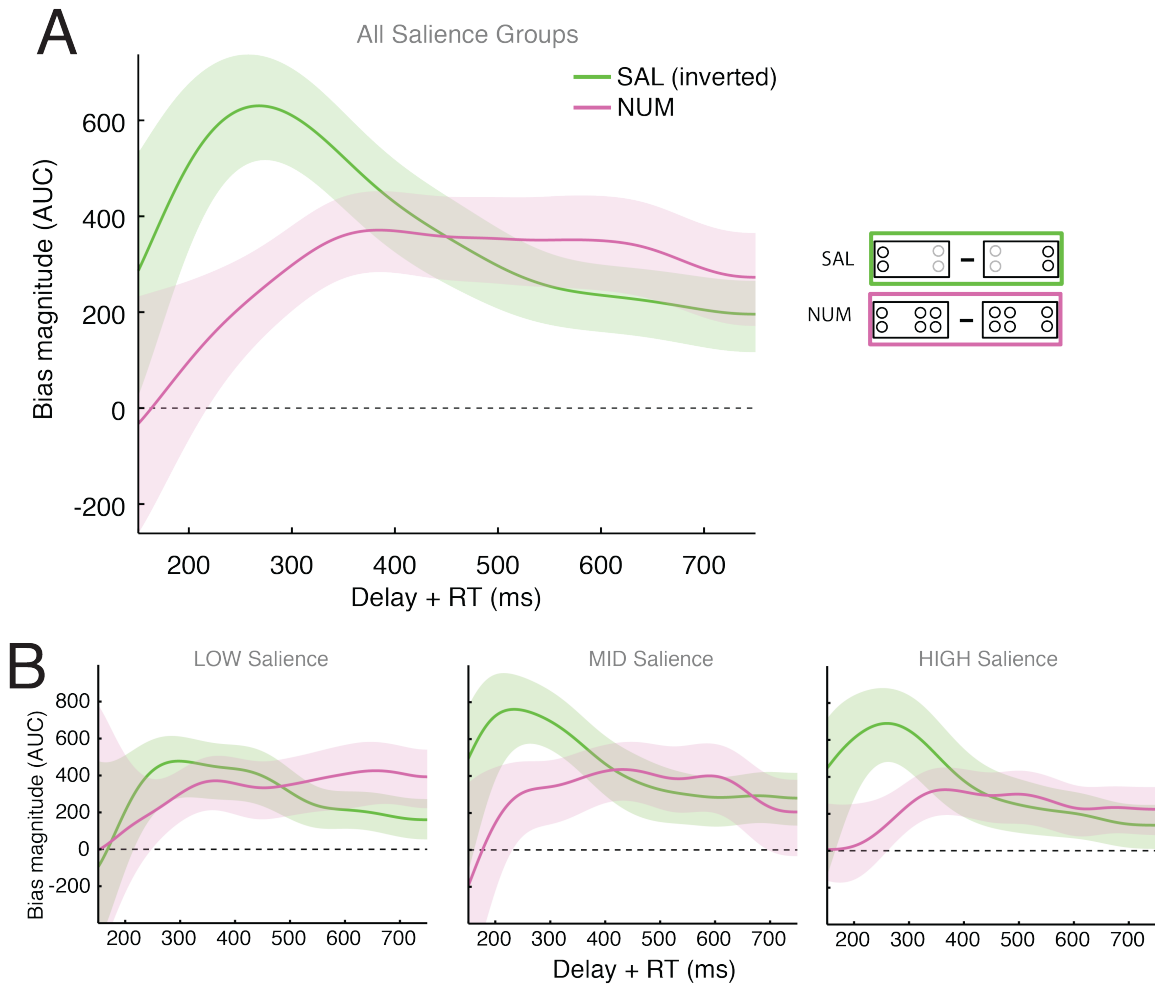


Figure 3.4 Pure salience (SAL) and pure numerosity (NUM) bias functions over time. *A*, Salience and numerosity bias strength averaged over all salience groups. *B*, Salience and numerosity bias functions averaged within salience groups. Note that the trace for the SAL condition is inverted for display purposes. Shaded regions indicate bootstrapped 95% confidence intervals.

Considered together, the SAL and NUM bias functions help explain the shape of the bias transition function, in particular its stabilization at equilibrium. Figure 3.4 isolates the SAL and NUM bias functions, and compares their magnitudes over time. At the earliest time points, there was no bias whatsoever in response to the NUM target display (see Figure 3.4A). In other words, reaches were going directly up the middle, presumably because these reaches were being initiated prior to any numerosity information arriving to the relevant neural pathways. After

150 ms of exposure to the targets, the numerosity bias came online and grew until it peaked at around 350 ms and then stayed constant across the remainder of the sampled time range (Figure 3.4A). This is in contrast to the SAL bias function, which peaked considerably higher and slightly earlier (i.e., by roughly 50-100 ms) than the NUM bias function, after which it logarithmically decayed until it reached what appeared to be a steady state of continued salience bias near the end of the sampled time range (Figure 3.4A). Notably, these two independent bias functions intersect at roughly 450 ms, which is exactly the time when the SAL-NUM bias transition function stabilized (compare intersection of pink and green curves in Figure 3.4A with the red curve in Figure 3.3A). The persistent effects of the pure NUM and SAL biases neatly accounts for the observation that the SAL-NUM bias transition function never completed a full transition to a numerosity bias. The fact that the salience bias exerted a persistent influence on visuomotor competition after at least 700 ms of visual exposure to the targets is one of the more surprising findings of this study, given the empirical precedent of a 250 ms window for the effect of salience.

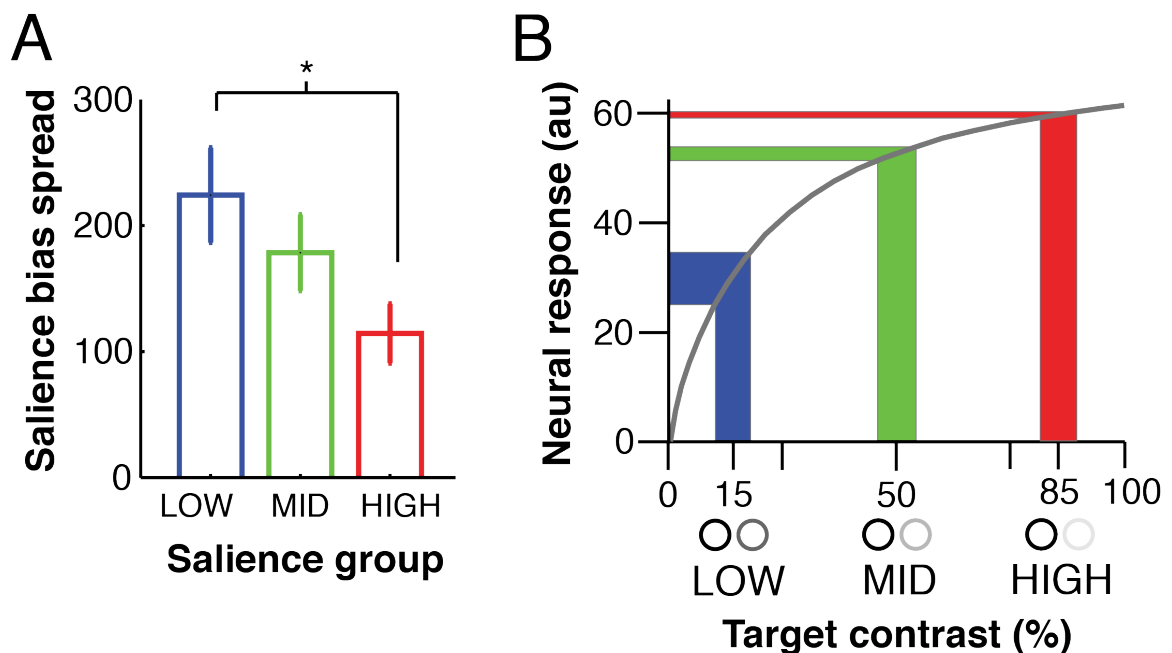


Figure 3.5 Between-group differences in salience-based bias function overlap. A, The degree of spread between the three salience-based bias functions (i.e., SAL-NUM, SAL,

and SAL+NUM), compared across salience groups. The magnitude of salience bias spread is inversely proportional to the influence of numerosity within a given target salience group. Error bars indicate SEM. * $p < 0.05$. *B*, Target contrast values of the three salience groups, mapped onto the logarithmic contrast response function. This figure illustrates the proposed mechanism underlying the results depicted in *A*.

We noted that the salience-based bias functions (i.e., SAL-NUM, SAL, and SAL+NUM) showed differing degrees of overlap between the three different salience groups (Figure 3.3 *B*). We quantified salience bias spread as follows: for each participant, we first averaged each of the three salience-based bias functions over the entire temporal range. We then assigned each of these values a difference score by subtracting the grand mean of all three from each individual bias function mean. Next, we took the slopes of a linear regression over the three resulting difference scores for each participant. In essence, the steepness of the slope is a measure of the degree of spread between the three salience-based bias functions. In turn, the degree of spread is indicative of the magnitude of the numerosity effect in the SAL-NUM and SAL+NUM bias functions. In other words, a smaller salience bias spread indicates a weaker influence of numerosity. Figure 3.5 *A* depicts the average regression slopes for the three target salience groups. Only the difference between the LOW and HIGH salience groups came out as significant ($p = 0.015$). Given the general direction of the effect and the significant difference between the LOW and HIGH groups, we take this as evidence that increasing the contrast difference between targets (and, by extension, the magnitude of salience) diminishes the effect of numerosity in visuomotor competition.

Figure 3.5 *B* depicts a possible mechanism to explain the groupwise differences in salience spread; it shows the target contrast values of the salience groups mapped onto the logarithmic contrast response function. The function is expansive at low contrasts and compressive at high contrasts (Boynton, Demb, Glover, & Heeger, 1999). In other words, a given span of contrast values at a

high range evokes a thinner band of neural responses than the same span of contrast values at a lower range.

3.4.2 Target salience affects the timing and magnitude of trajectory biases

The group-average bias functions reported above (i.e., Figures 3.3 and 3.4) are informative with respect to important general trends in the data. However, they would not reveal potentially interesting individual differences in the shapes of those functions for the different participants. To investigate what those shapes were, we fitted individual participants' bias transition functions with logistic, cubic, and linear functions (see Figure 3.2 C). For the logistic fit, we used a variant of the generalized logistic function:

$$Y(x) = A + K \left(\frac{1}{1 + e^{-(M+Bx)}} \right)$$

where A (value at maximum growth) and K (scaling factor) define the asymptotes and carrying capacity, B is the growth rate, and M is the time of maximum growth.

Overall, the best fit to the individual bias transition functions was with a cubic function (mean SSE = 0.46 au), followed by the logistic (mean SSE = 0.67 au) and linear (mean SSE = 1.88 au) functions (t-tests yielded $p < 10^{-7}$ for all contrasts). None of the participants had data that were best fit by a linear function, while 58.23% had data best fit by a cubic, and 41.77% had data best fit by a logistic function. In those cases where the best fit was logistic (and, indeed, in most other cases), the cubic function typically approximated the sigmoidal shape of a logistic function (see Figure 3.2 C).

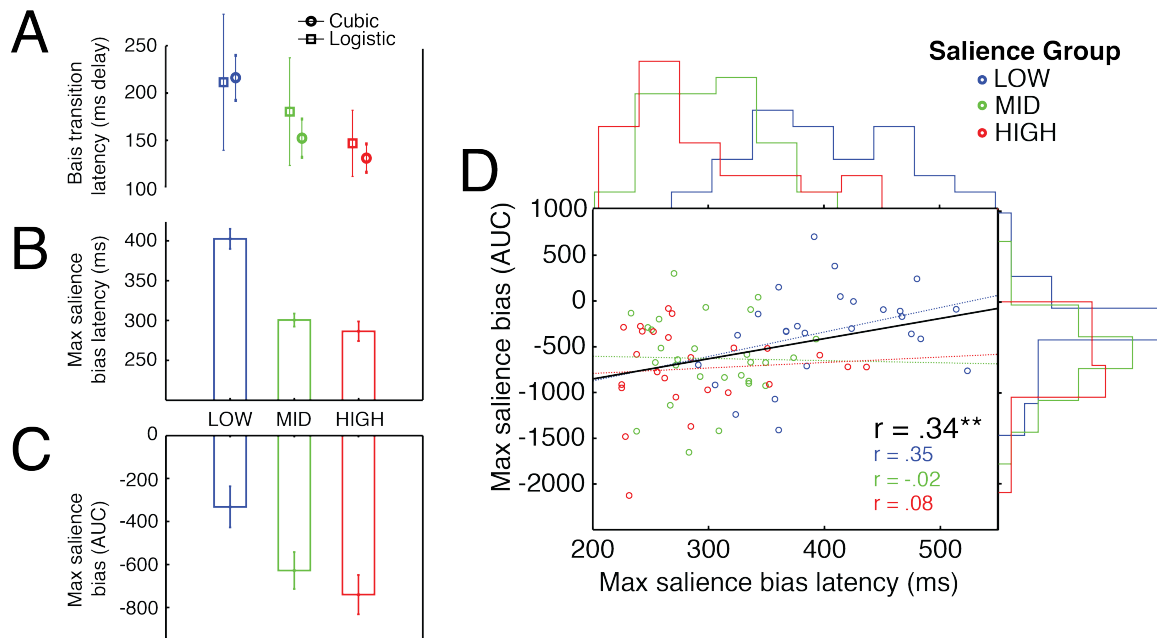


Figure 3.6 Maximum salience bias and bias transition latency. *A*, Measures of bias transition latency extracted from cubic and logistic fits to individual performance in the SAL-NUM display condition (see Figure 3.2D). In spite of the resemblance of the two fits, there were no significant latency differences between salience groups for the logistic fits, due to significantly higher variability. *B*, Average latency of the max salience bias for the respective salience groups. *C*, Average max salience bias for the respective salience groups. *D*, The magnitude of the maximum salience bias predicts the latency of the point where the maximum is reached. Participants with a stronger maximum salience bias tended to reach that maximum earlier than others. Histograms depict, on their respective axes, the distribution of data points for the three different salience groups. All error bars indicate SEM.

We characterized the latency of the SAL-NUM bias transition in three separate ways. First, we took the latency of the max salience bias (Figure 3.2 D). Second, we took latency of the inflection point on the logistic fit of the bias transition function (i.e., the bias function for the SAL-NUM condition). Third, we took the first inflection point of the cubic fit of the bias transition function (Figure 3.2 C). In cases where this first inflection point occurred after the first positive bias peak of

the fit (i.e., the first zero-crossing of the cubic's first derivative was from negative to positive instead of positive to negative), we approximated an inflection point by taking the midpoint between the peak and the previous lowest point in the data.

These three independent measures of bias transition latency all pointed to the same conclusion, although with varying degrees of reliability. In each case, the mean bias transition latency was inversely related to target salience (see Figure 3.6 A and B). There was a main effect of contrast on max salience bias latency, $F(2,76) = 32.21$, $p < 10^{-5}$. The same was true of cubic inflection latency, $F(2,76) = 4.56$, $p < 0.05$. The test for an effect of contrast on logistic inflection latency, however, failed to reach significance, $p = 0.078$. The pairwise comparisons for the max salience bias latency and the cubic inflection latency revealed a significant difference between the LOW and HIGH salience groups (max salience bias: $p < 10^{-5}$; cubic inflection latency: $p < 0.05$), and a significant difference between the LOW and MID salience groups in the case of max salience bias latency, $p < 10^{-5}$. Taken together, these three separate analytical approaches provide converging evidence that bias transition latency increases as the luminance contrast of the low-contrast target increases (or, in other words, as the salience of the high-contrast target decreases).

We also found a main effect of salience group on max salience bias, $F(2,76) = 5.25$, $p < 0.01$. Pairwise comparisons were significant only between the LOW and HIGH contrast groups, $p < 0.01$ (although the comparison between LOW and MID groups approached significance, $p = 0.068$ after correction). We conclude that the manipulation of luminance contrast produced a graded effect upon the degree of bias toward the more salient target. In other words, the more salient the high-contrast targets, the more participants reached in the direction of those targets.

The relationship between the magnitude of the salience bias and how quickly it began to transition toward a numerosity bias was illustrated in the moderate correlation between max salience bias and max salience bias latency, $r = 0.34$, p

< 0.01 (Figure 3.6 *D*). Given that this correlation was not significant within the individual salience groups, the significance of the correlation across all groups points to the differences between them. These differences could also be observed in the respective distributions of these variables for the respective salience groups, as seen in the histograms plotted on the axes of Figure 3.6 *D*.

3.4.3 Individual differences in maximum salience bias are predicted by target enumeration speed

During pilot testing for the reaching task, we took note of the considerable variability in the degree to which individual participants were susceptible to the respective salience and numerosity biases, even within a given salience group. We suspected that this variability was attributable to differences in low-level visual processing, and that the latter might be quantified in a separate psychophysical task that measured speed in reporting the number of targets (of varying luminance contrasts) briefly flashed on a screen.

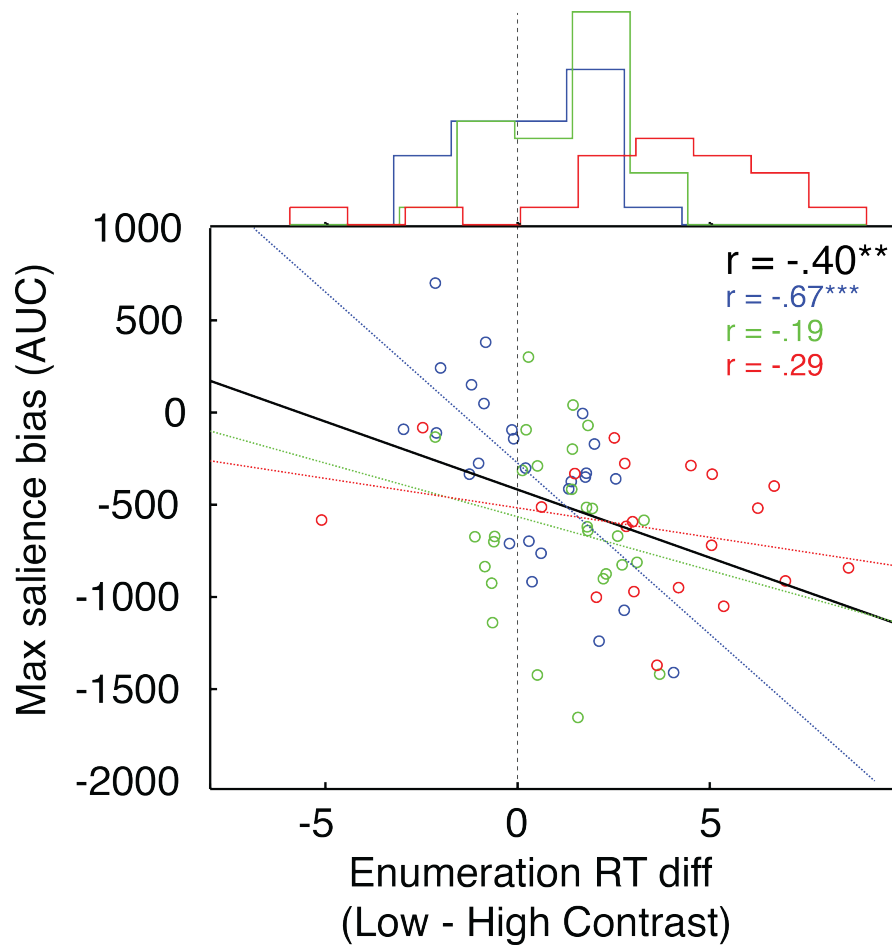


Figure 3.7 Target enumeration accuracy and RT are correlated with max salience bias. The RT difference between low- and high-contrast conditions is correlated with max salience bias in the reaching task. The black regression line represents the regression over all three salience groups, and corresponds to the Pearson's r value in black text. ** $p < 0.01$, *** $p < 0.001$

In our view, the most important result of the present study was a significant correlation observed between maximum salience bias and the RT difference between low- and high-contrast targets (collapsed over all target quantity conditions), $r = -0.40$, $p < 0.01$. The direction of the correlation indicates that the participants who took longer to respond to the low-contrast (relative to the high-contrast) targets in the enumeration task were more influenced by salience in the reaching task. In other words, individual differences in differential processing

speeds for targets of varying luminance contrasts predicted the degree to which target salience biased reaching vectors.

Intriguingly, participants who were actually faster at detecting and enumerating low-contrast stimuli tended to have max salience biases that were inverted (i.e., the closest they got to a salience bias was still a numerosity bias; see upper-left quadrant of Figure 3.7). Recall that the max salience bias measure is derived from the SAL-NUM target pattern, in which there are two high-contrast targets on one side and four low-contrast targets on the other side. Thus, the participants with the inverted RT relationship in the enumeration task (i.e., faster at detecting low- than high-contrast stimuli) were actually more biased toward the four low-salience targets from the very beginning. If that bias was due to low-contrast targets actually being more salient for these participants, then the same participants may also have displayed a bias toward the low-contrast stimuli even when there were twice as many high-contrast stimuli on the other side of space (i.e., target display SAL+NUM).

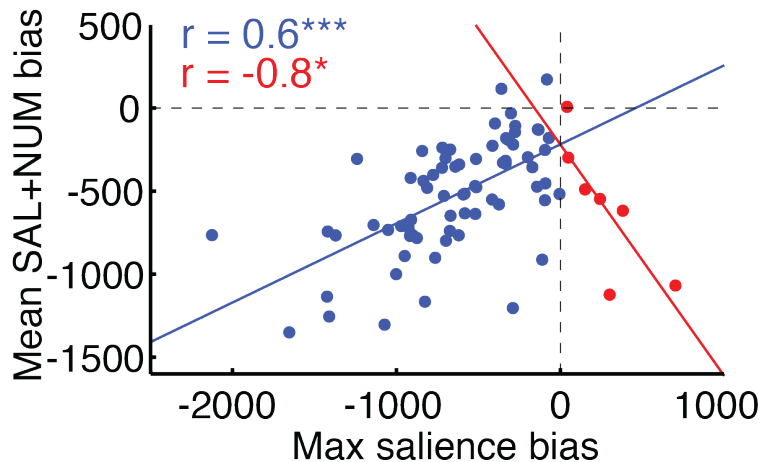


Figure 3.8 Numerosity-tuning in a subset of participants. We regressed max salience bias (taken from SAL+NUM performance) against the mean of the entire bias function for the SAL-NUM display trials. We then divided participants according to negative or positive max salience bias scores (blue and red dots, respectively). The resulting groups showed a striking reversal in the relationship between the two variables, revealing a

subset of participants who were tuned to the numerosity of the target display, regardless of which targets were salient. * $p < 0.05$, *** $p < 10^{-7}$

To test this possibility, we regressed max salience bias against the average of the entire SAL+NUM bias function for each participant (Figure 3.8). The result was unexpected: the participants who had inverted max salience bias scores simply had increasingly stronger biases toward the higher number of targets, regardless of which targets were more salient. Of the 7 participants who showed this pattern (red dots in Figure 3.8), 5 of them were in the LOW salience group, and 2 were in the MID salience group. Note that this does not rule out the possibility that, for these participants, the low-contrast targets were also slightly more salient due to faster processing (but not salient enough to overcome their powerful tuning to numerosity). What it does indicate is that, for those participants who showed salience-invariant numerosity tuning, the difference between low- and high-contrast target enumeration time was either reversed (compared to the average) or eradicated.

3.5 Discussion

This study employed a variant of the multiple target reaching task (C. S. Chapman, Gallivan, Wood, Milne, Culham, & Goodale, 2010a) to (1) explore the interaction of numerosity and salience throughout an extended period of visuomotor competition, and (2), critically, to test for a correlation between relative processing speed and susceptibility to salience bias. While the present study yielded a number of findings, for the sake of brevity we focus our discussion upon two primary contributions: (1) luminance contrast differences between competing targets result in persistent biases that diminish, but are not extinguished, over the course of 750 ms, and (2) visual processing speed predicts the degree of capture by salience.

3.5.1 Target salience persistently influences reach directions over a broad temporal range

By combining the instructed delay (0-450 ms) and the spontaneous RT of each trial, we were able to sample reaches at latencies from 150 to 750 ms. We observed persistent effects of salience on initial reach vectors across this entire range (see Figure 3.4). Two findings support this claim: (1) the SAL bias function never diminished to zero, as would be expected if the effects of salience were only transient, and (2) the SAL-NUM bias transition function never fully made the transition from the salience bias to the numerosity bias (even in the LOW salience group, in which the high- and low-contrast targets only differed in contrast by 15%), but instead settled at equilibrium between the two biases. Again, if salience were not a factor during the last half of the sampled range, we would have expected to see a clear transition to a numerosity bias.

Other studies have reported that salience exerts only a brief effect upon movement trajectories. This question has been addressed in detail for the oculomotor system. Using various measures, including RT (Dombrowe et al., 2010; Donk & Soesman, 2010), accuracy (Donk & van Zoest, 2008), and saccade trajectory deviations (van Zoest et al., 2012), Donk and colleagues have provided convincing evidence that the facilitative effects of salience typically abate by 250-300 ms. Aside from the fact that these studies measured eye movements instead of reaching movements, another important difference is that they used visual search tasks, in which there is typically one correct target and a distractor that varies in salience. In contrast, our task lacked a search element; it was designed such that participants could immediately distinguish and enumerate the stimuli, each of which was a potential target for the reach, and therefore task-relevant. Indeed, at the point of the reach sampled in the present analysis (i.e., 20% of reach distance), participants were still treating all of the stimuli on the screen as potential targets. It is likely that the distributed attention to (and ongoing intention to act upon) the individual targets had a continuous facilitative effect on the processing of those targets (Anton-Erxleben & Carrasco,

2013; Baldauf & Deubel, 2010). Such facilitation may have extended the temporal profile of any concurrent salience responses, effectively countering the reflexive inhibition of the salience response typically observed when the site of the salient stimulus is not task-relevant (as is the case in the studies of Donk and colleagues). This is consistent with the observation that, in primate lateral intraparietal area (which many researchers consider to be a candidate location for the salience map), responses to salient targets are stronger and more prolonged than responses to a salient distractor (Arcizet, Mirpour, & Bisley, 2011).

In summary, bottom-up salience exerts a transient effect only when the salient stimulus is task irrelevant. When task relevance and visual salience overlap (which, at the very least, is the case any time there are salience differences between multiple targets for action in our environment), the effects of salience persist much longer.

3.5.2 Range of visual processing speed predicts susceptibility to capture by target salience

The results of our study are consistent with the hypothesis that trajectory deviations toward salient stimuli are caused by differential processing times for the competing stimuli. Previous support for this hypothesis has been limited to showing differences in average latency-to-peak-salience effects between levels of a contrast manipulation (Dombrowe et al., 2010), an effect that we also demonstrate here in the form of various timing differences between the three salience groups (see Figure 3.6 A and B). Critically, we demonstrate that the peak magnitude of salience bias for a participant's reaching performance scales with the degree to which their detection and enumeration of high-contrast stimuli is faster than their performance for low-contrast stimuli (Figure 3.7). It is not surprising that there are individual differences in salience bias, nor is it surprising that there are individual differences in the speed with which targets of different contrasts are processed. What is striking is that these two are correlated.

We offer some possible interpretations of this finding. In traditional salience map models, salience is sculpted by an iterative application of the difference-of-Gaussians filter properties of the centre-surround cells in the map. While this mechanism is based upon rate-coding of spikes, it does not rule out the possibility that other mechanisms may contribute to the formation of activity peaks in the salience map. For example, Nakamura (1998) showed that spike order coding could plausibly work in concert with lateral inhibition to suppress later spikes for less salient locations. This combination of the two models (i.e., salience map and spike order coding) is appealing in the case of visuomotor processing, since it retains the unique ability of salience map models to represent the competition of multiple simultaneous targets while also opening the door to the fast, efficient coding of salience through spike order coding.

We stress here that differential processing speeds for targets of varying contrast could be the result of a straightforward rate-coding computation in the salience map. If this is the case, our results suggest that there are individual differences in the sensitivity of the spatial summation process, and that these differences would predict susceptibility to salience bias in a reaching task. On the other hand, if spike order coding is at all involved in the coding of salience, then our results suggest that individual differences in retinal contrast sensitivity would be correlated with salience bias. The lag between retinal ganglion spikes for low- and high-contrast targets would be preserved throughout visual processing (Van Rullen & Thorpe, 2001). Whatever the coding strategy, our results indirectly suggest that the intensity of the salience response in the visuomotor system depends upon differences in the speed with which the various locations of a scene are processed. A prediction that follows from our results (and is consistent with both mechanisms above) is that psychophysical testing should reveal individual differences in contrast sensitivity thresholds that correlate with susceptibility to salience bias.

The key to understanding many of the effects reported here resides in the logarithmic response function for visual contrast (2011; Heeger et al., 2000). Due

to the same normalization mechanisms responsible for the contrast response function (Carandini & Heeger, 2012), if two stimuli of differing contrast are presented simultaneously, the response for the high-contrast stimulus is a logarithmic function of the contrast of the low-contrast stimulus (Busse et al., 2009). We interpret the pattern of differences between the three salience groups in our study as evidence of response saturation. In other words, due to the logarithmic relationship between relative contrast (i.e., salience) and neural response, the high-contrast targets in the MID and HIGH salience groups are already near the upper asymptote of the response function, which means that there should be a sharper distribution of data points within these conditions. A clear example of this is illustrated in Figure 3.6 *D*, where the max salience bias latency values tend to cluster near the lower end of the range for the MID and HIGH groups, while the distribution of the LOW group values is more broadly tuned across the possible range.

A logarithmic response function for target salience explains (1) the increase of salience bias spread as target salience decreased (see Figure 3.5), including the near overlap and occasional reversal of expected differences between bias functions of the MID and HIGH salience groups (see Figure 3.3 *B* and Figure 3.4 *B*), (2) the large difference between the LOW group and the other two groups (and the lack of any difference between those other two groups) in both the bias transition latency and the max salience bias measures (see Figure 3.6 *A-C*), and (3) the high correlation between max salience bias and RT difference for the LOW salience group, compared to the lack thereof for the MID and HIGH groups.

3.5.3 Conclusions

Here we characterized, at a fine temporal scale, the interaction of salience and numerosity as biasing factors in visuomotor competition. The influence of numerosity was relatively slow to come online, first appearing at ~150 ms, peaking at ~350 ms, and then remaining stable throughout the rest of the sampled time range. The influence of salience came online prior to the earliest of

RTs, peaked at ~300 ms, and proceeded to decay logarithmically until it relaxed (at ~450 ms) into a diminished but persistent state of bias throughout the rest of the delay range. This latter finding prompts a qualification of the relatively well-established dogma that salience exerts only a short (~250 ms) influence on visuomotor processing: when the entire salience landscape happens to spatially overlap with task-relevant target locations, then the time course of salience is extended. Finally, we showed that individual differences in relative processing time for stimuli of differing contrasts predict the degree of capture by target salience. This result provides indirect support for the hypothesis that the magnetic effect of contrast-induced salience on goal-directed movements during visuomotor competition arises out of differences in the speed with which targets of varying contrast are processed by the visuomotor system.

Chapter 4: Target luminance contrast modulates stimulus-locked responses on human pectoralis major

4.1 Abstract

Primates and other vertebrates possess a wide range of involuntary, reflexive responses to stimuli. These involuntary responses often precede, and bleed into, more voluntary, controlled responses. A class of stimulus-locked muscle responses to peripheral targets have recently been observed in neck and upper limb muscles. These muscle responses are precisely locked to the timing and the location of the stimulus, regardless of the timing or direction of the ensuing voluntary response. In the present study, we set out to test the hypothesis that these stimulus-locked responses are mediated by a fast visual pathway that directly transforms visual information into muscle commands for the purpose of reflexive orienting. We show that the latency and magnitude of the upper limb stimulus-locked response is modulated by the luminance contrast of the target. We also show that, when the visuomotor system is primed for an immediate movement, both spatially informative and spatially uninformative cues-to-move will elicit a spatially tuned stimulus-locked response, even after a delay. Finally, we report a 12-15 Hz oscillation in the stimulus-locked response. This last finding has implications for the possible origins and purpose of the stimulus-locked response.

4.2 Introduction

The onset of moving or stationary stimuli has been shown to give rise to fast, reflexive, and highly tuned recruitment of proximal limb musculature in humans, monkeys, and cats (Fautrelle, Prablanc, Berret, Ballay, & Bonnetblanc, 2010; Perfiliev, Isa, Johnels, Steg, & Wessberg, 2010; Saijo, Murakami, Nishida, & Gomi, 2005; Schepens & Drew, 2003). Recently, Pruszynski et al. (2010) demonstrated the existence of a fast pulse of upper limb muscle activity that was locked to the onset of a visual target in a reaching task with humans. This stimulus-locked response (SLR) showed clear spatial tuning in chest and shoulder muscles approximately 100 ms after stimulus presentation, regardless of the ensuing manual reaction time for the reach. The temporal and spatial precision of the SLR suggests that it could have functional consequences for reaching behaviors that rely on rapid visual feedback, such as online trajectory correction and protective reflexes. However, the existing literature has little to say about the degree to which the SLR is exclusively a reflexive, involuntary response toward salient stimuli.

One clue comes from the literature on neck muscle activity during eye-head gaze shifts, where stimulus-locked activity has been observed and investigated more thoroughly (Corneil, Munoz, Chapman, Admans, & Cushing, 2008; Corneil, Olivier, & Munoz, 2004). Chapman et al. (2011) recently demonstrated that monkeys performing an anti-saccade task showed a SLR recruiting neck muscles used to orient the head toward the target, even when the monkeys correctly looked in the opposite direction on anti-saccade trials. If, as this latter result suggests, the SLR is mediated by a short-latency pathway that directly transforms visual information into motor commands, it may be that the quality of the visual information is reflected the SLR. Here we tested this idea and specifically we assessed whether the SLR might play a role in the well-established tendency of reach and saccade trajectories to reflexively deviate toward salient targets or distractors (Van der Stigchel, 2010; Wood et al., 2011) in a manner that scales with the relative salience of the stimulus (Schütz et al.,

2012). We addressed this question by recording electromyographic activity from a muscle involved in rapid shoulder rotation (pectoralis major, clavicular head) while subjects reached toward targets that varied in luminance contrast. This allowed us to test the prediction that the conspicuity of the target onset would modulate the timing and intensity of the SLR.

Note that there are reasons to doubt that the SLR is exclusively driven by the onset of a salient stimulus. For example, anticipatory postural adjustments in the limb muscles of cats performing an instructed delay task are time-locked not to the onset of a spatially informative target stimulus, but rather to a delayed, spatially uninformative cue to move (Schepens & Drew, 2003). Thus, to further test the hypothesis that the SLR is primarily a reflexive response tuned to the onset of a target, subjects also performed an instructed delay task in which the cue-to-move was the disappearance of a central fixation circle.

Consistent with past reports (Corneil et al., 2004; 2008; Pruszynski et al., 2010), our results confirmed the presence of stimulus-locked muscle activity in response to the onset of a reach target. We report here three main results that highlight the sensitivity of this phenomenon. First, we demonstrate that the magnitude and latency of the upper limb SLR is modulated by the conspicuity of the stimulus. Second, we show that, when the visuomotor system is primed for an immediate movement, both spatially informative and spatially uninformative cues-to-move will elicit a spatially tuned SLR, even after a delay. Third, we report the presence of a 12-15 Hz oscillation in the SLR. This latter finding has implications for the possible origins and purpose of the SLR phenomenon.

4.3 Materials and Methods

A total of 15 human subjects (ages 21-41; all male) participated with informed consent, and were paid for their participation. Six of the subjects participated in both of the two experiments reported here. All procedures were approved by the University Research Ethics Board for Health Science Research at the University of Western Ontario. All subjects reported no history of visual, neurological, or

musculoskeletal disorder. One of the subjects was left-handed; all others were right-handed.

Apparatus. Subjects performed reaching movements while grasping the handle of a robotic manipulandum (InMotion Technologies) with their right hand (Figure 4.1A). A six-axis force transducer (ATI Industrial Automation, Apex, NC; resolution: 0.05 N), which was located inside the handle, measured manual forces. The position of the manipulandum in the horizontal plane was sampled at 600Hz. Subjects sat at a desk and interacted with the robot in a horizontal plane at shoulder height. A custom air sled, secured below the subject's right elbow, supported the arm during movements. All stimuli were presented on a horizontal mirror, placed just below chin height, that reflected the display of a downward-facing LCD monitor. The mirror occluded the subject's view of his/her arm. Real-time visual feedback of hand position was provided by way of a small red dot projected on the mirror by the LCD monitor. The precise timing of visual events on the screen was determined with a photodiode.

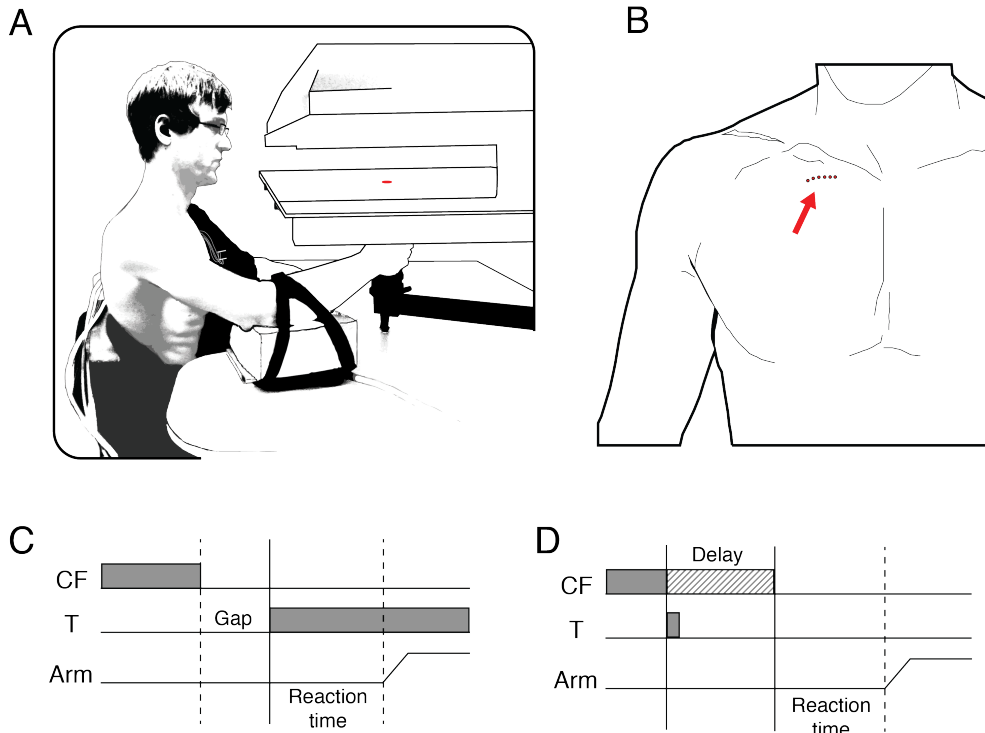


Figure 4.1 Experimental paradigm. *A*, Subjects held the handle of a robotic arm, with their arm supported by an air sled. They viewed both the reach targets and a cursor representing real-time position of their hand on a mirror surface that reflected the output of a downward-facing LCD screen. *B*, The arrow indicates the approximate placement of electrodes in the clavicular head of pectoralis major (cPM). *C*, Trials in the luminance contrast task started with subjects holding the cursor in the central fixation circle (CF). The CF disappeared 200 ms prior to target (T) onset, after which subjects immediately reached toward the target. *D*, Trials in the delay task also started with the cursor in the CF. The target then briefly flashed for 150 ms. The CF disappeared either at target onset, or after a 1 sec delay. CF disappearance was the cue to reach toward the remembered location of the target.

Muscle electromyography. We recorded electromyographic (EMG) activity from the clavicular head of the right pectoralis major (cPM). Recordings were made with intramuscular electrodes, using staggered monopolar insertions to characterize cPM recruitment across multiple motor units. Six insertions (i.e., 3 channels with 2 electrodes each) were spaced ~1cm apart, typically 1cm below (inferior to) the clavicle, with the most lateral insertions placed just under the

lower clavicular convexity (see Figure 4.1B). A surface ground electrode was placed on the left clavicle. EMG data were recorded with a Myopac Jr system (Run Technologies; low-pass filter modified to 2 kHz). The EMG data were amplified and sampled at 4 kHz. Offline, EMG signals were then full-wave rectified and downsampled to 1000 KHz. The MATLAB function that we used to downsample (i.e., the *decimate* function) performs a low-pass filter prior to resampling, which reduces aliasing.

4.3.1 Experimental tasks

In both tasks, subjects were instructed to move as quickly as possible, and to overshoot the target. During piloting, we found that a higher baseline EMG signal, induced by a constant load force on the arm, had a beneficial effect on the detectability of the stimulus-locked response (SLR). Thus, we used the robotic arm to generate a constant load force of 5.3 N (5 N to the right, 1.75 N down) opposite to the direction of the upper left target from the starting position.

Luminance contrast. Subjects ($n = 11$) performed a centre-out reaching task toward a single target. A trial started when the subject brought the cursor (a red dot representing real-time hand position) into a central fixation circle and maintained that position for 2.5 s. The fixation circle then changed color to signal the beginning of the trial. After 1 – 1.5 s (randomized), the fixation circle disappeared. Exactly 200 ms later, a target appeared 10 cm from fixation, in one of two locations: (1) 160 degrees (i.e., upper left target), or (2) 340 degrees (i.e., lower right target) from fixation.

We used four different levels of target luminance contrast. The targets were different shades of gray against a white background (350 cd/m^2). The lowest contrast target (TC1: 335 cd/m^2) had a Weber contrast ratio of 5%. The second lowest contrast target (TC2: 300 cd/m^2) had a Weber contrast ratio of 15%. The second highest contrast target (TC3: 230 cd/m^2) had a Weber contrast ratio of 35%. Finally, the highest contrast target (TC4: 5 cd/m^2) had a Weber contrast ratio of 99%. Luminance was measured with a Minolta LS-110 photometer.

Delayed reaching. Subjects ($n = 10$) performed an immediate/delayed reaching task. After a variable inter-trial interval, subjects were presented with a single target in one of the two locations (and at the same level of contrast as the TC4 condition) described in the luminance contrast task. Subjects were instructed to initiate the reach only after the disappearance of the central fixation circle. This could happen either (1) immediately, concurrent with target onset, or (2) 1 s after target onset. Critically, the no-delay and delay trials were randomly interleaved. In both conditions, the target was on the screen for only 150 ms. The target reappeared momentarily once the hand reached it.

4.3.2 Data Analysis

Kinematic analysis

In order to achieve sample-to-sample locking between kinematic and EMG data, kinematic data were up-sampled from 600 to 1000 Hz with a lowpass interpolation algorithm, and then lowpass filtered with a second-order Butterworth filter, using a cutoff at 150 Hz. Reaction time was calculated as the time from the appearance of the reach target, as measured by the photo-diode located on the LCD screen (luminance contrast task) or the disappearance of the central fixation point (delay task) to the initiation of the reach. Reach initiation was identified by first finding the peak tangential hand velocity, and then finding the closest previous point at which the velocity profile reached 5% of the peak. Errors in reach direction were determined by sampling the position of the hand 100 ms after reach initiation. If the position was not within $\pm 45^\circ$ of the true target location, the reach was classified as an error and was excluded from analysis. Since the RT distributions with the longest tails extended, at most, into the 600 ms range, RTs slower than 700 ms were also excluded from analysis.

Receiver-operating characteristic analysis

Receiver-operating characteristic (ROC) analysis was used to determine the presence and timing of stimulus-locked activity in the cPM muscle recordings.

The specific method used here is similar to what has been used in past studies (Corneil et al., 2004; Pruszynski et al., 2010). We separated EMG waveforms by target location and target contrast (luminance contrast task) or delay duration (delay task). These waveforms were then smoothed with a 7-point (7 ms) running average. For every sample (1 ms) between 100 ms before and 300 ms after target presentation (both tasks) or fixation disappearance (delay task), we calculated the area under an ROC curve. This metric indicated the probability that an ideal observer could discriminate between a leftward (cPM as agonist) and rightward (cPM as antagonist) reaching movement, based on the distribution of EMG activity at that particular sample. A value of .5 indicates chance discrimination of the ideal observer, while values of 0 and 1 indicate perfect discrimination. We set the threshold for discrimination at .675 (or .325 for the opposite direction), which is similar to (although slightly more conservative than) what was used in Pruszynski et al. (2010). Time of earliest discrimination was defined as the time after stimulus onset (luminance contrast task) or fixation disappearance (delay task) at which the ROC area surpassed .675, and remained above that threshold for at least 5 of the next 10 samples.

One of the primary goals of the present study was to test whether or not the luminance contrast of a target modulates the timing of stimulus-locked muscle activity. We used the ROC analysis to address this question. There were two practical hurdles, however. First, differences between target contrast conditions in the distribution of RTs meant that any differences in the timing of the earliest ROC discrimination for a given condition might simply be a function of the underlying RT distribution. The second practical hurdle was that reaction times were often very fast, even in conditions where no directional errors were committed (i.e., subjects were not merely guessing). Often, the large burst of muscle activity associated with the voluntary movement for these earliest RTs overlapped considerably with the temporal range where we expected to see evidence of stimulus-locked activity. This had the effect of “washing out” any potential signature of the stimulus-locked activity. This is illustrated in Figure 4.3A.

We addressed these difficulties by removing trials with the earliest RTs (and, by extension, EMG activity that overlapped the range of interest), thus simplifying the process of distinguishing between the presence or absence of stimulus-locked activity. Specifically, we removed trials in ascending order of RT while dividing the remaining trials into “early” and “late” RT groups (Figure 4.3A) and finding the slope of the relationship between the average RT and the earliest discrimination times for these two groups (Figure 4.3B & C). Whenever the slope of this relationship exceeded 67.5 degrees (i.e., halfway between unity at 45 degrees and perfectly vertical at 90 degrees), we combined the RT groups and performed the ROC analysis again. If a simple peak detection algorithm could detect a peak in the ROC time course between the time of discrimination and 30 ms thereafter (see Figure 4.3B and 4.4B), we assumed the presence of stimulus-locked activity. If (1) the slope of the discrimination time and RT relationship between the groups failed to exceed 67.5 degrees, or (2) a peak was never detected in the combined ROC where the slope did exceed 67.5 degrees, we assumed the absence of stimulus-locked activity.

Note that, in order for the analysis to reach the stage where the peak was detected, there had to be prior evidence that the timing of such a peak would be invariant with respect to RT. Thus, the latency of the ROC peak was assumed to be a faithful measure of the latency of stimulus-locked activity, in spite of differences between the RT distributions between target contrast conditions. We quantified the magnitude of the SLR for a given subject and contrast condition by taking the associated latency of the ROC peak and averaging the EMG activity within an 11 ms window with the peak latency at the center (i.e., 5 ms before to 5 ms after the peak). To normalize between electrodes (given large variability in mean EMG signal strength between electrodes), we then subtracted a baseline EMG value, calculated by taking the average of EMG activity 100 ms prior to stimulus presentation. Since we were interested in the within-subject relationships between SLR magnitudes for the various contrast conditions, and not necessarily patterns of SLR magnitude across subjects, we normalized the magnitude measures within subjects. Accordingly, we divided the magnitude

score for each contrast condition by the mean score across all contrast conditions. We performed ANOVAs and planned comparisons on the peak latencies and average SLR magnitudes for the four target contrast conditions. The p values for reported t-tests are therefore uncorrected.

For the delay experiment, we were less concerned with the latency or magnitude of any possible stimulus-locked activity, and more concerned with simply testing our hypotheses regarding the purpose of the SLR, and the associated predictions regarding its appearance in the various epochs of interest. We therefore ended the analysis at the stage where the slope of the relationship between RT and ROC discrimination time was quantified for the early and late RT trials.

4.4 Results

4.4.1 Luminance contrast task

We report here that the luminance contrast of the target in a reaching task modulated the timing and magnitude of the stimulus-locked response (SLR) in the muscle. This is illustrated in Figure 4.2, which shows raw and average EMG signal, locked to stimulus onset, for a single subject and for each of the four target contrast conditions. The SLR appears as a vertical band of excitation (agonist movement) or suppression (antagonist movement), approximately 100 ms after stimulus onset, regardless of RT. As shown in Figure 4.2, this band is more intense, and appears earlier, as the luminance contrast of the target increases.

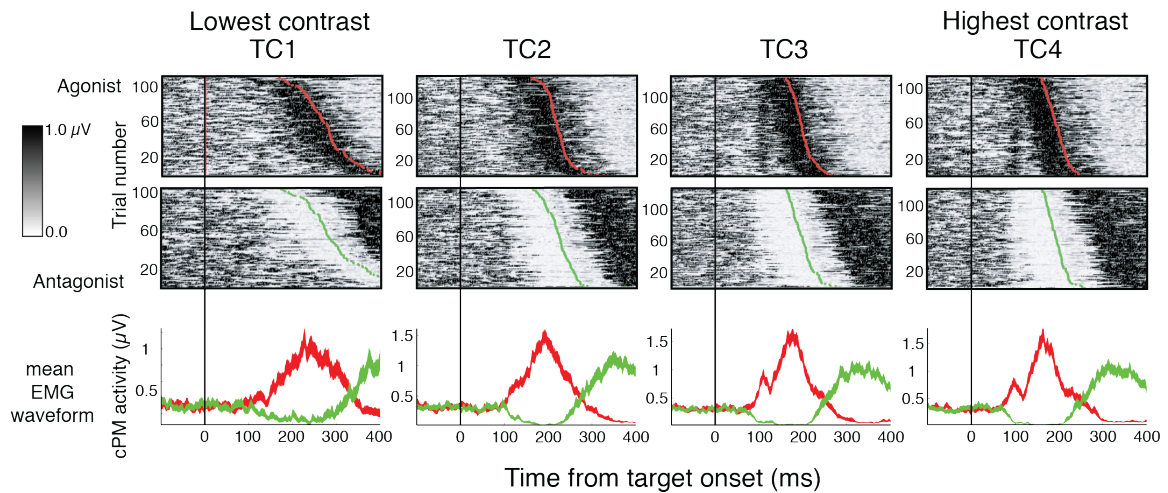


Figure 4.2 Exemplar EMG recordings from pectoralis major (clavicular head; cPM) of a single subject in the luminance contrast experiment. The top row of panels depicts activity for movements toward the upper-left target, where cPM acts as an agonist. The middle row depicts cPM activity for movements toward the lower-right target. Data are aligned to visual target presentation (black vertical line at 0 ms) and are sorted according to RT in descending order. Manual RT for each trial is marked with red (agonist) or green (antagonist) circles. Bottom row depicts mean EMG traces. The width of the trace subtends SEM. Columns are grouped by target contrast (TC) condition, with TC4 being the highest contrast.

Of the 11 subjects that participated in the luminance contrast experiment, 7 of them demonstrated stimulus-locked activity in response to at least one of the target contrast conditions (Figure 4.3D). That is, 7 of the subjects had a performance in at least one of the target contrast conditions such that the slope of the relationship between the average RT and ROC discrimination times of the muscle activity for slow and fast RT trials was above the threshold of 67.5 degrees. In each of these 7 subjects, a SLR was detected in the TC4 (i.e., highest contrast target) condition. We note here that the four subjects who failed to show evidence of stimulus-locked activity also had the highest percentage of trials discarded due to directional errors and RT violations. Without exception, these subjects had RTs that were exceptionally fast, which resulted in

considerable overlap between the expected range of the SLR and the robust EMG activity associated with the voluntary movement. Divergence between mean EMG traces for the two movement directions occurred shortly after target presentation, suggesting that these participants were engaging the task in a fundamentally different way, emphasizing speed by anticipating the position of the target, but at the cost of accuracy.

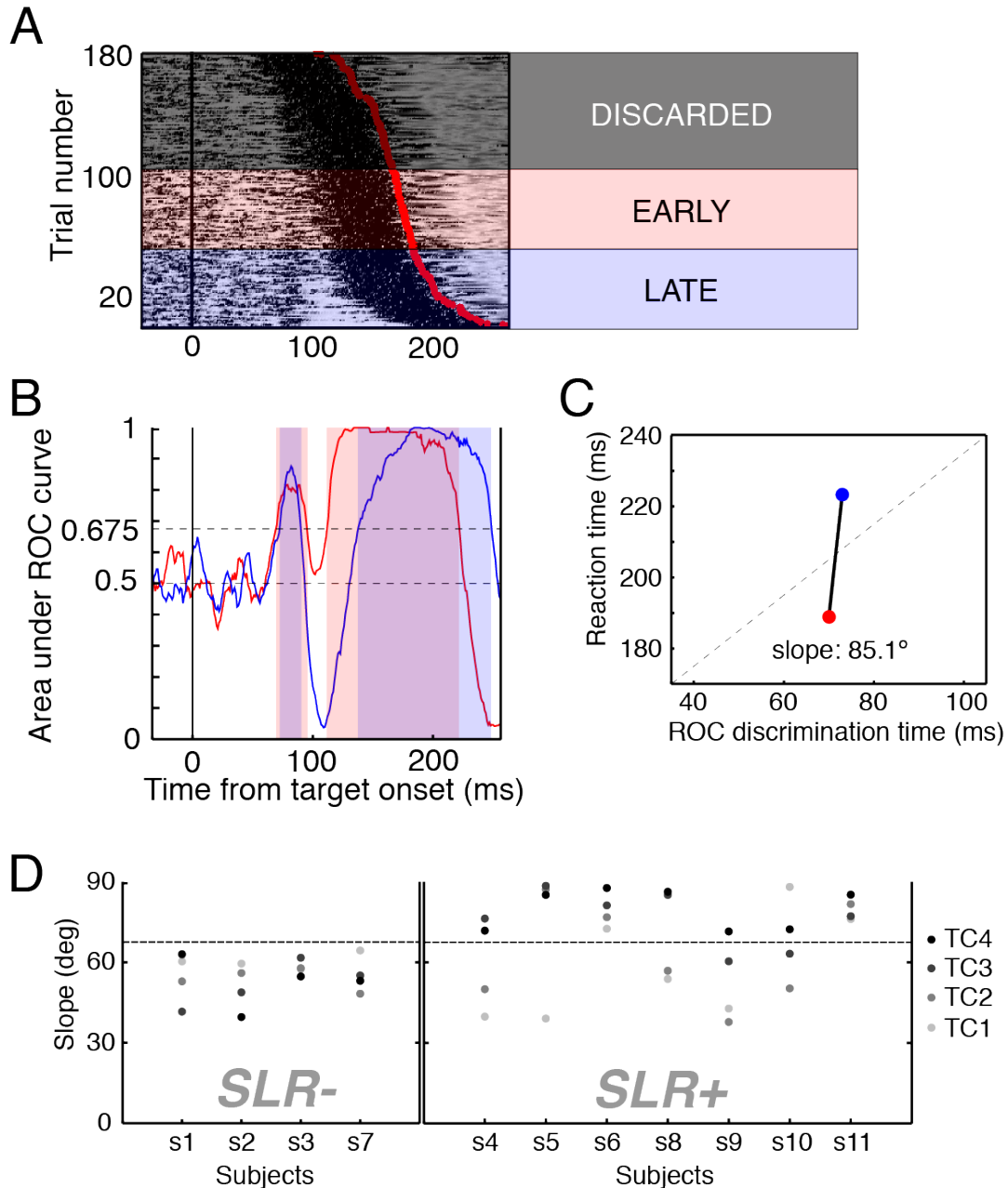


Figure 4.3 Detection of stimulus-locked activity. *A*, Exemplary EMG data, sorted by RT and locked to stimulus onset (black vertical line at time 0). Red circles indicate RT for a given trial. Trials were either discarded (due to temporal overlap between robust voluntary movement-related activity and the stimulus-locked band of activity) or separated into early (red) or late (blue) RT groups. *B*, Area under the ROC curve was calculated for each EMG sample (here, from Figure 4.3A) between 100 ms before and 300 ms after stimulus presentation (only a constrained time window is displayed here), for both RT groups (i.e., early and late). ROC discrimination time (RDT) was defined as

the time at which the ROC area first surpassed a value of .675. Red (early RT) and blue (late RT) transparent bands indicate samples at which the corresponding ROC area is over threshold. *C*, The slope of the relationship between RDT and average RT for early and late RT groups was calculated. Shown here is the slope for the data depicted in *A* and *B*. *D*, The slope threshold for detecting a SLR was set at 67.5 degrees (horizontal dotted line). Performance of all subjects in the luminance contrast task is shown. Individual dots represent the slope of the relationship between RDT and RT for the fast and slow RT trials, and the intensity of the dot corresponds to different target contrast conditions (see legend). The subjects are grouped into those who show the presence of stimulus-locked activity in at least one target contrast condition (SLR+) and those who do not (SLR-).

To test our prediction that target luminance contrast would modulate the timing of the SLR, we compared the latencies of the first peaks past threshold in the ROC time course for the 4 target contrast conditions. There was a significant effect of target contrast on SLR latency, $F(3,14) = 117.2$, $p < 10^{-9}$, $\eta_p^2 = 0.93$. Since we performed this analysis only where an SLR was detected, the target contrast conditions had unequal sample sizes. Accordingly, we used Welch's t test for planned comparisons. SLR latencies for TC4 ($N=7$, $M=94.14 \pm 1.52$ SEM) were significantly faster than those for TC3 ($N=5$, $M=107.6 \pm 1.97$ SEM, $p < 0.05$), TC2 ($N=3$, $M=122.33 \pm 2.41$ SEM, $p < 10^{-5}$), and TC1 ($N=3$, $M=152 \pm 1$ SEM, $p < 10^{-12}$). Latencies for TC3 were faster than those for TC2 ($p < .05$) and TC1 ($p < 10^{-15}$). Finally, latencies for TC2 were faster than those for TC1, $p < 10^{-10}$. These results demonstrate that stimulus-locked activity appears sooner when the luminance contrast of the target is higher (Figure 4.4A).

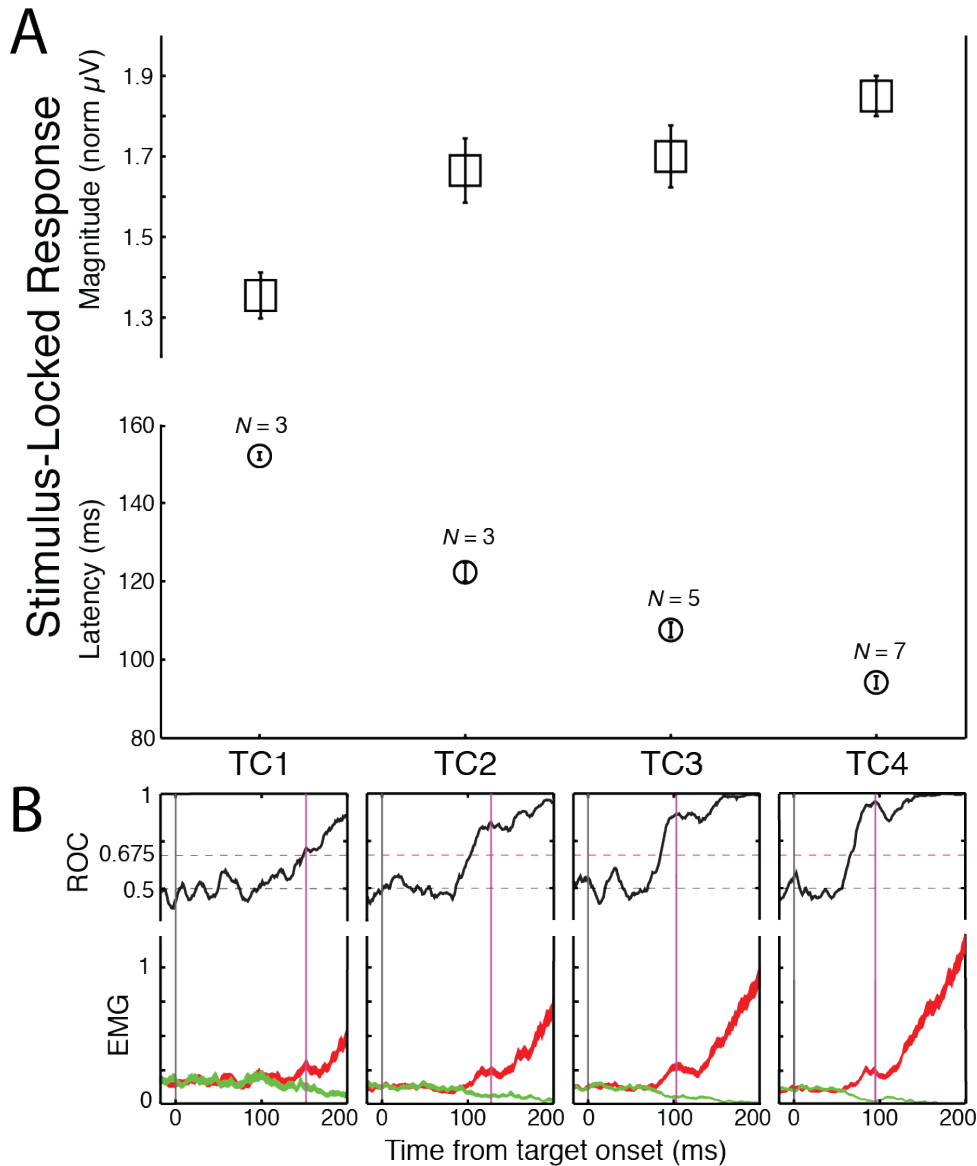


Figure 4.4 Contrast-modulated latency and magnitude of stimulus-locked activity. *A*, Average SLR magnitude (squares in upper axis) and latency (circles in lower axis) for the four target contrast conditions. Error bars (within the circles for latency values) indicate SEM. With the exception of TC2 vs TC3 in the magnitude data, all comparisons between conditions were significant for both measures, $p < 0.05$. *B*, Exemplary data from a single subject (different from individual subjects in Figures 4.2 and 4.3), illustrating the identification of peaks and their latencies in the ROC time course (black trace plotted above) for the four target contrast conditions. Black dotted line is .5 (chance discrimination), and red dotted line is .675 (discrimination threshold). Average EMG traces for agonist (red) and antagonist (green) movements are plotted below. Width of

traces subtends SEM. Magenta vertical line indicates timing of SLR peak in the ROC time course. Black vertical line at time 0 indicates stimulus onset.

Whenever stimulus-locked activity was detected, we used the timing of the associated ROC peak to define a 10 ms window (i.e., 5 ms before and after the peak) within which we calculated the average EMG activity, and then compared across target contrast conditions in order to test for differences in magnitude. To account for raw magnitude differences between different recordings within individual subjects, magnitude was calculated as the mean of the raw EMG signal within the 10 ms window, minus the mean of all activity 100 ms prior to stimulus presentation. Note that, while we report the actual magnitude values for each condition, we calculated the inferential statistics on normalized magnitude values (due to substantial differences between subjects). Thus, in order to preserve the subject-specific relations between magnitude values (rather than the idiosyncrasies of individual subjects' range of values), normalization was carried out by dividing each magnitude value by the within-subject mean of all magnitude values. There was a significant effect of target contrast on the magnitude of the SLR, $F(3,13) = 14.18$, $p < 0.001$, $\eta_p^2 = 0.62$. SLR magnitudes for TC4 ($N=6$, $M=1.85 \pm .05$ SEM) were significantly higher than those for TC3 ($N=5$, $M=1.7 \pm .07$ SEM, $p < 0.05$), TC2 ($N=3$, $M=1.67 \pm .08$ SEM, $p < 0.005$), and TC1 ($N=3$, $M=1.36 \pm .06$ SEM, $p < 0.001$). There was no difference between TC3 and TC2, but TC3 had higher SLR magnitudes than TC1, $p < 0.05$. Finally, magnitudes were higher for TC2 than for TC1, $p < 0.05$. These results suggest that stimulus-locked activity in the muscle is more vigorous when the luminance contrast of the target is higher (Figure 4.4 A).

4.4.2 Delay task

In the delay task, subjects reached toward a briefly-flashed (150 ms duration) high-contrast target. The cue to move was the disappearance of a central fixation circle. This cue was given at one of two times: (1) immediately, with stimulus

presentation, or (2) 1000 ms after stimulus presentation. One of the main goals of this experiment was to see if the onset of a spatially informative cue-to-move (in this case, the target) was sufficient to evoke stimulus-locked activity, even when the required movement was delayed. A second goal was to see if the presentation of a spatially uninformative cue to move (in this case, the disappearance of the central fixation circle) would also invoke a time-locked response in the muscle. Note that here we use the term SLR to refer to activity that is locked either to the target onset in both tasks or to the disappearance of the fixation circle in the delay trials.

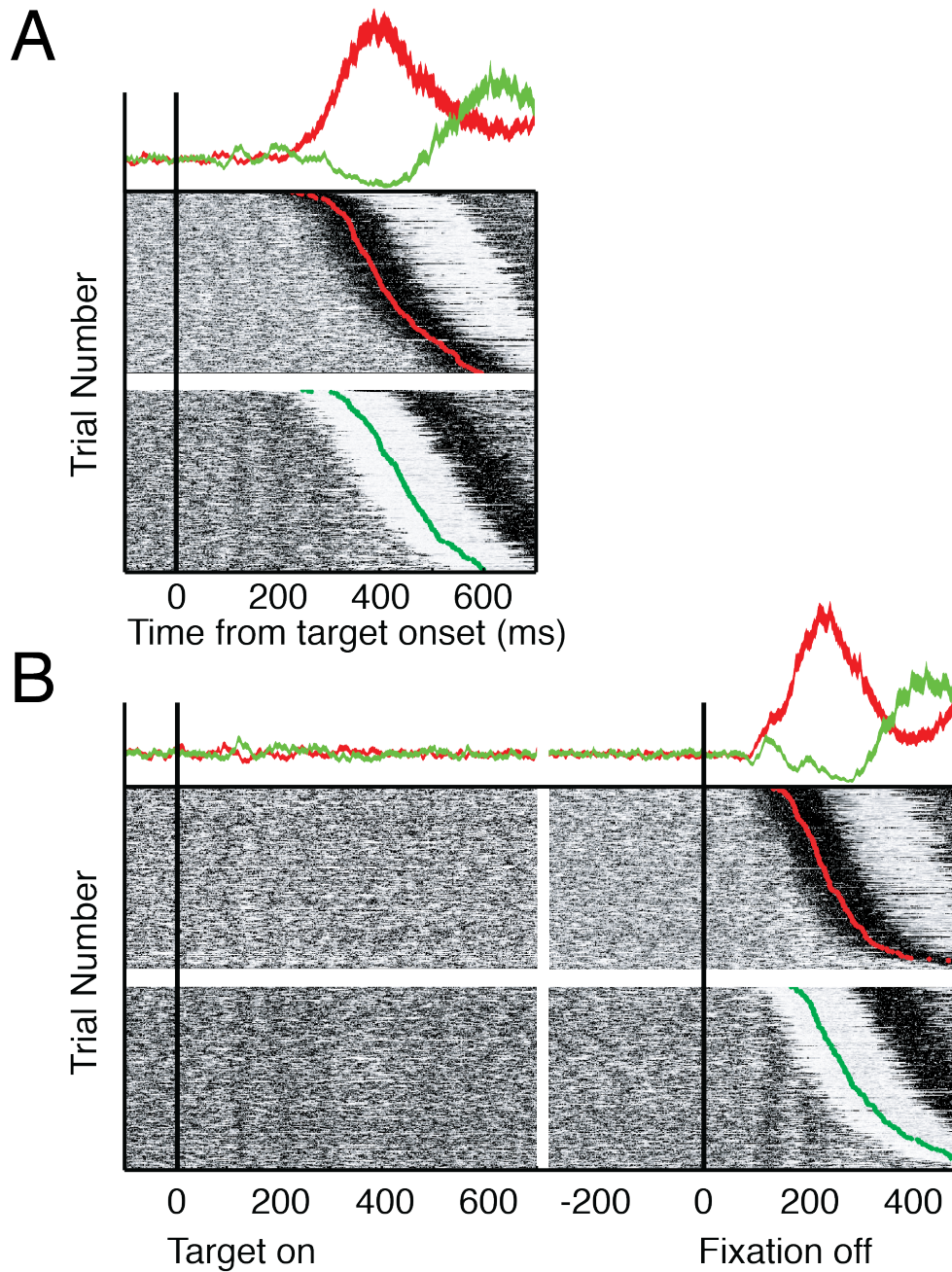


Figure 4.5 Exemplar recordings from a single subject in the delay experiment. Both panels contain EMG activity for individual trials, sorted by RT. Darker colors represent greater EMG activity. Red (agonist movement) and green (antagonist movement) dots represent manual RT. Mean EMG traces are plotted above each pair of panels. *A*, Data from the no-delay condition, locked to stimulus onset. *B*, Data from the delay condition. The first 800 ms (i.e., -100 to 700) are locked to stimulus onset, while the last 800 ms

(i.e., -300 to 500) are locked to disappearance of central fixation. Approximately 150 trials are depicted in each cluster (on the ordinate).

We observed stimulus-locked activity in three separate EMG epochs: (1) stimulus-locked with no delay, (2) stimulus-locked, but with a delay, and (3) locked to disappearance of the fixation circle after a delay. We used the same analysis described for the luminance contrast task. In short, we searched for cases where the slope of the relationship between average RT and ROC discrimination time for early and late RT trials exceeded the threshold of 67.5 degrees.

Figure 4.6 shows the performance of a single subject in the delay task. In this particular subject, we detected an SLR in each of the epochs. Here the SLR appeared as an oscillating band, primarily in the antagonist EMG recordings, starting at around 100 ms. Figure 4.6 A (stimulus-locked, no delay) is essentially a replication of the TC4 condition in the luminance contrast task. Figure 4.6 B demonstrates that the SLR can be detected even when it is not immediately followed by a movement, and that it occurs in response to go-cues that convey no spatial information (e.g., the disappearance of the central fixation circle).

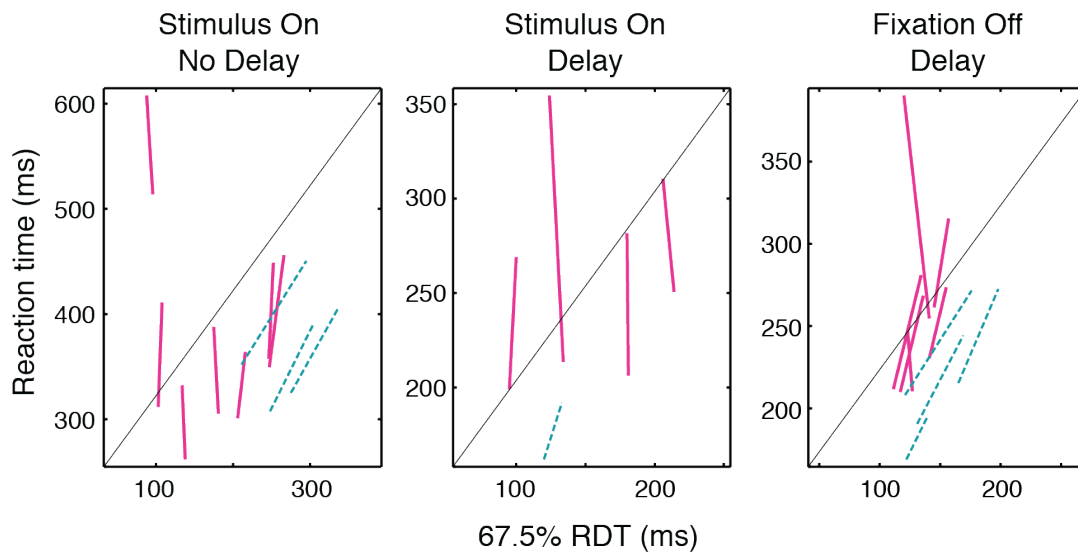


Figure 4.6 Stimulus-locked activity in the delay task. ROC discrimination slopes (67.5% RDT versus RT) for individual subjects in three different epochs: (1) locked to stimulus onset, no delay, (2) locked to stimulus onset, delay, (3) locked to fixation disappearance, delay. Slopes over the cutoff of 67.5° (SLR detected) are in pink solid lines, while slopes below the cutoff (no SLR detected) are in blue dotted lines.

This pattern of results was consistent across subjects. At the group level, we found strong evidence of stimulus-locked activity in each of the three different epochs. Figure 4.7 depicts the results of the analysis. Of the 10 subjects who participated in the delay task, 7 had a statistically-reliable SLR in the no delay condition. When there was a delay, 4 of the subjects showed an SLR immediately after stimulus presentation, and 6 subjects showed an SLR after the disappearance of the central fixation circle. Note the relatively large SLR latencies for the stimulus-locked epochs (i.e., left and middle plots). These are due to oscillations in the SLR. Essentially, there were some cases where the ROC analysis detected the SLR only after the second or third cycle of the oscillation, resulting in a longer ROC discrimination time.

While all 10 subjects are depicted for the no-delay and the delay/fixation-disappearance epochs (left and right plots in Figure 4.7), only 5 subjects are

depicted in the delay/stimulus-locked epoch (central plot in Figure 4.7). This is due to the fact that only 5 subjects had ROC time courses with values that actually exceeded the discrimination threshold. We also note here that any interesting patterns in the relationship between average RT and ROC discrimination time for early and late RT trials were, for this latter epoch, qualified by the fact that subjects did not actually react until 1000 ms later, making RT just one possible ordering variable among many others. Indeed, we would have expected the same results if we had randomly shuffled the trials for this epoch.

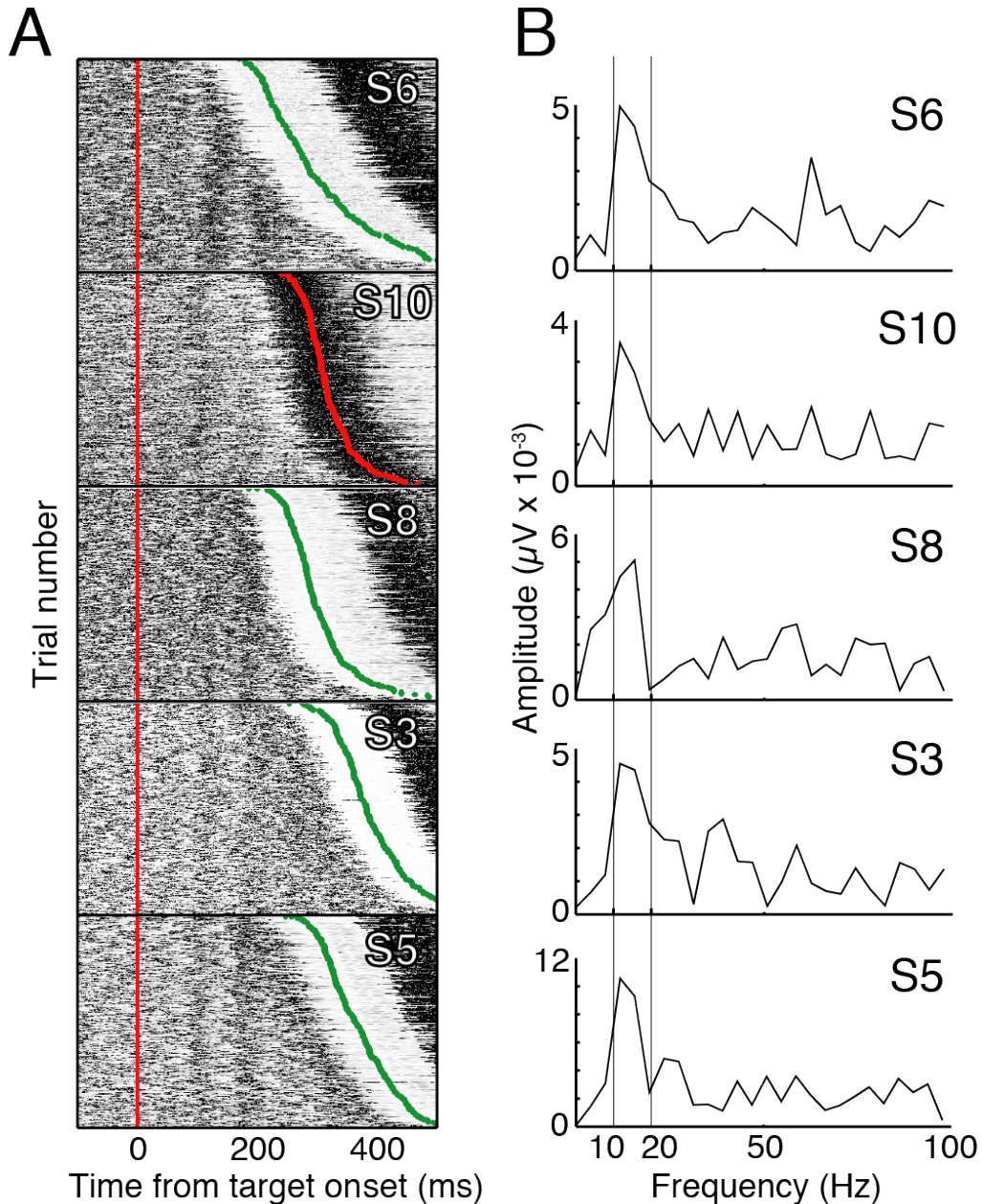


Figure 4.7 Stimulus-locked oscillations in muscle activity. *A*, EMG activity for individual trials, sorted by RT and locked to stimulus presentation (red vertical line), for 5 of the subjects in the delay experiment. Red (agonist movement) and green (antagonist movement) dots represent manual RT. Darker colors represent greater EMG activity. Approximately 150-200 trials are depicted for each subject (on the ordinate). *B*, Single-sided frequency-amplitude spectra for the corresponding epochs (sampled between 50 and 250 ms) in *A*. The two vertical lines indicate the location of 10 and 20 Hz. Note that peak amplitude consistently occurs between 12 and 15 Hz.

The relatively long RTs in this task (due, in part, to a more demanding task and the absence of a 200 ms gap between fixation disappearance and stimulus onset, as in the luminance contrast task) revealed the presence of stimulus-locked oscillations in the 12-15 Hz range (i.e., separated by 60-80 ms). This oscillation was remarkably stereotyped across the different subjects in whom it appeared (Figure 4.8). We searched for, but were unable to detect systematic oscillations in kinematics that corresponded to the oscillations in muscle activity. The absence of correlated hand movement may be due to the degrees of freedom intervening between the pectoral muscle and the hand. In other words, coordinated elbow and wrist movements may have compensated for the small, involuntary movements of the humerus during the muscle activity oscillations.

4.5 Discussion

The first key finding of the present study is that the luminance contrast of a target modulates the timing and magnitude of the SLR in upper limb muscles (Figure 4.4). This demonstration of the sensitivity of the SLR to intrinsic features of the target reveals that the SLR is more than a simple marker of the impending motor consequences of a visual cue to move. Broad tuning to the conspicuity of the stimulus is what would be expected if the SLR does indeed play a functional role in behaviors that involve the involuntary deviation of reach and saccade trajectories toward salient stimuli, and it is consistent with cases where the trajectory deviations scale in magnitude with the relative salience of those stimuli (Schütz et al., 2012; Wood et al., 2011).

The delay task in the present study revealed two important findings (Figure 4.7). First, we showed that, in 4 of the 10 subjects, the SLR inexorably followed target onset, even in cases where the go-cue had not been given and the reach was successfully inhibited. Second, we showed that, in 6 of the 10 subjects, the SLR appeared following the disappearance of the fixation circle after a 1 s delay. The first, but not the second, finding is broadly consistent with Pruszynski et al.

(2010), who also included an instructed delay task in their study. While they reported an absence of the SLR in the delay condition, both immediately after target onset and after the disappearance of the central marker, it is important to note that they blocked the presentation of delay and no-delay trials. In designing our version of the delay task, we reasoned that if the delay and no-delay trials were randomly interleaved, subjects would have to maintain a constant state of readiness. We predicted that this readiness, when combined with the onset of a target, would elicit a SLR even in cases when the go-cue was not immediately given. Our results confirmed this prediction (see Figure 4.7, central panel).

The absence of the target-induced SLR in the delay task of Pruszynski et al. demonstrated that the onset of a visual stimulus is not sufficient, in and of itself, to evoke a SLR. Given that these delay trials were essentially a precue paradigm, their finding suggests that the SLR is not evoked by the shifts in attention that would be associated with the onset of the target. Our results extend this finding, demonstrating that when some minimal degree of motor readiness is involved, the onset of a visual stimulus is sufficient to evoke a SLR. This is consistent with the finding that SLRs in neck muscles are evoked by the onset of a stimulus, even when an anti-saccade is required and successfully performed (B. B. Chapman & Corneil, 2011).

It is slightly more difficult to reconcile the discrepancy between our demonstration of SLRs that were locked to a delayed go-cue and the absence of such an effect in Pruszynski et al. There were only three differences between the two versions of the task. As already mentioned, we randomly interleaved delay and immediate trials while Pruszynski et al. blocked them. The other two differences were that (1) we included a constant force acting upon the arm and (2) we removed the target 150 ms after its onset, while Pruszynski et al. left it on the screen for the duration of the trial. Essentially, the fact that the stimulus was absent after 150 ms meant that our task was a memory-guided reaching task. This last difference between the duration of the initial stimuli turns out to be a possible explanation of the discrepancy. Basso and Liu (2007) demonstrated that substantia nigra pars

reticulata (SNr) suppresses saccades bilaterally when stimulated, and that it preferentially modulates memory-guided saccades. These two roles of SNr are mediated through its widespread and tonic inhibition of SC. Interestingly, SNr neurons are in turn inhibited by both caudate neurons, which have been shown to integrate nonspatial signals for volitional actions (Watanabe & Munoz, 2010), as well as putamen neurons, which have been shown to process information about the timing of movement onset after a precue and a delay (Jaeger, Gilman, & Aldridge, 1993). In essence, the concerted action of these basal ganglia structures could potentially withhold a stimulus-driven orienting response, direct a memory-guided response to that location later in time after a spatially uninformative go-cue, and do all of this by acting upon a region (the superior colliculus) that is strongly implicated in the pathway responsible for neck muscle SLRs, and potentially responsible for upper limb SLRs (as we will argue below).

The majority of what we already understand about the source of the SLR comes from the neck muscle literature. Neck muscle activity is profoundly influenced by the SC (Corneil, Olivier, & Munoz, 2002a; 2002b; Rezvani & Corneil, 2008), and there is strong evidence that SLRs and other reflexive orienting responses in neck muscles are mediated through a tecto-reticulo-spinal pathway (Corneil et al., 2004; 2008). However, despite the resemblance between neck muscle SLRs and those found in upper-limb muscles, there are many potential pathways that could be involved in the generation of SLRs during reaching. A number of them, including various corticospinal paths and, in particular, the tecto-reticulo-spinal pathway, are considered in detail in Pruszynski et al. (2010). We will limit ourselves here to laying out a brief summary of the evidence supporting a tecto-reticulo-spinal pathway for the upper-limb SLR, and how it is strengthened by the present results.

Cells in the superior colliculus (SC) are known for their role in mediating the transformation of visual information into motor commands for eye movements. However, SC cells also work in concert with reticular formation cells to code for arm movements in gaze-related coordinates (Stuphorn, Bauswein, & Hoffmann,

2000; Stuphorn, Hoffmann, & Miller, 1999; Werner, Dannenberg, & Hoffmann, 1997a; Werner, Hoffmann, & Dannenberg, 1997b). Moreover, the SC is particularly sensitive to the luminance of targets. Marino et al. (2012) found that SC responses increased in magnitude and decreased in latency as the luminance contrast of a visual stimulus increased. They also found that these modulations of SC activity were directly related to the timing of saccades. This could potentially explain our observation that the magnitude and latency of the upper-limb SLR are modulated by the luminance contrast of the target. It also suggests a clear prediction: given the relationship between the magnitude of neck muscle SLR and saccade RT during orienting responses (Corneil et al., 2004), we predict that the neck muscle SLR should also show a sensitivity to the luminance contrast of visual stimuli.

Our results, particularly those that show that a SLR can be elicited by a delayed and spatially uninformative cue-to-move, bear a close resemblance to those of Schepens and Drew (2003), who observed a similar phenomenon in cats. The cats heard a tone and, after a delay, were given a (spatially uninformative) cue to report which tone they heard by reaching for a reward with their right or left front limb. An anticipatory postural adjustment in the limb muscles, locked to the presentation of the go-cue, was observed. Over the last decade, Schepens and Drew have convincingly demonstrated that these postural adjustments are the result of signals from the pontomedullary reticular formation (Schepens & Drew, 2004; 2006; Schepens, Stapley, & Drew, 2008).

Another important link to reticular processing is found in our demonstration of 12-15 Hz oscillations during the SLR in upper limb muscles (Figure 4.8). Synchronous oscillations within this range have been frequently observed in neck muscles. Blouin et al. (2007) showed a 10-15 Hz coherence between a wide range of neck muscles during isometric contractions, and attributed this coherence to widespread monosynaptic excitatory connections between reticular formation neurons and motoneurons in the different neck muscles (Iwamoto & Sasaki, 1990; Sasaki, 1999; Shinoda, Kakei, & Muto, 1996). Similarly, Tijssen et

al. (2000) observed 10-15 Hz synchrony between three neck muscles (splenius capitis, sternocleidomastoid, and levator scapulae) during tonic contractions. Thus, the 10-15 Hz oscillation is a signature of muscular synchrony during neck movements, and this synchrony is most likely generated by reticular formation neurons. Some have argued that such oscillations could play a role in sensorimotor integration (Nicoletis, Baccala, Lin, & Chapin, 1995). This is supported by evidence that patients with idiopathic torticollis (in which the muscles of the neck are locked into a painful involuntary contraction), who are believed to have deficits in sensorimotor integration, lack the synchronous 10-15 Hz neck muscle oscillations observed in healthy individuals (Tijssen et al., 2000).

Further evidence of the link between reticular processing and the 10-15 Hz bandwidth is found in the startle response literature. Like the SLR, the startle response involves fast, reflexive movements indexed to hyper-salient stimuli. Unlike the SLR, a pure startle response involves bilateral muscle responses that habituate over time. However, when a startle response is combined with a target-directed movement, the response becomes mostly unilateral and it will not habituate, resulting in a hastening of the initially planned movement (Siegmund, Inglis, & Sanderson, 2001). The expression (but not the acquisition) of startle responses can be blocked by injecting muscimol into superior colliculus/mesencephalic reticular formation neurons (Meloni & Davis, 1999). This is consistent with findings that show increased bicep EMG responses elicited by tetanic stimulation of SC during startle-responses (C. Lin et al., 2002), as well as the finding that giant neurons in the reticular formation create a sensorimotor interface between sensory inputs and spinal motoneurons during the startle response (Lingenhöhl & Friauf, 1994). Critically, synchronous 10-15 Hz oscillations have been observed in deltoid and biceps muscles during the startle response (Grosse & Brown, 2003). Taken together with the observation of 12-15 Hz SLR oscillations in the present study, these findings imply a common pathway between the startle response and the SLR, and provide strong support for the idea that this pathway involves the SC and reticular formation.

Taken in isolation, the 10-15 Hz oscillation in neck and upper limb muscles ties together a number of empirical findings and provides some explanatory power, but it is not sufficient to warrant strong conclusions about the pathway that mediates the SLR in upper limb muscles. At the most, it provides a strong impetus for future studies. We note here that oscillations in the 16 to 35 Hz range have been previously linked to a corticospinal drive to distal limb motoneurons (Baker, Kilner, Pinches, & Lemon, 1999; Kilner et al., 1999), and while the frequencies observed in the present study marginally overlap with this bandwidth, there is a much better overlap with the 10 to 15 Hz range that has been repeatedly associated with the tecto-reticulo-spinal pathway. This, and the relatively low number of corticospinal projections to proximal (versus distal) musculature (Murayama, Lin, Salenius, & Hari, 2001), strongly suggest that the SLR is not generated by a corticospinal pathway.

In sum, both neck and upper limb muscles have been shown to synchronously oscillate within the 10-15 Hz bandwidth during tonic contraction (and during acoustic startle responses in the case of upper limb muscles). Stimulus-locked activity in neck muscles, the startle response, anticipatory postural adjustments, and muscle oscillations in the 10-15 Hz bandwidth have all been directly associated with neural signals deriving from the collicular-reticular axis. Further, there have been numerous demonstrations of cells in the SC that code—sometimes exclusively—for reaching movements. Finally, the timing and magnitude of visual responses in SC scale with luminance contrast of the target, similar to the contrast-related scaling of the timing and magnitude of upper-limb SLRs.

When considered in light of all these findings, the results of the present study strongly suggest that the upper-limb SLR is mediated by the tecto-reticulo-spinal pathway. In particular, our observation of 12-15 Hz oscillations in cPM muscles, along with the suggestion of such oscillations in past work on the SLR in neck muscles, raise the intriguing possibility that the separately observed SLRs in neck and upper limb muscles are actually part of a coordinated synchronization

of these muscle groups during orienting responses to stimuli in situations that require fast, unfiltered sensorimotor transformation. There is a large literature on eye-hand coordination, but few (if any) studies have rigorously explored the properties of eye-neck-limb coordination in situations of reflexive responding to salient stimuli, and how such coordination might be reflected in both neural processing and the motor periphery.

A final point involves the wide range of sensory modalities that are processed through the tecto-reticulo-spinal pathway (Meredith & Stein, 1985; Yeomans, Li, Scott, & Frankland, 2002). Especially in light of our finding that delayed, spatially uninformative cues-to-move are able to elicit the SLR, it is reasonable to wonder whether any type of cue would suffice. We predict that any sensory modality with high temporal sensitivity and some degree of spatial sensitivity (e.g., hearing, vision, touch) could produce the SLR in upper limb-muscles, and presumably in neck muscles as well.

4.5.1 Conclusions

Our results suggest the existence of a pathway that is able to quickly and sensitively transmit sensory information about imperatives (e.g., when to release the inhibition on a pre-programmed response), as well as low-level visual information about the intensity of the stimulus. This pathway would presumably bypass the stochastic processes that result in the variable latencies associated with voluntary reaction times. The discovery of 12-15 Hz oscillations in the SLR adds to the growing body of evidence that the SLR is mediated by the tecto-reticulo-spinal pathway.

Chapter 5: General Discussion

5.1 Summary of objectives and findings

In Chapters 2 and 3, I demonstrated that salience, induced by luminance contrast differences between targets, overpowers the effect of numerosity at early response latencies. Initial reach trajectories deviated toward high-salience targets, even in cases where there were twice as many low-salience targets (and therefore twice the likelihood of the final target appearing) on the opposite side. Between the two studies, I tested the relative potency of salience and numerosity biases as they evolved over a ~750 ms time frame. This was accomplished by imposing a variable delay (from 0 to 500 ms) between the presentation of the potential target display and the administration of the auditory go-cue. After a 500 ms delay (which was roughly 750 ms after stimulus presentation once RT was accounted for), the influence of salience had all but disappeared.

In Chapter 2, the salience bias was replaced by a weak but significant numerosity bias after 500 ms. In Chapter 3, the salience bias appeared to reach an equilibrium with the numerosity bias after roughly 400 ms, after which it persisted until the end of the 750 ms epoch. Due to constraints upon space, this was not addressed in the original manuscript found in Chapter 3, so I will address it now. In Chapter 2, I originally interpreted the admittedly small numerosity bias at 500 ms as evidence that the effect of salience had entirely dissipated by that time. A more probable interpretation (especially in light of the results of Chapter 3) is that salience was still a factor, but by 500 ms it had been slightly eclipsed in magnitude by the effect of numerosity. The modest numerosity bias observed at 500 ms, in comparison with the much stronger bias consistently observed in no-delay versions of the task (C. S. Chapman, Gallivan, Wood, Milne, Culham, & Goodale, 2010a), is evidence of this.

The preceding does not explain, however, why the effect of salience in Chapter 2 would be smaller than that observed in Chapter 3. It may have been due to the type of stimuli used. In Chapter 2, luminance contrast was manipulated in two ways: (1) by changing the RGB value of the target outline (i.e., the same as in

Chapter 3), and (2) by holding RGB at full black, but adding or subtracting a cross from the target outline. Both of these manipulations changed the luminance contrast of the entire space of the target with the background, but only the former changed the local luminance contrast of the boundaries of the target with the background. In Chapter 3, the primary motivation for using the RGB manipulation was that its effect of salience was at least 50% stronger than that of the cross manipulation (a fact that was not mentioned in Chapter 2). Thus, the discrepancy in salience bias magnitude between the two Chapters may have been due to differences in the ability of the two contrast manipulations to capture attention and therefore bias reaching.

Another outcome of Chapter 3 was the detailed description of the interaction between salience and numerosity as biasing factors in visuomotor competition. The influence of numerosity first appeared at ~150 ms, peaked at ~350 ms, and then stabilized throughout the range of delay times at which we tested. The salience bias was already online at the earliest samples, suggesting that it is capable of influencing the motor periphery before 150 ms. This salience bias reached its peak at ~300 ms, after which it followed a nonlinear decay until relaxing into an apparent equilibrium (at ~450 ms) with the numerosity bias throughout the rest of the delay range.

The unique persistence of the salience bias after relatively long delays is inconsistent with the fairly well established time course of excitation and inhibition associated with bottom up attentional capture, inhibition-of-return, and trajectory deviations in response to distractors, which puts the transition between positive and negative biasing of exogenously attended space at around 250 ms. I argue that the longer time course of excitation (i.e., deviation toward the location of the salient stimulus) in Chapter 4 is due to the fact that the multiple target reaching task requires participants to treat all targets as relevant; there is no point prior to the initiation of movement at which the inhibition of a target location would be appropriate or helpful in accomplishing the task. If this is true, it suggests that the inhibitory rebound that typically appears around 250 ms (in situations where the

inhibition of that location is typically helpful) may not be as reflexive as some researchers suggest, but may rather be a mechanism susceptible to contextual modulation, given the nature of the task at hand.

Finally, it was demonstrated that individual differences in relative processing time for stimuli of differing luminance contrast can predict the extent to which reach trajectories will deviate toward high contrast targets in an array of targets. This finding indirectly supports the hypothesis that the transient trajectory biases evoked by contrast-induced salience arise out of differences in processing speed for the different stimulus intensities.

The research presented in Chapter 4 was designed to test the hypothesis that the stimulus-locked responses (SLRs) that had been previously demonstrated in both neck and upper-limb muscles (Corneil et al., 2004; Pruszynski et al., 2010) are mediated by a short-latency pathway that directly transforms visual information into muscle commands for the purpose of reflexive orienting. One prediction of this hypothesis is that the SLR should be sensitive to the intensity of the visual stimulus to which it is a response. Another prediction is that the SLR should not be detected in response to a delayed, spatially uninformative go-cue. The results presented in Chapter 4 confirmed the first prediction, but not the second.

The magnitude and latency of SLRs was dependent upon the intensity of the stimulus. As the luminance contrast of the target increased, the SLR latency decreased and the magnitude of the EMG signal increased. A surprising observation in Chapter 4 was that the SLR was consistently present following a delayed go-cue that conveyed no spatial information about the direction of the reach (this information had been previously supplied 1000 ms earlier with the brief flash of the target location). In the same delayed response task, the SLR appeared following the flash of the spatially informative target, even in cases when the go-cue had not yet been given, and the participant successfully withheld a voluntary response. Taken together, these results suggest the

possible existence of a circuit that is not only able to quickly transform visual information into muscle commands for reflexive orienting, but is also capable of suppressing voluntary responses until a go-cue is detected. Among the possible candidates for such a circuit, the most promising seems to be a retino-tecto-spinal circuit with a basal ganglia loop.

5.2 Future directions

The studies reported in this thesis generated a number of new avenues for future research. Some of the more promising proposals are sketched out here.

Does the retinal contrast response function determine visuomotor capture by luminance contrast?

There is strong evidence that the relative strengths of responses to stimuli of varying luminance contrast are largely preserved from the first volley of spikes that arrive from the retina (Carandini & Heeger, 2012; Thorpe, Delorme, & Van Rullen, 2001; Vanrullen, 2003). The results reported in Chapters 3 and 4 are broadly consistent with the idea that there is a preservation of the rank order of visual response intensities (and latencies) throughout the visual processing pathways, and that the preservation of this order has implications for both involuntary and voluntary responses during target directed movements. Specifically, there are interesting implications of the finding that individual differences in the differential processing speeds for low- and high-contrast stimuli predict how strongly reach trajectories will deviate toward a salient target. Do these processing speed differences arise from individual idiosyncrasies in the retinal contrast response function? Or are there individual differences in the speed of integration of retinal signals, somewhere along the visual pathway?

Marino et al (2012) demonstrated that the intensity of a visual stimulus was correlated with the timing and magnitude of the visual response in SC, as well as the latency and metrics of the ensuing saccade. Thus, the SC would be an ideal location to test for similar effects when there are intensity differences between

multiple simultaneous stimuli. This would be a step in the direction of characterizing the ability of SC to flexibly categorize stimuli in terms of their visual intensity. After characterizing the temporal and spatial effects of multiple stimuli with varying intensity, it would be interesting to find a way to test whether the dynamics observed in the SC are a direct function of the retinal contrast response function. One way to do this would be to assess retinal transduction efficiency with electroretinography.

How correlated are saccadic and reach trajectory curvature during visually guided pointing tasks?

As noted in the general introduction of this thesis, there is a striking similarity between the results of Ghez et al (1997) and Van der Stigchel et al. (2013). Taken together, these two studies showed that eye movements and reaching movements share a common range of target separation within which trajectory averaging is most likely to occur. Specifically, the transition from a unimodal distribution of endpoints between the targets to a bimodal distribution with modes centered on the two targets occurred at roughly 40 degrees of angular separation between the two targets. This is broadly consistent with the idea that, at some point in the intermingling of saccadic and reach-related sensorimotor processing, a common map is exerting an influence (Zehetleitner et al., 2011).

A simple first approach to this question would be to design a compelled response task in which reaches and saccades to presented targets of varying angular separation are recorded. The degree of correlation between the averaging of eye and hand trajectories would be a good test of the hypothesis that they are mutually influenced by a common priority map. A negative result would allow us to throw this hypothesis out. A positive result would be less instructive, however. It could be the case that significant correlations between eye and hand curvature are simply due to general computational principles common to neural circuits that mediate sensorimotor transformation.

How visual is the visual response in neck and upper limb muscles?

This proposal is fairly straightforward. Given the evidence presented in Chapter 4 that the upper limb SLR can be evoked by a delayed, spatially uninformative go-cue, it is reasonable to ask whether that go-cue must be visual, or whether it can be any sensory modality. There are solid reasons to predict that the latter is the case. There is strong evidence that the SLR is mediated by a retino-tecto-spinal pathway. An extensive argument for this can be found in the discussion of Chapter 4. Moreover, both the SC and reticular formation perform operations on inputs from multiple sensory modalities (Meredith & Stein, 1985; Yeomans et al., 2002).

A simple instructed delay task would allow us to test this hypothesis. After the brief presentation of a visual target in the periphery, the participant would wait until an auditory cue to begin the reach. Other modalities, such as touch (e.g., an air puff on the cheek or forehead) could easily be adapted to the task.

5.3 Conclusions

Unlike previous studies that were unable to disentangle the effects of salience from the effects of the mere presence of a distractor or extra target, the original research presented in this thesis demonstrates that the luminance contrast of targets exerts a sharp, transient effect upon the trajectories of reaching movements. Specifically, reach trajectories deviate toward the target(s) with the highest luminance contrast. It was further demonstrated that salience and numerosity have distinct, separable time courses with respect to their effect upon the reach vector. Salience comes online quickly and vigorously, after which it logarithmically diminishes in influence. Numerosity takes longer to come online, but it exerts a persistent, non-diminishing influence after it plateaus. The degree to which a given individual is likely to reach toward a salient target can be predicted by how quickly they are able to process visual stimuli of varying intensities. This relationship between the magnitude and the speed of salience-induced effects was also demonstrated in human upper limb muscles during a

reaching task. Stimulus-locked muscle responses diminished in magnitude and increased in latency as the intensity of the stimulus grew weaker. Finally, oscillations observed in the stimulus-locked muscle responses were consistent with an account in which such responses are mediated by a tecto-reticulo-spinal pathway. Taken together, the findings in this thesis represent a solid contribution to the scientific understanding of how bottom-up salience influences sensorimotor processing for the skeletomuscular system.

References

- Anton-Erxleben, K., & Carrasco, M. (2013). Attentional enhancement of spatial resolution: linking behavioural and neurophysiological evidence. *Nature Reviews Neuroscience*, *14*(3), 188–200. doi:10.1038/nrn3443
- Arai, K., & Keller, E. L. (2005). A model of the saccade-generating system that accounts for trajectory variations produced by competing visual stimuli. *Biological Cybernetics*, *92*(1), 21–37. doi:10.1007/s00422-004-0526-y
- Arcizet, F., Mirpour, K., & Bisley, J. W. (2011). A Pure Saliency Response in Posterior Parietal Cortex. *Cerebral Cortex (New York, NY : 1991)*. doi:10.1093/cercor/bhr035
- Asadollahi, A., Mysore, S. P., & Knudsen, E. I. (2010). Stimulus-driven competition in a cholinergic midbrain nucleus. *Nature Neuroscience*, *13*(7), 889–895. doi:10.1038/nn.2573
- Baker, S. N., Kilner, J. M., Pinches, E. M., & Lemon, R. N. (1999). The role of synchrony and oscillations in the motor output. *Experimental Brain Research Experimentelle Hirnforschung Expérimentation Cérébrale*, *128*(1-2), 109–117.
- Baldauf, D., & Deubel, H. (2010). Attentional landscapes in reaching and grasping. *Vision Research*, *50*(11), 999–1013. doi:10.1016/j.visres.2010.02.008
- Baldauf, D., Cui, H., & Andersen, R. A. (2008). The posterior parietal cortex encodes in parallel both goals for double-reach sequences. *The Journal of Neuroscience : the Official Journal of the Society for Neuroscience*, *28*(40), 10081–10089. doi:10.1523/JNEUROSCI.3423-08.2008
- Basso, M. A., & Liu, P. (2007). Context-dependent effects of substantia nigra stimulation on eye movements. *Journal of Neurophysiology*, *97*(6), 4129–4142. doi:10.1152/jn.00094.2007
- Basso, M. A., & Wurtz, R. H. (1997). Modulation of neuronal activity by target uncertainty. *Nature*, *389*(6646), 66–69. doi:10.1038/37975
- Bell, A. H., Meredith, M. A., Van Opstal, A. J., & Munoz, D. P. (2006). Stimulus intensity modifies saccadic reaction time and visual response latency in the superior colliculus. *Experimental Brain Research Experimentelle Hirnforschung Expérimentation Cérébrale*, *174*(1), 53–59. doi:10.1007/s00221-006-0420-z
- Bisley, J. W., & Goldberg, M. E. (2010). Attention, intention, and priority in the parietal lobe. *Annual Review of Neuroscience*, *33*, 1–21. doi:10.1146/annurev-neuro-060909-152823
- Blouin, J. S., Siegmund, G. P., Carpenter, M. G., & Inglis, J. T. (2007). Neural Control of Superficial and Deep Neck Muscles in Humans. *Journal of Neurophysiology*, *98*(2), 920–928. doi:10.1152/jn.00183.2007
- Boehnke, S. E., & Munoz, D. P. (2008). On the importance of the transient visual response in the superior colliculus. *Current Opinion in Neurobiology*, *18*(6), 544–551. doi:10.1016/j.conb.2008.11.004
- Bonin, V., Mante, V., & Carandini, M. (2005). The suppressive field of neurons in lateral geniculate nucleus. *The Journal of Neuroscience : the Official Journal*

- of the Society for Neuroscience, 25(47), 10844–10856.
doi:10.1523/JNEUROSCI.3562-05.2005
- Boynton, G. M., Demb, J. B., Glover, G. H., & Heeger, D. J. (1999). Neuronal basis of contrast discrimination. *Vision Research*, 39(2), 257–269.
- Buetti, S., & Kerzel, D. (2009). Conflicts during response selection affect response programming: Reactions toward the *Journal of Experimental Psychology: Human Perception and Performance*.
- Buschman, T. J., & Miller, E. K. (2007). Top-Down Versus Bottom-Up Control of Attention in the Prefrontal and Posterior Parietal Cortices. *Science (New York, NY)*, 315(5820), 1860–1862. doi:10.1126/science.1138071
- Busse, L., Wade, A. R., & Carandini, M. (2009). Representation of concurrent stimuli by population activity in visual cortex. *Neuron*, 64(6), 931–942. doi:10.1016/j.neuron.2009.11.004
- Carandini, M., & Heeger, D. J. (2012). Normalization as a canonical neural computation. *Nature Reviews Neuroscience*, 13(1), 51–62. doi:10.1038/nrn3136
- Cattell, J. M. (1886). The influence of the intensity of the stimulus on the length of the reaction time. *Brain*, 8(4), 512–515. doi:10.1093/brain/8.4.512
- Chapman, B. B., & Corneil, B. D. (2011). Neuromuscular recruitment related to stimulus presentation and task instruction during the anti-saccade task. *The European Journal of Neuroscience*, 33(2), 349–360. doi:10.1111/j.1460-9568.2010.07496.x
- Chapman, C. S., & Goodale, M. A. (2008). Missing in action: the effect of obstacle position and size on avoidance while reaching. *Experimental Brain Research Experimentelle Hirnforschung Expérimentation Cérébrale*, 191(1), 83–97. doi:10.1007/s00221-008-1499-1
- Chapman, C. S., Gallivan, J. P., Wood, D. K., Milne, J. L., Culham, J. C., & Goodale, M. A. (2010a). Reaching for the unknown: multiple target encoding and real-time decision-making in a rapid reach task. *Cognition*, 116(2), 168–176. doi:10.1016/j.cognition.2010.04.008
- Chapman, C. S., Gallivan, J. P., Wood, D. K., Milne, J. L., Culham, J. C., & Goodale, M. A. (2010b). Short-term motor plasticity revealed in a visuomotor decision-making task. *Behavioural Brain Research*, 214(1), 130–134. doi:10.1016/j.bbr.2010.05.012
- Churchland, A. K., Kiani, R., & Shadlen, M. N. (2008). Decision-making with multiple alternatives. *Nature Neuroscience*, 11(6), 693–702. doi:10.1038/nn.2123
- Cisek, P. (2006). Integrated neural processes for defining potential actions and deciding between them: a computational model. *The Journal of Neuroscience : the Official Journal of the Society for Neuroscience*, 26(38), 9761–9770. doi:10.1523/JNEUROSCI.5605-05.2006
- Cisek, P. (2007). Cortical mechanisms of action selection: the affordance competition hypothesis. *Philosophical Transactions of the Royal Society B: Biological Sciences*, 362(1485), 1585.
- Cisek, P. (2012). Making decisions through a distributed consensus. *Current Opinion in Neurobiology*, 1–10. doi:10.1016/j.conb.2012.05.007

- Cisek, P., & Kalaska, J. F. (2005). Neural correlates of reaching decisions in dorsal premotor cortex: specification of multiple direction choices and final selection of action. *Neuron*, *45*(5), 801–814. doi:10.1016/j.neuron.2005.01.027
- Cisek, P., & Kalaska, J. F. (2010). Neural mechanisms for interacting with a world full of action choices. *Annual Review of Neuroscience*, *33*, 269–298. doi:10.1146/annurev.neuro.051508.135409
- Cohen, B., & Komatsuzaki, A. (1972). Eye movements induced by stimulation of the pontine reticular formation: evidence for integration in oculomotor pathways. *Experimental Neurology*, *36*(1), 101–117.
- Collinger, J. L., Wodlinger, B., Downey, J. E., Wang, W., Tyler-Kabara, E. C., Weber, D. J., et al. (2013). High-performance neuroprosthetic control by an individual with tetraplegia. *Lancet*, *381*(9866), 557–564. doi:10.1016/S0140-6736(12)61816-9
- Corneil, B. D., Munoz, D. P., Chapman, B. B., Admans, T., & Cushing, S. L. (2008). Neuromuscular consequences of reflexive covert orienting. *Nature Neuroscience*, *11*(1), 13–15. doi:10.1038/nn2023
- Corneil, B. D., Olivier, E., & Munoz, D. P. (2002a). Neck muscle responses to stimulation of monkey superior colliculus. I. Topography and manipulation of stimulation parameters. *Journal of Neurophysiology*, *88*(4), 1980–1999.
- Corneil, B. D., Olivier, E., & Munoz, D. P. (2002b). Neck muscle responses to stimulation of monkey superior colliculus. II. Gaze shift initiation and volitional head movements. *Journal of Neurophysiology*, *88*(4), 2000–2018.
- Corneil, B. D., Olivier, E., & Munoz, D. P. (2004). Visual responses on neck muscles reveal selective gating that prevents express saccades. *Neuron*, *42*(5), 831–841.
- Demb, J. B. (2002). Multiple mechanisms for contrast adaptation in the retina. *Neuron*, *36*(5), 781–783.
- Desimone, R. (1998). Visual attention mediated by biased competition in extrastriate visual cortex. *Philosophical Transactions of the Royal Society of London Series B, Biological Sciences*, *353*(1373), 1245–1255. doi:10.1098/rstb.1998.0280
- Deubel, H., Wolf, W., & Hauske, G. (1984). The evaluation of the oculomotor error signal. In A. G. Gale & F. Johnson (Eds.), (p. 55). Theoretical and applied aspects of eye movement research.
- Dombrowe, I. C., Olivers, C. N. L., & Donk, M. (2010). The time course of color- and luminance-based salience effects. *Frontiers in Psychology*, *1*, 1–6. doi:10.3389/fpsyg.2010.00189
- Donk, M., & Soesman, L. (2010). Salience is only briefly represented: evidence from probe-detection performance. *Journal of Experimental Psychology: Human Perception and Performance*, *36*(2), 286–302. doi:10.1037/a0017605
- Donk, M., & van Zoest, W. (2008). Effects of salience are short-lived. *Psychological Science : a Journal of the American Psychological Society / APS*, *19*(7), 733–739. doi:10.1111/j.1467-9280.2008.02149.x
- Edelman, J. A., & Keller, E. L. (1998). Dependence on target configuration of express saccade-related activity in the primate superior colliculus. *Journal of*

- Neurophysiology*, 80(3), 1407–1426.
- Elder, J., & Zucker, S. (1993). The effect of contour closure on the rapid discrimination of two-dimensional shapes. *Vision Research*, 33(7), 981–991.
- Fautrelle, L., Prablanc, C., Berret, B., Ballay, Y., & Bonnetblanc, F. (2010). Pointing to double-step visual stimuli from a standing position: very short latency (express) corrections are observed in upper and lower limbs and may not require cortical involvement. *Neuroscience*, 169(2), 697–705. doi:10.1016/j.neuroscience.2010.05.014
- Fecteau, J. H., & Munoz, D. P. (2006). Saliency, relevance, and firing: a priority map for target selection. *Trends in Cognitive Sciences*, 10(8), 382–390. doi:10.1016/j.tics.2006.06.011
- Findlay, J. M., & Walker, F. (1999). A model of saccade generation based on parallel processing and competitive inhibition. *The Behavioral and Brain Sciences*, 22(4), 661–74; discussion 674–721.
- Fisk, J. D., & Goodale, M. A. (1985). The organization of eye and limb movements during unrestricted reaching to targets in contralateral and ipsilateral visual space. *Experimental Brain Research Experimentelle Hirnforschung Expérimentation Cérébrale*, 60(1), 159–178.
- Furman, M., & Wang, X.-J. (2008). Similarity Effect and Optimal Control of Multiple-Choice Decision Making. *Neuron*, 60(6), 1153–1168. doi:10.1016/j.neuron.2008.12.003
- Gallivan, J. P., Chapman, C. S., Wood, D. K., Milne, J. L., Ansari, D., Culham, J. C., & Goodale, M. A. (2011). One to four, and nothing more: nonconscious parallel individuation of objects during action planning. *Psychological Science : a Journal of the American Psychological Society / APS*, 22(6), 803–811. doi:10.1177/0956797611408733
- Gawne, T. J., Kjaer, T. W., & Richmond, B. J. (1996). Latency: another potential code for feature binding in striate cortex. *Journal of Neurophysiology*, 76(2), 1356–1360.
- Geyer, T., Müller, H. J., & Krummenacher, J. (2008). Expectancies modulate attentional capture by salient color singletons. *Vision Research*, 48(11), 1315–1326. doi:10.1016/j.visres.2008.02.006
- Ghez, C., Favilla, M., Ghilardi, M. F., Gordon, J., Bermejo, R., & Pullman, S. (1997). Discrete and continuous planning of hand movements and isometric force trajectories. *Experimental Brain Research Experimentelle Hirnforschung Expérimentation Cérébrale*, 115(2), 217–233. doi:10.1007/PL00005692
- Glimcher, P. W., & Sparks, D. L. (1993). Representation of averaging saccades in the superior colliculus of the monkey. *Experimental Brain Research Experimentelle Hirnforschung Expérimentation Cérébrale*, 95(3), 429–435.
- Godijn, R., & Theeuwes, J. (2002). Programming of endogenous and exogenous saccades: Evidence for a competitive integration model. *Journal of Experimental Psychology: Human Perception and Performance*, 28(5), 1039–1054. doi:10.1037//0096-1523.28.5.1039
- Gold, J. I., & Shadlen, M. N. (2007). The neural basis of decision making. *Annual Review of Neuroscience*, 30, 535–574.

- doi:10.1146/annurev.neuro.29.051605.113038
- Goodale, M. A., & Milner, A. D. (1992). Separate visual pathways for perception and action. *Trends in Neurosciences*, 15(1), 20–25.
- Goodale, M., & Milner, D. (2013). *Sight Unseen*. Oxford University Press.
- Goossens, H. H. L. M., & Van Opstal, A. J. (2006). Dynamic ensemble coding of saccades in the monkey superior colliculus. *Journal of Neurophysiology*, 95(4), 2326–2341. doi:10.1152/jn.00889.2005
- Goossens, H. H. L. M., & Van Opstal, A. J. (2012). Optimal control of saccades by spatial-temporal activity patterns in the monkey superior colliculus. *PLoS Computational Biology*, 8(5), e1002508. doi:10.1371/journal.pcbi.1002508
- Gottlieb, J. P., Kusunoki, M., & Goldberg, M. E. (1998). The representation of visual salience in monkey parietal cortex. *Nature*, 391(6666), 481–484. doi:10.1038/35135
- Grosse, P., & Brown, P. (2003). Acoustic startle evokes bilaterally synchronous oscillatory EMG activity in the healthy human. *Journal of Neurophysiology*, 90(3), 1654–1661. doi:10.1152/jn.00125.2003
- Guyonneau, R., Vanrullen, R., & Thorpe, S. J. (2004). Temporal codes and sparse representations: A key to understanding rapid processing in the visual system. *Journal of Physiology-Paris*, 98(4-6), 487–497. doi:10.1016/j.jphysparis.2005.09.004
- Heeger, D. J. (1992). Normalization of cell responses in cat striate cortex. *Visual Neuroscience*, 9(2), 181–197.
- Heeger, D. J., Huk, A. C., Geisler, W. S., & Albrecht, D. G. (2000). Spikes versus BOLD: what does neuroimaging tell us about neuronal activity? *Nature Neuroscience*, 3, 631–632.
- Hickey, C., McDonald, J. J., & Theeuwes, J. (2006). Electrophysiological evidence of the capture of visual attention. *Journal of Cognitive Neuroscience*, 18(4), 604–613. doi:10.1162/jocn.2006.18.4.604
- Hikosaka, O., & Wurtz, R. H. (1983a). Visual and oculomotor functions of monkey substantia nigra pars reticulata. I. Relation of visual and auditory responses to saccades. *Journal of Neurophysiology*, 49(5), 1230–1253.
- Hikosaka, O., & Wurtz, R. H. (1983b). Visual and oculomotor functions of monkey substantia nigra pars reticulata. II. Visual responses related to fixation of gaze. *Journal of Neurophysiology*, 49(5), 1254–1267.
- Hikosaka, O., & Wurtz, R. H. (1983c). Visual and oculomotor functions of monkey substantia nigra pars reticulata. III. Memory-contingent visual and saccade responses. *Journal of Neurophysiology*, 49(5), 1268–1284.
- Hikosaka, O., & Wurtz, R. H. (1983d). Visual and oculomotor functions of monkey substantia nigra pars reticulata. IV. Relation of substantia nigra to superior colliculus. *Journal of Neurophysiology*, 49(5), 1285–1301.
- Hochberg, L. R., Bacher, D., Jarosiewicz, B., Masse, N. Y., Simeral, J. D., Vogel, J., et al. (2012). Reach and grasp by people with tetraplegia using a neurally controlled robotic arm. *Nature*, 485(7398), 372–375. doi:10.1038/nature11076
- Hudson, T. E., Maloney, L. T., & Landy, M. S. (2007). Movement planning with probabilistic target information. *Journal of Neurophysiology*, 98(5), 3034–

3046. doi:10.1152/jn.00858.2007
- Ipata, A. E., Gee, A. L., Gottlieb, J., Bisley, J. W., & Goldberg, M. E. (2006). LIP responses to a popout stimulus are reduced if it is overtly ignored. *Nature Neuroscience*, 9(8), 1071–1076. doi:10.1038/nn1734
- Itti, L., & Koch, C. (2001). Computational modelling of visual attention. *Nature Reviews Neuroscience*, 2(3), 194–203. doi:10.1038/35058500
- Itti, L., Koch, C., & Niebur, E. (1998). A model of saliency-based visual attention for rapid scene analysis. *IEEE Transactions on Pattern Analysis and Machine Intelligence*, 20(11), 1–6.
- Iwamoto, Y., & Sasaki, S. (1990). Monosynaptic excitatory connexions of reticulospinal neurones in the nucleus reticularis pontis caudalis with dorsal neck motoneurons in the cat. *Experimental Brain Research Experimentelle Hirnforschung Expérimentation Cérébrale*, 80(2), 277–289.
- Jaeger, D., Gilman, S., & Aldridge, J. W. (1993). Primate basal ganglia activity in a precued reaching task: preparation for movement. *Experimental Brain Research Experimentelle Hirnforschung Expérimentation Cérébrale*, 95(1), 51–64.
- Johannes, S., Münte, T. F., Heinze, H. J., & Mangun, G. R. (1995). Luminance and spatial attention effects on early visual processing. *Brain Research Cognitive Brain Research*, 2(3), 189–205.
- Johansson, R. S., & Birznieks, I. (2004). First spikes in ensembles of human tactile afferents code complex spatial fingertip events. *Nature Neuroscience*, 7(2), 170–177. doi:10.1038/nn1177
- Katnani, H. A., & Gandhi, N. J. (2011). Order of operations for decoding superior colliculus activity for saccade generation. *Journal of Neurophysiology*, 106(3), 1250–1259. doi:10.1152/jn.00265.2011
- Katnani, H. A., Van Opstal, A. J., & Gandhi, N. J. (2012). A test of spatial temporal decoding mechanisms in the superior colliculus. *Journal of Neurophysiology*, 107(9), 2442–2452. doi:10.1152/jn.00992.2011
- Keller, E. L. (1974). Participation of medial pontine reticular formation in eye movement generation in monkey. *Journal of Neurophysiology*, 37(2), 316–332.
- Kerzel, D., & Schönhammer, J. (2013). Salient stimuli capture attention and action. *Attention, Perception, & Psychophysics*, 75(8), 1633–1643. doi:10.3758/s13414-013-0512-3
- Kilner, J. M., Baker, S. N., Salenius, S., Jousmäki, V., Hari, R., & Lemon, R. N. (1999). Task-dependent modulation of 15-30 Hz coherence between rectified EMGs from human hand and forearm muscles. *The Journal of Physiology*, 516 (Pt 2), 559–570.
- Kim, M. S., & Cave, K. R. (1999). Top-down and bottom-up attentional control: on the nature of interference from a salient distractor. *Perception & Psychophysics*, 61(6), 1009–1023.
- Knudsen, E. I. (2011). Control from below: the role of a midbrain network in spatial attention. *The European Journal of Neuroscience*, 33(11), 1961–1972. doi:10.1111/j.1460-9568.2011.07696.x
- Koch, C., & Ullman, S. (1985). Shifts in selective visual attention: towards the

- underlying neural circuitry. *Human Neurobiology*, 4(4), 219–227.
- Kusunoki, M., Gottlieb, J., & Goldberg, M. E. (2000). The lateral intraparietal area as a salience map: the representation of abrupt onset, stimulus motion, and task relevance. *Vision Research*, 40(10-12), 1459–1468.
- Lamme, V. A. F., & Roelfsema, P. R. (2000). The distinct modes of vision offered by feedforward and recurrent processing. *Trends in Neurosciences*, 23(11), 571–579.
- Lamy, D., & Zoaris, L. (2009). Task-irrelevant stimulus salience affects visual search. *Vision Research*, 49(11), 1472–1480.
doi:10.1016/j.visres.2009.03.007
- Lee, D. K., Itti, L., Koch, C., & Braun, J. (1999). Attention activates winner-take-all competition among visual filters. *Nature Neuroscience*, 2(4), 375–381.
doi:10.1038/7286
- Leys, C., Ley, C., Klein, O., Bernard, P., & Licata, L. (2013). Journal of Experimental Social Psychology. *Journal of Experimental Social Psychology*, 49(4), 764–766. doi:10.1016/j.jesp.2013.03.013
- Li, X., & Basso, M. A. (2008). Preparing to move increases the sensitivity of superior colliculus neurons. *The Journal of Neuroscience : the Official Journal of the Society for Neuroscience*, 28(17), 4561–4577.
doi:10.1523/JNEUROSCI.5683-07.2008
- Li, Z. (2002). A saliency map in primary visual cortex. *Trends in Cognitive Sciences*, 6(1), 9–16.
- Lin, C., Wan, X., Zhao, W., Ma, C., Ma, C., Gao, Y., et al. (2002). Enhancement of electrically evoked startle-like responses by tetanic stimulation of the superior colliculus. *Neuroreport*, 13(14), 1769–1773.
- Lingenhöhl, K., & Friauf, E. (1994). Giant neurons in the rat reticular formation: a sensorimotor interface in the elementary acoustic startle circuit? *The Journal of Neuroscience : the Official Journal of the Society for Neuroscience*, 14(3 Pt 1), 1176–1194.
- Louie, K., Gratton, L. E., & Glimcher, P. W. (2011). Reward value-based gain control: divisive normalization in parietal cortex. *The Journal of Neuroscience : the Official Journal of the Society for Neuroscience*, 31(29), 10627–10639.
doi:10.1523/JNEUROSCI.1237-11.2011
- Mansfield, R. J. (1973). Latency functions in human vision. *Vision Research*, 13(12), 2219–2234.
- Marino, R. A., Levy, R., Boehnke, S., White, B. J., Itti, L., & Munoz, D. P. (2012). Linking visual response properties in the superior colliculus to saccade behavior. *European Journal of Neuroscience*, 35(11), 1738–1752.
doi:10.1111/j.1460-9568.2012.08079.x
- Martin, G. R. (1982). An owl's eye: Schematic optics and visual performance in *Strix aluco* L. *Journal of Comparative Physiology*, 145(3), 341–349.
- Mazaheri, A., Diquattro, N. E., Bengson, J., & Geng, J. J. (2011). Pre-Stimulus Activity Predicts the Winner of Top-Down vs. Bottom-Up Attentional Selection. *PLoS ONE*, 6(2), e16243. doi:10.1371/journal.pone.0016243.g004
- Mazer, J. A., & Gallant, J. L. (2003). Goal-related activity in V4 during free viewing visual search. Evidence for a ventral stream visual salience map.

- Neuron*, 40(6), 1241–1250.
- McPeck, R. M., Han, J. H., & Keller, E. L. (2003). Competition between saccade goals in the superior colliculus produces saccade curvature. *Journal of Neurophysiology*, 89(5), 2577–2590. doi:10.1152/jn.00657.2002
- McPeck, R. M., Skavenski, A. A., & Nakayama, K. (2000). Concurrent processing of saccades in visual search. *Vision Research*, 40(18), 2499–2516.
- Meloni, E. G., & Davis, M. (1999). Muscimol in the deep layers of the superior colliculus/mesencephalic reticular formation blocks expression but not acquisition of fear-potentiated startle in rats. *Behavioral Neuroscience*, 113(6), 1152–1160.
- Meredith, M. A., & Stein, B. E. (1985). Descending efferents from the superior colliculus relay integrated multisensory information. *Science (New York, NY)*, 227(4687), 657–659.
- Milne, J. L., Chapman, C. S., Gallivan, J. P., Wood, D. K., Culham, J. C., & Goodale, M. A. (2013). Connecting the Dots: Object Connectedness Deceives Perception but Not Movement Planning. *Psychological Science : a Journal of the American Psychological Society / APS*. doi:10.1177/0956797612473485
- Murayama, N., Lin, Y. Y., Salenius, S., & Hari, R. (2001). Oscillatory interaction between human motor cortex and trunk muscles during isometric contraction. *NeuroImage*, 14(5), 1206–1213. doi:10.1006/nimg.2001.0907
- Mysore, S. P., & Knudsen, E. I. (2012). Reciprocal inhibition of inhibition: a circuit motif for flexible categorization in stimulus selection. *Neuron*, 73(1), 193–205. doi:10.1016/j.neuron.2011.10.037
- Mysore, S. P., & Knudsen, E. I. (2013). A shared inhibitory circuit for both exogenous and endogenous control of stimulus selection. *Nature Neuroscience*, 16(4), 473–478. doi:10.1038/nn.3352
- Mysore, S. P., Asadollahi, A., & Knudsen, E. I. (2010). Global inhibition and stimulus competition in the owl optic tectum. *The Journal of Neuroscience : the Official Journal of the Society for Neuroscience*, 30(5), 1727–1738. doi:10.1523/JNEUROSCI.3740-09.2010
- Nakamura, K. (1998). Neural processing in the subsecond time range in the temporal cortex. *Neural Computation*, 10(3), 567–595.
- Neggers, S. F., & Bekkering, H. (2000). Ocular gaze is anchored to the target of an ongoing pointing movement. *Journal of Neurophysiology*, 83(2), 639–651.
- Nicolelis, M. A., Baccala, L. A., Lin, R. C., & Chapin, J. K. (1995). Sensorimotor encoding by synchronous neural ensemble activity at multiple levels of the somatosensory system. *Science (New York, NY)*, 268(5215), 1353–1358.
- Ozen, G., Helms, M. C., & Hall, W. C. (2004). The intracollicular neuronal network. In W. C. Hall & A. K. Moschovakis (Eds.), *The Superior Colliculus: New Approaches for Studying Sensorimotor Integration*. Boca Raton, FL: CRC Press.
- Pastor-Bernier, A., & Cisek, P. (2011). Neural correlates of biased competition in premotor cortex. *The Journal of Neuroscience : the Official Journal of the Society for Neuroscience*, 31(19), 7083–7088. doi:10.1523/JNEUROSCI.5681-10.2011

- Perfiliev, S., Isa, T., Johnels, B., Steg, G., & Wessberg, J. (2010). Reflexive limb selection and control of reach direction to moving targets in cats, monkeys, and humans. *Journal of Neurophysiology*, *104*(5), 2423–2432. doi:10.1152/jn.01133.2009
- Port, N. L., & Wurtz, R. H. (2003). Sequential activity of simultaneously recorded neurons in the superior colliculus during curved saccades. *Journal of Neurophysiology*, *90*(3), 1887–1903. doi:10.1152/jn.01151.2002
- Pruszynski, J. A., King, G. L., Boisse, L., Scott, S. H., Flanagan, J. R., & Munoz, D. P. (2010). Stimulus-locked responses on human arm muscles reveal a rapid neural pathway linking visual input to arm motor output. *The European Journal of Neuroscience*, *32*(6), 1049–1057. doi:10.1111/j.1460-9568.2010.07380.x
- Rezvani, S., & Corneil, B. D. (2008). Recruitment of a head-turning synergy by low-frequency activity in the primate superior colliculus. *Journal of Neurophysiology*, *100*(1), 397–411. doi:10.1152/jn.90223.2008
- Saijo, N., Murakami, I., Nishida, S., & Gomi, H. (2005). Large-field visual motion directly induces an involuntary rapid manual following response. *The Journal of Neuroscience : the Official Journal of the Society for Neuroscience*, *25*(20), 4941–4951. doi:10.1523/JNEUROSCI.4143-04.2005
- Sailer, U., Eggert, T., Ditterich, J., Straube, A., & (null). (2002). Global effect of a nearby distractor on targeting eye and hand movements. *Journal of Experimental Psychology: Human Perception and Performance*, *28*(6), 1432–1446.
- Sasaki, S. (1999). Direct connection of the nucleus reticularis gigantocellularis neurons with neck motoneurons in cats. *Experimental Brain Research Experimentelle Hirnforschung Expérimentation Cérébrale*, *128*(4), 527–530.
- Schepens, B., & Drew, T. (2003). Strategies for the integration of posture and movement during reaching in the cat. *Journal of Neurophysiology*, *90*(5), 3066–3086. doi:10.1152/jn.00339.2003
- Schepens, B., & Drew, T. (2004). Independent and convergent signals from the pontomedullary reticular formation contribute to the control of posture and movement during reaching in the cat. *Journal of Neurophysiology*, *92*(4), 2217–2238. doi:10.1152/jn.01189.2003
- Schepens, B., & Drew, T. (2006). Descending signals from the pontomedullary reticular formation are bilateral, asymmetric, and gated during reaching movements in the cat. *Journal of Neurophysiology*, *96*(5), 2229–2252. doi:10.1152/jn.00342.2006
- Schepens, B., Stapley, P., & Drew, T. (2008). Neurons in the Pontomedullary Reticular Formation Signal Posture and Movement Both as an Integrated Behavior and Independently. *Journal of Neurophysiology*, *100*(4), 2235–2253. doi:10.1152/jn.01381.2007
- Schneider, K. A., & Kastner, S. (2005). Visual responses of the human superior colliculus: a high-resolution functional magnetic resonance imaging study. *Journal of Neurophysiology*, *94*(4), 2491–2503. doi:10.1152/jn.00288.2005
- Schütz, A. C., Trommershäuser, J., & Gegenfurtner, K. R. (2012). Dynamic integration of information about salience and value for saccadic eye

- movements. *Proceedings of the National Academy of Sciences of the United States of America*, 109(19), 7547–7552. doi:10.1073/pnas.1115638109/-DCSupplemental
- Shinoda, Y., Kakei, S., & Muto, N. (1996). Morphology of single axons of tectospinal and reticulospinal neurons in the upper cervical spinal cord. *Progress in Brain Research*, 112, 71–84.
- Siegmund, G. P., Inglis, J. T., & Sanderson, D. J. (2001). Startle response of human neck muscles sculpted by readiness to perform ballistic head movements. *The Journal of Physiology*, 535(Pt 1), 289–300.
- Song, J.-H., & Nakayama, K. (2006). Role of focal attention on latencies and trajectories of visually guided manual pointing. *Journal of Vision*, 6(9), 982–995. doi:10.1167/6.9.11
- Song, J.-H., & Nakayama, K. (2007). Automatic adjustment of visuomotor readiness. *Journal of Vision*, 7(5), 2.1–9. doi:10.1167/7.5.2
- Song, J.-H., & Nakayama, K. (2008). Target selection in visual search as revealed by movement trajectories. *Vision Research*, 48(7), 853–861. doi:10.1016/j.visres.2007.12.015
- Sparks, D. L. (2002). The brainstem control of saccadic eye movements. *Nature Reviews Neuroscience*, 3(12), 952–964. doi:10.1038/nrn986
- Stritzke, M., Trommershäuser, J., & Gegenfurtner, K. R. (2009). Effects of salience and reward information during saccadic decisions under risk. *Journal of the Optical Society of America a, Optics, Image Science, and Vision*, 26(11), B1–13. Retrieved from http://academia.edu/194819/Effects_of_salience_and_reward_information_during_saccadic_decisions_under_risk
- Stuphorn, V., Bauswein, E., & Hoffmann, K. P. (2000). Neurons in the primate superior colliculus coding for arm movements in gaze-related coordinates. *Journal of Neurophysiology*, 83(3), 1283–1299.
- Stuphorn, V., Hoffmann, K.-P., & Miller, L. E. (1999). Correlation of Primate Superior Colliculus and Reticular Formation Discharge With Proximal Limb Muscle Activity. *The Journal of Neuroscience : the Official Journal of the Society for Neuroscience*, 19(10), 3978–3982.
- Theeuwes, J. (2010). Top-down and bottom-up control of visual selection. *Acta Psychologica*, 135(2), 77–99. doi:10.1016/j.actpsy.2010.02.006
- Theeuwes, J., Kramer, A., & Hahn, S. (1998). Our eyes do not always go where we want them to go: Capture of the eyes by new objects. *Psychological Science : a Journal of the American Psychological Society / APS*, 9(5), 379–385.
- Thompson, K. G., & Bichot, N. P. (2005). A visual salience map in the primate frontal eye field. *Progress in Brain Research*, 147, 251–262. doi:10.1016/S0079-6123(04)47019-8
- Thorpe, S., Delorme, A., & Van Rullen, R. (2001). Spike-based strategies for rapid processing. *Neural Networks : the Official Journal of the International Neural Network Society*, 14(6-7), 715–725.
- Tijssen, M. A., Marsden, J. F., & Brown, P. (2000). Frequency analysis of EMG activity in patients with idiopathic torticollis. *Brain*, 123 (Pt 4), 677–686.

- Tipper, S. P., Howard, L. A., & Houghton, G. (1998). Action-based mechanisms of attention. *Philosophical Transactions of the Royal Society of London Series B, Biological Sciences*, 353(1373), 1385–1393. doi:10.1098/rstb.1998.0292
- Tipper, S., Howard, L., & Houghton, G. (2000). Behavioral Consequences of Selection from Neural Population Codes. *Control of Cognitive Processes: Attention and Performance XVIII*, 223.
- Torralba, A. (2003). Modeling global scene factors in attention. *Journal of the Optical Society of America a, Optics, Image Science, and Vision*, 20(7), 1407–1418.
- Töllner, T., Zehetleitner, M., Gramann, K., & Müller, H. J. (2011). Stimulus saliency modulates pre-attentive processing speed in human visual cortex. *PLoS ONE*, 6(1), e16276. doi:10.1371/journal.pone.0016276
- Trappenberg, T. P., Dorris, M. C., Munoz, D. P., & Klein, R. M. (2001). A model of saccade initiation based on the competitive integration of exogenous and endogenous signals in the superior colliculus. *Journal of Cognitive Neuroscience*, 13(2), 256–271.
- Ungerleider, L. G., & Mishkin, M. (1982). Two cortical visual systems. In D. J. Ingle, M. A. Goodale, & R. Mansfield (Eds.), *Analysis of Visual Behavior* (pp. 549–586). Cambridge, MA: MIT Press.
- Van der Stigchel, S. (2010). Recent advances in the study of saccade trajectory deviations. *Vision Research*, 50(17), 1619–1627. doi:10.1016/j.visres.2010.05.028
- Van der Stigchel, S., & Nijboer, T. C. W. (2013). How global is the global effect? The spatial characteristics of saccade averaging. *Vision Research*, 84(C), 6–15. doi:10.1016/j.visres.2013.03.006
- Van der Stigchel, S., Meeter, M., & Theeuwes, J. (2006). Eye movement trajectories and what they tell us. *Neuroscience and Biobehavioral Reviews*, 30(5), 666–679. doi:10.1016/j.neubiorev.2005.12.001
- Van Gisbergen, J. A. M., Van Opstal, A. J., & Roebroek, J. G. H. (1987). Stimulus-induced midflight modification of saccade trajectories. In J. K. O'Regan & A. Levy-Schoen (Eds.), *Eye Movements: From Physiology to Cognition* (pp. 1–11). North Holland: Elsevier.
- Van Opstal, A. J., & Goossens, H. H. L. M. (2008). Linear ensemble-coding in midbrain superior colliculus specifies the saccade kinematics. *Biological Cybernetics*, 98(6), 561–577. doi:10.1007/s00422-008-0219-z
- Van Rullen, R., & Thorpe, S. J. (2001). Rate coding versus temporal order coding: what the retinal ganglion cells tell the visual cortex. *Neural Computation*, 13(6), 1255–1283.
- van Zoest, W., Donk, M., & Van der Stigchel, S. (2012). Stimulus-salience and the time-course of saccade trajectory deviations. *Journal of Vision*, 12(8), 16. doi:10.1167/12.8.16
- Vanrullen, R. (2003). Visual saliency and spike timing in the ventral visual pathway. *Journal of Physiology-Paris*, 97(2-3), 365–377. doi:10.1016/j.jphysparis.2003.09.010
- Walker, R., Mccorley, E., & Haggard, P. (2006). The control of saccade

- trajectories: direction of curvature depends on prior knowledge of target location and saccade latency. *Perception & Psychophysics*, 68(1), 129–138.
- Watanabe, M., & Munoz, D. P. (2010). Presetting basal ganglia for volitional actions. *The Journal of Neuroscience : the Official Journal of the Society for Neuroscience*, 30(30), 10144–10157. doi:10.1523/JNEUROSCI.1738-10.2010
- Welsh, T. N. (2011). The relationship between attentional capture and deviations in movement trajectories in a selective reaching task. *Acta Psychologica*, 137(3), 300–308. doi:10.1016/j.actpsy.2011.03.011
- Welsh, T. N., & Elliot, D. (2004). Effects of response priming and inhibition on movement planning and execution. *Journal of Motor Behavior*, 36(2), 200–211. doi:10.3200/JMBR.36.2.200-211
- Welsh, T. N., Neyedli, H., & Tremblay, L. (2013). Refining the time course of facilitation and inhibition in attention and action. *Neuroscience Letters*. doi:10.1016/j.neulet.2013.08.055
- Werner, W., Dannenberg, S., & Hoffmann, K. P. (1997a). Arm-movement-related neurons in the primate superior colliculus and underlying reticular formation: comparison of neuronal activity with EMGs of muscles of the shoulder, arm and trunk during reaching. *Experimental Brain Research*, 115, 191–205.
- Werner, W., Hoffmann, K.-P., & Dannenberg, S. (1997b). Anatomical distribution of arm-movement-related neurons in the primate superior colliculus and underlying reticular formation in comparison with visual and saccadic cells. *Experimental Brain Research Experimentelle Hirnforschung Expérimentation Cérébrale*, 115(2), 206–216. doi:10.1007/PL00005691
- White, B. J., & Munoz, D. P. (2011). Separate visual signals for saccade initiation during target selection in the primate superior colliculus. *The Journal of Neuroscience : the Official Journal of the Society for Neuroscience*, 31(5), 1570–1578. doi:10.1523/JNEUROSCI.5349-10.2011
- Wolfe, J. M., & Horowitz, T. S. (2004). What attributes guide the deployment of visual attention and how do they do it? *Nature Reviews Neuroscience*, 5(6), 495–501. doi:10.1038/nrn1411
- Wolpert, D. M., Ghahramani, Z., & Flanagan, J. R. (2001). Perspectives and problems in motor learning. *Trends in Cognitive Sciences*, 5(11), 487–494.
- Wong, P., Collins, C. E., & Kaas, J. H. (2010). Overview of Sensory Systems of Tarsius. *International Journal of Primatology*, 31(6), 1002–1031. doi:10.1007/s10764-009-9388-4
- Wood, D. K., Gallivan, J. P., Chapman, C. S., Milne, J. L., Culham, J. C., & Goodale, M. A. (2011). Visual salience dominates early visuomotor competition in reaching behavior. *Journal of Vision*, 11(10), 16–16. doi:10.1167/11.10.16
- Yantis, S., & Egeth, H. E. (1999). On the distinction between visual salience and stimulus-driven attentional capture. *Journal of Experimental Psychology: Human Perception and Performance*, 25(3), 661–676.
- Yarbus, A. (1967). *Eye Movements and Vision*. New York: Plenum Press.
- Yeomans, J. S., Li, L., Scott, B. W., & Frankland, P. W. (2002). Tactile, acoustic

- and vestibular systems sum to elicit the startle reflex. *Neuroscience and Biobehavioral Reviews*, 26, 1–11.
- Zehetleitner, M., Hegenloh, M., & Müller, H. J. (2011). Visually guided pointing movements are driven by the salience map. *Journal of Vision*, 11(1). doi:10.1167/11.1.24
- Zehetleitner, M., Koch, A. I., Goschy, H., & Müller, H. J. (2013). Salience-Based Selection: Attentional Capture by Distractors Less Salient Than the Target. *PLoS ONE*, 8(1), e52595. doi:10.1371/journal.pone.0052595.s002

Appendix A: Supplemental Information for Chapter 2

SUPPLEMENTARY INFORMATION

Visual salience dominates early visuomotor competition in reaching behaviour

Daniel K. Wood, Jason P. Gallivan, Craig S. Chapman, Jennifer L. Milne,
Jody C. Culham and Melvyn A. Goodale



Centre for Brain & Mind

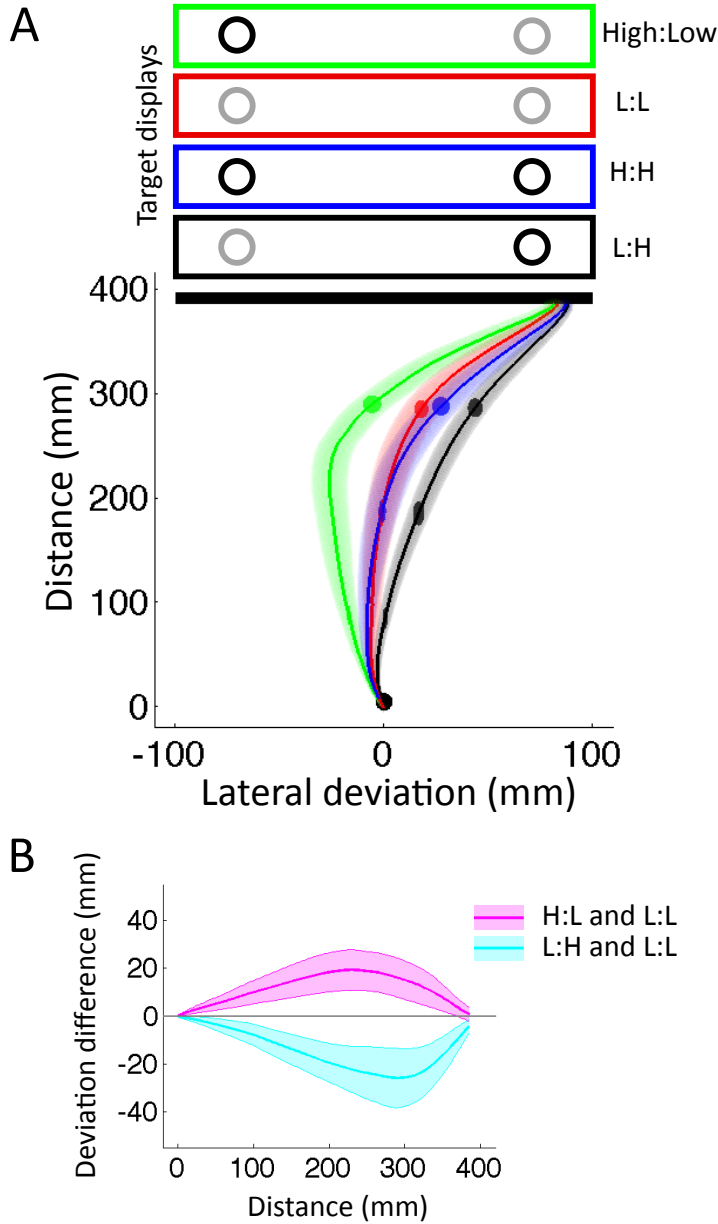
Department of Neuroscience

University of Western Ontario

London, Ontario, Canada N6A 5B7

Saliency Bias for Rightward Reaches in Experiment 1

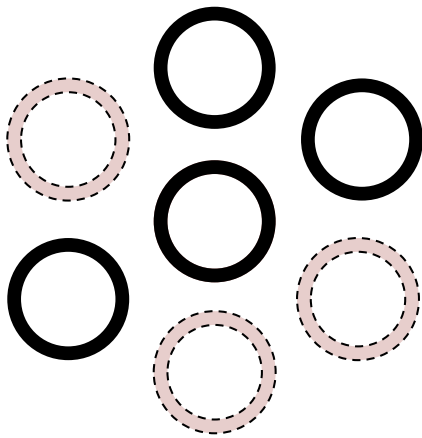
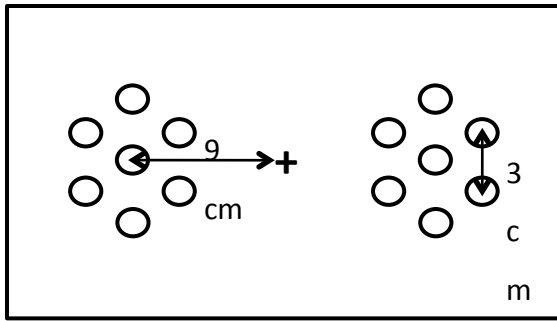
In the main manuscript of the present study, we presented the results of experiment 1 (E1) only in the context of trials where the final target appeared on the left side of space. This was done for the sake of simplicity. However, as mentioned in the main manuscript, in nearly every case, the effects observed in trials where the final target appeared on the left (i.e., end-left) were also observed in trials where the final target appeared on the right side of space (i.e., end-right). For example, in E1, a robust effect of saliency was observed not only for end-left trials (Figure 2.2, main manuscript), but also for end-right trials (Supplementary Figure 1).



Supplementary Figure 1. Results from E1: an overhead plot of average reach trajectories (A) toward the target displays indicated above the plot. Only end-right trials are shown. Shaded areas in the trajectory plot represent average standard error. The dark lines in (B) indicate the lateral deviation difference between trajectories in the H:L (i.e., *high* salience target left versus *low* salience target right) and L:L conditions (magenta) and between trajectories in the L:H and L:L conditions (cyan). Shaded areas in the difference plot represent 95% confidence intervals.

Supplementary Methods for Experiment 2

The present study is the latest in a string of studies that suggest that when participants are required to reach toward a display of multiple potential targets, initial trajectories reflect the spatial distribution of those targets. This means that biases in the trajectories reflect not only the number of targets on each side of space, but the lateral position of those targets as well (Chapman et al., 2010a). In order to control for this factor in experiment 2 (E2) of the present study, we determined the location of the potential targets for the initial display of a given trial by choosing them from a hexagonal cluster of seven targets (Supplementary Figure 2A). Whenever targets were displayed from a cluster, the central target was always displayed, along with other randomly selected targets (Supplementary Figure 2B). Thus, over the course of the experiment, the lateral position of potential targets was balanced.

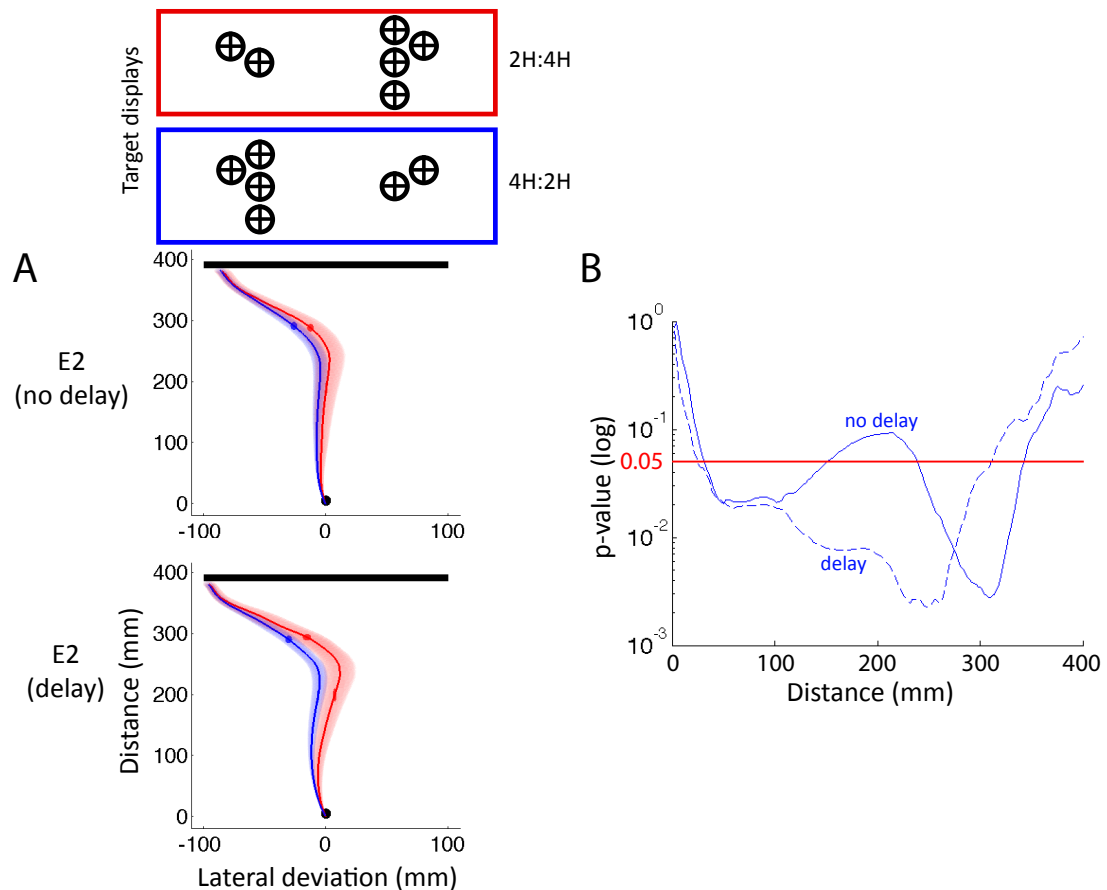


Supplementary Figure 2. Configuration of target display (A) and method of selecting locations for the potential targets (B). For a given trial, potential targets were chosen from two hexagonal clusters of seven targets. The central target of each cluster was located 9 cm to the left or right of the central fixation cross. All targets within a cluster were 3 cm apart (from center to center). Out of the seven possible targets in a cluster, only zero, two, or four were chosen to be targets in the initial display for a given trial (B). If any targets were displayed, the central target was always displayed, along with other randomly selected targets from the cluster.

Attenuation of Spatial Averaging Bias in Experiment 2

One interesting result of the salience manipulation we employed in E2 was that it apparently attenuated the typically strong spatial averaging bias. That is, even when target salience was held constant, participants in the no-delay group initiated reaches that were only weakly drawn toward the side of space with more

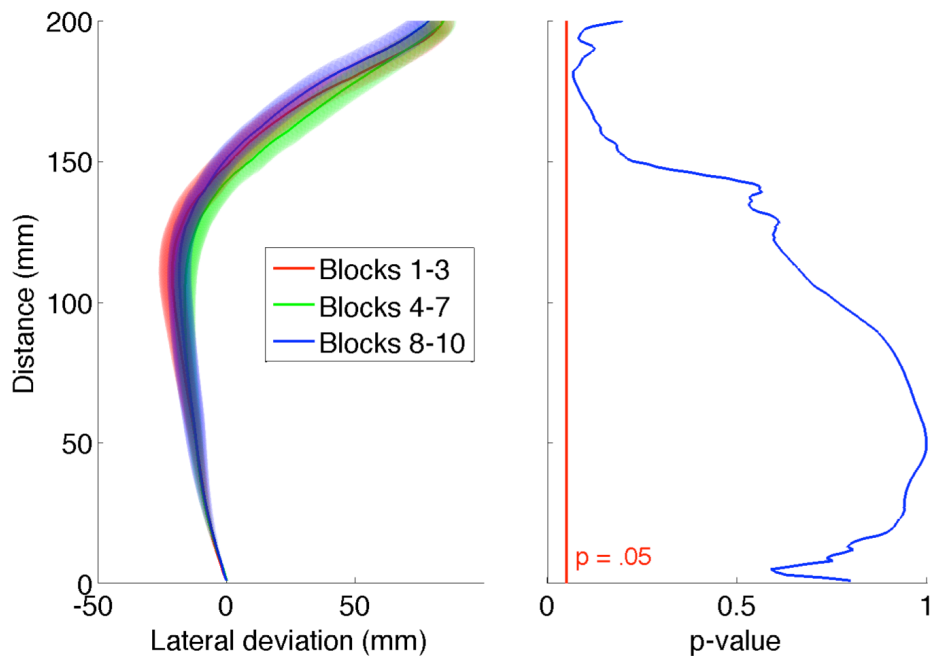
targets (Supplemental Figure 3A), as evidenced by a significance function that only intermittently dipped below 0.05 (Supplemental Figure 3B). The spatial averaging bias was also attenuated in the delay group participants, although the separation between the trajectories was larger (Supplemental Figure 3A) and more significant (Supplemental Figure 3B) than that of the no-delay participants.



Supplementary Figure 3. Results from E2: an overhead plot of average reach trajectories (A) toward the target displays indicated above the plot. Data from both no-delay (top plot) and delay (bottom plot) groups are shown. Only end-left trials are shown. Shaded areas in the trajectory plot represent average standard error. The graph (B) shows the results of the functional ANOVA that evaluated differences between the trajectories presented in (A). Significance functions for both the no-delay (solid blue line) and delay (dotted blue line) groups are shown.

No Practice Effects in Experiment 2

We tested whether the task irrelevance of target salience would, over time, become more evident in the behaviour of participants in the no-delay group. We binned trials into three groups based on block order (i.e., blocks 1-3, blocks 4-7, and blocks 8-10) and ran a functional ANOVA upon the associated average trajectories (Supplementary Figure 4). There was no point at which the trajectories significantly differed from one another. This leads us to conclude that, within the time frame of an experimental session, participants were not able to learn to ignore the salience of potential targets.



Supplementary Figure 4. Overhead view of no-delay group average trajectories for the 2H:4L display (left plot). Shaded bands represent average standard error. Also plotted are the results of the corresponding functional ANOVA (right plot) that compared the average trajectories of blocks 1-3, blocks 4-7, and blocks 8-10. The plot shows the p-value as a function of the distance of the hand from the touchscreen. The red line represents the *alpha* at 0.05.

As mentioned in the main manuscript, we speculate that this could be due to the overwhelming task-relevance of salience in many other natural contexts.

Breaking this instinct may be a possibility, but this would require more trials (and therefore more feedback) than this experiment provided.

Traditional Statistical Analysis of Trajectory Differences

Due to the relative novelty of functional data analysis in the context of movement kinematics, we supply here a supplemental statistical analysis of trajectory differences with ANOVA. Instead of assessing differences in variance as an entire function of some other variable (as one would do in functional data analysis), we instead sampled the lateral deviation function at a specific point (i.e., at 30% of the reach) and submitted the resulting data points to an ANOVA. For those interested in functional data analysis, the text by Ramsay and Silverman (2005) is a good resource. For details on how we applied this technique to our data, please see supplemental materials in past publications (Chapman et al., 2010a, 2010b; Gallivan et al., in press). The results of the traditional analysis are displayed in Supplementary Table 1 below.

Conditions		No Delay			
		EndLeft		EndRight	
Conditions		AvDiff(SE)	p-value	AvDiff(SE)	p-value
2H:4H	4H:2H	4.2(2.3)	0.078	.92(1.9)	0.6
2L:4L	4L:2L	3.2(2.3)	0.169	2.7(2.3)	0.26
2L:2H	2H:2L	13.5(2.5)	0.000002	11.3(2.5)	0.00004
4L:4H	4H:4L	13.1(2.4)	0.000001	10.7(2.6)	0.0001
4L:2H	2H:4L	10.2(2.8)	0.001	11.6(2.5)	0.0001
baseline	4H:2H, 2H:4H	-28.9(2.3)	0.000001	21.1(2.3)	0.0001
Conditions		Delay			
		EndLeft		EndRight	
Conditions		AvDiff(SE)	p-value	AvDiff(SE)	p-value
2H:4H	4H:2H	7.65(2.38)	0.002	7.1(1.9)	0.001
2L:4L	4L:2L	5.6(2.31)	0.019	5.9(2.4)	0.016
2L:2H	2H:2L	1.88(2.56)	0.465	2.0(2.5)	0.424
4L:4H	4H:4L	.98(2.42)	0.686	-1.0(2.6)	0.701
4L:2H	2H:4L	-7.047(2.83)	0.016	-5.59(2.5)	0.033
baseline	4H:2H, 2H:4H	-22.17(2.37)	0.000001	10.6(2.3)	0.00003

Supplementary Table 1. Traditional repeated-measures ANOVA comparing average trajectories for various conditions of interest at 30% of the movement distance. Average

differences between conditions, along with standard error of those differences, are displayed in milliseconds. Significant comparisons are highlighted in pink.

Notice the reversal of significance between delay groups in the first four conditions. The first two conditions tested the effect of spatial probability (i.e., how much of a bias was introduced by the distribution of potential targets) within the two levels of salience. While for the no-delay group there was no detectable effect of spatial probability at the point sampled here (30% of the reach), we note that the functional ANOVA reached significance earlier in the reach for this particular comparison. The third and fourth conditions tested the effect of salience. There were relatively large and significant differences for these comparisons in the no-delay group, but there was a striking eradication of these differences in the delay group.

The fifth condition compared responses to mirror images of a display with two high salience targets on one side and four low salience targets on the other. There were significant differences in both the delay and no-delay groups, but there was a reversal in the sign of the difference, as noted in the main manuscript. The sixth condition compared baseline trials (i.e., only two targets on one side of space, with trajectories that move in a straight line toward the targets) with a spatially uneven condition (four high salience versus two high salience). The motivation for showing the results of this comparison was to highlight the fact that trajectories in the delay group were still quite different from baseline, even when trajectories were biased toward the four targets instead of the two on the other side. This suggests that participants were not engaging in a conscious strategy, and that their reach trajectories, even after a 500 ms preview, were still primarily controlled by non-conscious mechanisms.

Analysis of Kinematic Measures in Experiment 2

We analyzed reaction times (Supplemental Table 2) from E2 with a mixed-design ANOVA. Reaction time was calculated as the time elapsed between the

sounding of the auditory go-cue (either concomitant with or 500 ms after presentation of the target display) and the release of a start button.

RT

Delay	Condition	No Delay
162.12	2L (left)	199.46
163.53	2L (right)	195.30
161.82	2H (right)	195.86
163.03	2H (left)	196.83
175.16	2L:2L	198.80
172.05	4L:4L	197.17
174.95	2L:4L	199.69
175.98	4L:2L	197.71
172.21	2L:2H	196.19
175.43	4L:4H	197.47
176.52	2L:4H	197.68
174.77	4L:2H	200.04
172.98	2H:2L	197.32
176.12	4H:4L	198.68
176.58	2H:4L	197.10
171.70	2H:2H	199.03
174.20	4H:4H	197.69

174.73	2H:4H	197.44
173.70	4H:2H	199.95

Supplementary Table 2. Average reaction times (ms) for all display configurations in E2, organized by delay group (i.e., delay or no-delay).

In the delay group, the first four conditions (baseline conditions) had significantly faster RTs than the rest of the conditions, among which there were no significant differences. There were no significant differences in RT for the no-delay group. The general absence of RT differences is a consistent finding in studies where the multiple target reaching task is employed. We have argued that this phenomenon is due to the stringent reaction time constraints that we impose upon the task itself (i.e., participants must react within 325 ms or the trial is aborted).

We also analyzed movement time (Supplemental Table 3) from E2 with a mixed-design ANOVA, this time including the factor of final target location (i.e., the side of space upon which the final target appeared). Movement was calculated as the time elapsed between the release of the start button and contact of the participant's finger with the touchscreen.

MT

Delay		Condition	No Delay	
Left	Right		Left	Right
393.31	N/A	2L (left)	407.32	N/A
N/A	383.15	2L (right)	N/A	388.98
N/A	382.79	2H (right)	N/A	390.52

397.48	N/A	2H (left)	401.76	N/A
465.71	425.60	2L:2L	448.73	427.04
466.60	430.78	4L:4L	459.87	433.72
469.33	426.62	2L:4L	459.89	431.76
458.03	433.30	4L:2L	449.55	422.38
464.14	431.73	2L:2H	462.59	420.00
467.13	432.29	4L:4H	467.30	424.58
468.52	425.53	2L:4H	470.14	425.63
458.40	433.33	4L:2H	458.53	422.11
462.98	432.95	2H:2L	438.68	433.83
463.45	438.10	4H:4L	442.35	435.96
465.80	430.56	2H:4L	445.48	442.90
460.40	431.13	2H:2H	452.17	430.53
464.34	434.28	4H:4H	452.50	429.16
474.47	433.10	2H:4H	455.60	431.84
460.85	433.98	4H:2H	451.31	436.72

Supplementary Table 3. Average movement time (ms) for all display configurations in E2, organized by delay group and whether the final target appeared on the left or the right side of the display.

There was a strong effect of condition upon movement time. This effect was driven predominately by the differences between baseline and non-baseline trials. As might be expected, baseline trials had significantly faster movement

times than non-baseline trials. This difference can be attributed to the fact that trajectories in the baseline conditions were essentially direct toward the target, and thus required no online correction. This effectively reduced the distance travelled, as well as any temporal cost associated with overcoming the momentum of the initial trajectory vector.

Also present was a strong effect of final target location. In both baseline and non-baseline conditions, trials where the final target appeared on the right had significantly faster movement times than trials where the final target appeared on the left. Presumably, this effect is a reflection of skeletomuscular constraints of the right arm and how these constraints interacted with the task requirements.

Appendix B: Copyright Permissions

Rightslink Printable License

2013-11-09 11:57 PM

SPRINGER LICENSE TERMS AND CONDITIONS

Nov 10, 2013

This is a License Agreement between daniel wood ("You") and Springer ("Springer") provided by Copyright Clearance Center ("CCC"). The license consists of your order details, the terms and conditions provided by Springer, and the payment terms and conditions.

All payments must be made in full to CCC. For payment instructions, please see information listed at the bottom of this form.

License Number	3265181369294
License date	Nov 10, 2013
Licensed content publisher	Springer
Licensed content publication	Experimental Brain Research
Licensed content title	Discrete and continuous planning of hand movements and isometric force trajectories
Licensed content author	C. Ghez
Licensed content date	Jan 1, 1997
Volume number	115
Issue number	2
Type of Use	Thesis/Dissertation
Portion	Figures
Author of this Springer article	No
Order reference number	
Title of your thesis / dissertation	Reaching for the light: The prioritization of conspicuous visual stimuli for reflexive target-directed reaching
Expected completion date	Jan 2014
Estimated size(pages)	180
Total	0.00 USD
Terms and Conditions	

Introduction

The publisher for this copyrighted material is Springer Science + Business Media. By clicking "accept" in connection with completing this licensing transaction, you agree that the following terms and conditions apply to this transaction (along with the Billing and Payment

<https://s100.copyright.com/App/PrintableLicenseFrame.jsp?publisherl...a2633-d272-4927-b3e4-0faf57f83291%20%20&targetPage=printablelicense>

Page 1 of 4

ELSEVIER LICENSE TERMS AND CONDITIONS

Nov 10, 2013

This is a License Agreement between daniel wood ("You") and Elsevier ("Elsevier") provided by Copyright Clearance Center ("CCC"). The license consists of your order details, the terms and conditions provided by Elsevier, and the payment terms and conditions.

All payments must be made in full to CCC. For payment instructions, please see information listed at the bottom of this form.

Supplier	Elsevier Limited The Boulevard, Langford Lane Kidlington, Oxford, OX5 1GB, UK
Registered Company Number	1982084
Customer name	daniel wood
Customer address	
License number	3265190248777
License date	Nov 10, 2013
Licensed content publisher	Elsevier
Licensed content publication	Vision Research
Licensed content title	How global is the global effect? The spatial characteristics of saccade averaging
Licensed content author	S. Van der Stigchel, T.C.W. Nijboer
Licensed content date	24 May 2013
Licensed content volume number	84
Licensed content issue number	
Number of pages	10
Start Page	6
End Page	15
Type of Use	reuse in a thesis/dissertation
Intended publisher of new work	other
Portion	figures/tables/illustrations

ELSEVIER LICENSE TERMS AND CONDITIONS

Nov 10, 2013

This is a License Agreement between daniel wood ("You") and Elsevier ("Elsevier") provided by Copyright Clearance Center ("CCC"). The license consists of your order details, the terms and conditions provided by Elsevier, and the payment terms and conditions.

All payments must be made in full to CCC. For payment instructions, please see information listed at the bottom of this form.

Supplier	Elsevier Limited The Boulevard, Langford Lane Kidlington, Oxford, OX5 1GB, UK
Registered Company Number	1982084
Customer name	daniel wood
Customer address	
License number	3265711333369
License date	Nov 10, 2013
Licensed content publisher	Elsevier
Licensed content publication	Neuron
Licensed content title	Neural Correlates of Reaching Decisions in Dorsal Premotor Cortex: Specification of Multiple Direction Choices and Final Selection of Action
Licensed content author	Paul Cisek, John F. Kalaska
Licensed content date	3 March 2005
Licensed content volume number	45
Licensed content issue number	5
Number of pages	14
Start Page	801
End Page	814
Type of Use	reuse in a thesis/dissertation
Portion	figures/tables/illustrations
Number of	1

Appendix C: Ethical Approval

copy



Department of Psychology



Use of Human Subjects - Ethics Approval Notice

Review Number	08 08 01	Approval Date	08 08 06
Principal Investigator	Mel Goodale/ Jason Gallivan/Craig Chapman/Daniel Wood	End Date	09 07 31
Protocol Title	Reaching and pointing experiment		
Sponsor	n/a		

This is to notify you that The University of Western Ontario Department of Psychology Research Ethics Board (PREB) has granted expedited ethics approval to the above named research study on the date noted above.

The PREB is a sub-REB of The University of Western Ontario's Research Ethics Board for Non-Medical Research Involving Human Subjects (NMREB) which is organized and operates according to the Tri-Council Policy Statement and the applicable laws and regulations of Ontario. (See Office of Research Ethics web site: <http://www.uwo.ca/research/ethics/>)

This approval shall remain valid until end date noted above assuming timely and acceptable responses to the University's periodic requests for surveillance and monitoring information.

During the course of the research, no deviations from, or changes to, the protocol or consent form may be initiated without prior written approval from the PREB except when necessary to eliminate immediate hazards to the subject or when the change(s) involve only logistical or administrative aspects of the study (e.g. change of research assistant, telephone number etc). Subjects must receive a copy of the information/consent documentation.

Investigators must promptly also report to the PREB:

- a) changes increasing the risk to the participant(s) and/or affecting significantly the conduct of the study;
- b) all adverse and unexpected experiences or events that are both serious and unexpected;
- c) new information that may adversely affect the safety of the subjects or the conduct of the study.

If these changes/adverse events require a change to the information/consent documentation, and/or recruitment advertisement, the newly revised information/consent documentation, and/or advertisement, must be submitted to the PREB for approval.

Members of the PREB who are named as investigators in research studies, or declare a conflict of interest, do not participate in discussion related to, nor vote on, such studies when they are presented to the PREB.



Clive Seligman Ph.D.

Chair, Psychology Expedited Research Ethics Board (PREB)

The other members of the 2087-2009 PREB are: David Dozois, Bill Fisher, Riley Hinson and Steve Lupker

CC: UWO Office of Research Ethics

This is an official document. Please retain the original in your files



Use of Human Participants - Ethics Approval Notice

Principal Investigator: Dr. Mel Goodale
Review Number: 06246E
Review Level: Delegated
Approved Local Adult Participants: 2400
Approved Local Minor Participants: 0
Protocol Title: The neural substrates of visual perception and visually-guided action in normal subjects.
Department & Institution: Physiology & Pharmacology, University of Western Ontario
Sponsor:
Ethics Approval Date: February 01, 2012 Expiry Date: March 31, 2012
Documents Reviewed & Approved & Documents Received for Information:

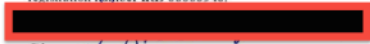
Table with 3 columns: Document Name, Comments, Version Date. Row 1: Addition of Co-investigator, Daniel Wood has been added as a co-investigator.

This is to notify you that The University of Western Ontario Research Ethics Board for Health Sciences Research Involving Human Subjects (HSREB) which is organized and operates according to the Tri-Council Policy Statement: Ethical Conduct of Research Involving Humans and the Health Canada/ICH Good Clinical Practice Practices: Consolidated Guidelines; and the applicable laws and regulations of Ontario has reviewed and granted approval to the above referenced revision(s) or amendment(s) on the approval date noted above.

The ethics approval for this study shall remain valid until the expiry date noted above assuming timely and acceptable responses to the HSREB's periodic requests for surveillance and monitoring information. If you require an updated approval notice prior to that time you must request it using the UWO Updated Approval Request Form.

Members of the HSREB who are named as investigators in research studies, or declare a conflict of interest, do not participate in discussion related to, nor vote on, such studies when they are presented to the HSREB.

The Chair of the HSREB is Dr. Joseph Gilbert. The UWO HSREB is registered with the U.S. Department of Health & Human Services under the IRB registration number IRB 00000940.



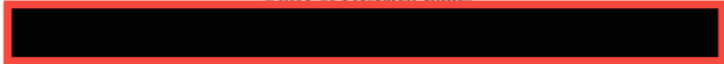
Signature

Ethics Officer to Contact for Further Information

Table with 3 columns: Janice Sutherland (jsuther@uwo.ca), Grace Kelly (grace.kelly@uwo.ca), Shantel Walcott (swalcot@uwo.ca)

This is an official document. Please retain the original in your files.

The University of Western Ontario
Office of Research Ethics





LAWSON FINAL APPROVAL NOTICE

RESEARCH OFFICE REVIEW NO.: R-13-277

PROJECT TITLE: Saliency responses in human arm muscles during reaching

PRINCIPAL INVESTIGATOR: Dr. Mel Goodale

LAWSON APPROVAL DATE: June 20, 2013

Health Sciences REB#: 103341

Please be advised that the above project was reviewed by the Clinical Research Impact Committee and the project:

Was Approved

Please inform the appropriate nursing units, laboratories, etc. before starting this protocol. The research office review number must be used when communicating with these areas.

Dr. David Hill
V.P. Research
Lawson Health Research Institute

All future correspondence concerning this study should include the Research Office Review



cc: Administration

Curriculum Vitae

Daniel Kent Wood

Education

2009 University of Western Ontario (London, ON)

M.Sc. Neuroscience

Thesis: The effects of ambiguity and trial order on the selection of goal-directed actions.

2006 Brigham Young University (Provo, UT)

B.A. Philosophy with Honors

Minors in Logic, Psychology, and Music

Thesis: Neuro-existentialism: The existential significance of the material body.

2001 Brigham Young University-Idaho (Rexburg, ID)

A.A. General Studies

Research Experience

2007-2013 The Brain and Mind Institute (Dr. Melvyn Goodale). Investigating the visuomotor system. Experimental techniques employed:

- *Behavioral*: psychophysics, kinematics (hand-tracking and eye-tracking), kinetics (object-lifting and force-fields in robot-arm environment) in healthy and neurological populations (blindsight, neglect, visual form agnosia)
- *Electrophysiological*: EEG, galvanic skin response, intramuscular and surface electromyography EMG.
- *Imaging*: fMRI
- *Stimulation*: TMS

2012 August Summer School in Computational Sensory-Motor Neuroscience (CoSMo). Two-week immersive course on robotics and BMI, computational neuroimaging, neuromechanics, etc. from leaders in computational neuroscience.

2005-2006 BYU Neuroscience Lab (Dr. Scott Steffensen). Studied spatial memory deficits in rats exposed to clinical levels of prenatal ultrasound.

Programming Experience

2012 TCL/TK

2007 Matlab

Teaching and Supervision

2012 Supervision of Western Physiology/Pharmacology Honours Student (Alex Major). Oversaw the design, data collection, analysis, and presentation of original research project.

2010 Supervision of Western Psychology Honours Student (Daryl Chambers).

2009 T.A. for Psych 2800E (Research Methods). Taught the lab portion for 21 students. Lectured (two hours weekly) on experimental design and statistical analysis, administered tests, held office hours, and graded tests and papers.

2008 Course Coordinator for Psych 280E (Research Methods). Responsible for designing the curriculum and overseeing the instruction in 10 labs. Also created and maintained various web materials for the course.

2007 T.A. for Psych 280E (Research Methods).

2006 T.A. for PHIL 305 (Predicate Logic). Taught classes, held office hours, graded coursework and term papers. Course instructor: Dr. Dennis Packard.

2005 R.A. for Dr. Mark Wrathall. Conducted research on the history of phenomenology and existentialism; assisted with preparation of manuscripts for *A Companion to Phenomenology and Existentialism*. Ed. Mark Wrathall and Hubert Dreyfus. USA: Blackwell Publishing, 2006.

Commentary

Gallivan, J.P., & **Wood, D.K.** (2009). Simultaneous encoding of potential grasping movements in macaque AIP. *Journal of Neuroscience*, 29(39), 12031-12032.

Peer-Reviewed Publications

Chapman, C.S., Gallivan, J.P., **Wood, D.K.**, Milne, J.L., Ansari, D., Culham, J.C., and Goodale, M.A. (Submitted). Counting on the motor system: Rapid action planning 'points' to format-dependent representations of number.

Milne, J.L., Chapman, C.S., Gallivan, J.P., **Wood, D.K.**, Culham, J.C., and Goodale, M.A. (2013). Object connectedness influences perceptual comparisons but not the planning or control of rapid reaches to multiple goals. *Psychological Science*.

Wood, D.K., Gallivan, J.P., Chapman, C.S., Milne, J.L., Culham, J.C., & Goodale, M.A. (2011). Visual salience dominates early visuomotor competition in reaching behaviour. *Journal of Vision*, 11(10):16, pp. 1-11.

Gallivan, J.P., Chapman, C.S., **Wood, D.K.**, Milne, J.L., Culham, J.C., Ansari, D., & Goodale, M.A. (2011). One to four, and nothing more: Non-conscious parallel object individuation in action. *Psychological Science*, 22(6) pp. 803-811.

Wood, D.K., & Goodale, M.A. (2011). Selection of wrist posture in conditions of motor ambiguity. *Exp Brain Res*, 208(4) pp. 607-20.

Chapman, C.S., Gallivan, J.P., **Wood, D.K.**, Milne, J.L., Culham, J.C., & Goodale, M.A. (2010). Short-term motor plasticity revealed in a visuomotor decision-making task. *Behavioural Brain Research*, 214(1), pp. 130-4.

Chapman, C.S., Gallivan, J.P., **Wood, D.K.**, Milne, J.L., Culham, J.C., & Goodale, M.A. (2010). Reaching for the unknown: multiple target encoding and real-time decision-making in a rapid reach task. *Cognition*, 116(2), pp. 168-76.

Awards and Fellowships

2012-2013 Queen Elizabeth II Graduate Scholarship in Science and Technology (QEIGSST). \$15,000.

2009-2012 Canadian Institutes of Health Research (CIHR) CGS Doctoral Research Award. \$105,000.

- 2010** University of Western Ontario, MSc Thesis Award in Neuroscience.
2008-2009 Canadian Institutes of Health Research (CIHR) graduate scholarship (MSc). \$17,500.
2007-2013 Western Graduate Research Scholarship. \$4,617 per semester.
2005 Brigham Young University Honors Research Grant. Amount: \$1,000.

Posters

- Wood, D.K.**, Chapman, C.S., Gallivan, J.P., Milne, J.L., Culham, J.C., & Goodale, M.A. (2013). The temporal decay of visual salience in a compelled response task. Poster presented at Gordon Research Conference: Eye Movements at Stonehill College in Easton, MA.
- Wood, D.K.**, Chapman, C.S., Gallivan, J.P., Milne, J.L., Culham, J.C., & Goodale, M.A. (2013) Characterizing the arrival of task-relevance: Parametric delays in a rapid reaching task reveal the transition from salience-based to task-based performance. Poster presented at the CAN/ACN conference in Toronto, ON.
- Wood, D.K.**, Cruse, D., & Goodale, M.A. (2012). Electrophysiological correlates of biomechanically induced bistability of preferred arm-postures. Poster presented at the Society for Neuroscience annual meeting in New Orleans, LA.
- Wood, D.K.**, Milne, J.L., Gallivan, J.P., Chapman, C.S., Culham, J.C., & Goodale, M.A. (2012). Implicit extraction of probability information from arbitrary color cues. Poster presented at ECVF (European Conference for Visual Perception) in Sardinia, Italy.
- Wood, D.K.**, Milne, J.L., Gallivan, J.P., Chapman, C.S., Culham, J.C., & Goodale, M.A. (2012). A reaching task reveals the rapid extraction of probability information from arbitrary colour cues. Poster presented at CSBBCS in Kingston, ON.
- Wood, D.K.**, Buckingham, G., Anwar, A., and Goodale, M.A. (2011) Foreknowledge of sequence optimizes fingertip force prediction in the absence of distinguishing visual cues. Poster presented at the *Society for Neuroscience*, Washington, DC.
- Chapman, C.S., Gallivan, J.P., **Wood, D.K.**, Milne, J.L., Culham, J.C., & Goodale, M.A. (2010) Rapid reaching task 'points' toward different representations of number. Poster presented at the *Society for Neuroscience*, San Diego, CA.
- Wood, D.K.**, Chapman, C.S., Gallivan, J.P., Milne, J.L., Culham, J.C., & Goodale, M.A. (2010) Visual salience of potential targets overrides spatial probabilities in a rapid visuomotor task. Poster presented at the *Society for Neuroscience*, San Diego, CA.
- Gallivan, J.P., Chapman, C.S., **Wood, D.K.**, Milne, J., Culham, J.C., & Goodale, M.A. (2009) Stuck in the middle: Kinematic evidence for optimal reaching in the presence of multiple potential reach targets. Poster presented at VSS (Vision Sciences Society) conference at Naples, Florida.
- Chapman C.S., Gallivan J.P., **Wood D.K.**, Milne J., Culham J.C., and Goodale M.A. (2009) Dynamic Target Acquisition: Rapid reach responses in the presence of multiple potential reach targets. Poster presented at the *Canadian Neuroscience Meeting*, Vancouver, BC.

- Wood, D.K.**, & Goodale, M.A. (2009). The effects of response ambiguity and trial order on the selection of goal-directed actions. Poster presented at VSS (Vision Sciences Society) conference at Naples, Florida.
- Wood, D.K.**, & Goodale, M.A. (2008). Grasping the ambiguous: The effect of ambiguous orientations on reach-to-grasp movements. Poster presented at CSBBCS (Canadian Society for Brain, Behaviour and Cognitive Science) conference.
- Wood, D.K.**, & Goodale, M.A. (2008). The selection of grip posture. Poster presented at SONA (Southern Ontario Neuroscience Association) conference. Received 3rd place award for best poster presentation.
- Wood, D.K.**, & Goodale, M.A. (2008). The effect of orientation on grasping strategies. Poster presented at the Western Research Forum at UWO, London, ON.
- Burnett, J., **Wood, D.K.**, & Steffensen, S. (2005). Does perinatal ultrasound produce neurocognitive defects? Poster presented at annual BYU Mentored Student Research Conference at BYU, Provo, UT.

Invited talks

- Wood, D.K.**, Goodale, M.A. (2013). Reaching and grasping in an uncertain world. Presented at University of Texas, Austin.
- Wood, D.K.**, Chapman, C.S., Gallivan, J.P., Milne, J.L., Culham, J.C., & Goodale, M.A. (2013). How does target salience influence reaching toward multiple targets? Presented at Northwestern University.
- Cieslak, M., Kluth, T., Stiels, M., & **Wood, D.K.** (2012). Deciding when to cut your losses. Presented at CoSMo Summer School, Northwestern University, Evanston, IL.
- Wood, D.K.**, Buckingham, G., & Goodale, M.A. (2011, February). Predictive fingertip force application in the absence of visual cues for weight. Presented at CAPNET (Canadian Action and Perception Network) conference at St. Adèle, Quebec.
- Wood, D.K.**, Monaco, S., McAdam, T., Dutton, G.N., Culham, J.C., & Goodale, M.A. (2009, October). Impaired selection of wrist posture in a patient with a parieto-occipital lesion. Presented at SFN (Society for Neuroscience) conference at Chicago, IL.
- Wood, D.K.** (2008, April). Grasping the ambiguous: The selection of grip posture. Talk given to the CIHR Group for Action and Perception at Elmhurst, Ontario, CA.